NOVEL REGULATORY MECHANISMS AFFECTING INSULIN SECRETION FROM SINGLE PANCREATIC BETA-CELLS

By

CRAIG ALAN ASPINWALL

A DISSERTATION PRESENTED TO THE GRADUATE SCHOOL
OF THE UNIVERSITY OF FLORIDA IN PARTIAL FULFILLMENT
OF THE REQUIREMENTS FOR THE DEGREE OF
DOCTOR OF PHILOSOPHY

UNIVERSITY OF FLORIDA

1999

To my parents, for a lifetime of love, guidance, and support

ACKNOWLEDGMENTS

I would like to express sincere appreciation to my advisor, Dr. Robert T. Kennedy for his guidance, support, and assistance throughout my graduate career. I would also like to thank all of the members of the Kennedy Research Group, past and present, for all of their assistance and encouragement during my time in the Kennedy Lab. I would like to especially thank Mr. Weijun Qian for his collaboration with calcium measurements presented in Chapter 5.

I would like to thank Dr. Jonathan R.T. Lakey for supplying islets used at various times throughout this research and for his valuable insight and collaboration. Deep appreciation is expressed to Drs. Olof Larsson and Robert Bränström for their assistance and willingness to answer any and all questions regarding β-cells and electrophysiological measurements and also for supplying the INS-1 cells used in this work. I would like to thank all of the members of my doctoral committee - Dr. Mark A. Atkinson, Dr. Jon D. Stewart, Dr. Kathryn R. Williams, and Dr. Richard A. Yost - for their wisdom, assistance, and encouragement. I would also like to express my gratitude to the UF Chemistry Department Division of Analytical Chemistry, the American Chemical Society, and Eastman Chemical Company for sponsoring fellowships to fund this work.

TABLE OF CONTENTS

page

ACKNOWLEDGMENTS iii

LIST OF ABBREVIATIONS vii

ABSTRACT x

CHAPTERS

1 INTRODUCTION 1

Pancreatic Islets and β-cells 2
Physiological Regulation of Insulin Secretion 4
Role of the β-cell in Diabetes Mellitus 8
Measurement of Insulin Secretion 11
Electrochemical Detection of Insulin Secretion 14
Dissertation Overview 16

2 AMPEROMETRIC DETECTION OF 5-HYDROXYTRYPTAMINE AS A MARKER OF EXOCYTOSIS FROM SINGLE PANCREATIC BETA-CELLS OF DIFFERENT SPECIES 25

Introduction 25
Experimental 28
Results 35
Discussion 42

3 EFFECTS OF INTRAVESICULAR H^+ AND EXTRACELLULAR H^+ AND ZN^{2+} ON INSULIN SECRETION IN PANCREATIC BETA-CELLS 64

Introduction 64
Experimental 67
Results 71
Discussion 75

4 INSULIN-STIMULATED INSULIN SECRETION IN SINGLE PANCREATIC BETA-CELLS.....94

Introduction.....94
Experimental.....97
Results.....102
Discussion.....106

5 INSULIN-STIMULATED INSULIN SECRETION IS MEDIATED BY RELEASE OF INTRACELLULAR CALCIUM STORES THROUGH A WORTMANNIN-SENSITIVE PATHWAY.....122

Introduction.....122
Experimental.....126
Results.....129
Discussion.....133

6 COMPARISON OF SECRETORY ACTIVITY FROM FRESH AND CRYOPRESERVED PANCREATIC ISLETS AND BETA-CELLS.....143

Introduction.....143
Experimental.....148
Results.....152
Discussion.....154

7 SUMMARY AND FUTURE DIRECTIONS.....161

Summary.....161
Future Directions.....165

APPENDICES.....169

A ISOLATION AND PREPARATION OF PANCREATIC ISLETS AND BETA-CELLS.....169

Procurement and Handling of Canine, Porcine, and Human Islets.....169
Isolation of Rodent Islets.....170
Dispersion of Human, Canine, and Porcine Islets into Single β-cells.....175
Dispersion of Rodent Islets into Single β-cells.....177

B AUTOMATED ANALYSIS OF AMPEROMETRIC CURRENT SPIKES............182

File Formats..........182
Fragmentation of Data Files..........183
Concerns Using Ts-findn..........185
Example File Types..........186
Program Code..........187

C MEASUREMENT OF INTRACELLULAR FREE Ca^{2+} IN SINGLE PANCREATIC BETA-CELLS USING FURA-2..........191

Use of Fura-2..........191
Instrumental Diagram..........192
Instrument Alignment..........193
Measurements of $[Ca^{2+}]_i$ in Single β-cells by Fura-2 Microfluorimetry..........194

REFERENCES..........199

BIOGRAPHICAL SKETCH..........211

LIST OF ABBREVIATIONS

5-HT	5-hydroxytryptamine
5-HTP	5-hydroxytryptophan
AC	Adenylate Cyclase
Ach	Acetylcholine
ADP	Adenosine diphosphate
Ag/AgCl	Silver/Silver Chloride Reference Electrode
AM	Acetoxymethyl Ester
amol	attomole (10^{-18} moles)
ATP	Adenosine triphosphate
βIRKO	β-cell Insulin Receptor Knockout
βTC3	Insulin secreting tumor line
$[Ca^{2+}]_i$	Intracellular free Ca^{2+} concentration
cAMP	Cyclic adenosine monophosphate
DAG	Diacylglycerol
DMEM	Dulbecco's Modified Eagle Medium
DMSO	Dimethylsulfoxide
EDTA	Ethylenediaminetetraacetic acid
EGTA	Ethylene glycol-bis(2-aminoethyl)-N,N,N',N'-tetraacetic acid
ER	Endoplasmic Reticulum

FBS	Fetal Bovine Serum
FWHH	Full Width at Half Height
G-100	Modified CMRL tissue culture medium
GK	Glucokinase
GLUT-2	Type 2 Glucose Transporter
HBSS	Hank's Balanced Salt Solution
HEPES	N-(2-hydroxyethyl)piperazine-N'-(2-ethanesulfonic acid)
IBMX	Isobutylmethylxanthine
IDDM	Insulin-Dependent Diabetes Mellitus
INS-1	Insulin secreting β-cell tumor line
IP_3	Inositol (1,4,5) triphosphate
IRS-1	Insulin Receptor Substrate-1
IRS-2	Insulin Receptor Substrate-2
K_{ATP}	ATP sensitive K^+ channel
KRB	Kreb's Ringer Buffer
MODY	Maturity Onset Diabetes of the Young
NIDDM	Non-Insulin-Dependent Diabetes Mellitus
P_{2y}	Type 2y purinergic receptor
PI-3K	Phosphoinositol 3-Kinase
PIP_2	Phosphatidyl inositol (4,5) diphosphate
PIP_3	Phosphatidyl inositol (3,4,5) diphosphate
PKA	Protein Kinase A
PKB	Protein Kinase B

PKC	Protein Kinase C
PLC	Phospholipase C
PMT	Photomultiplier Tube
RIA	Radioimmunoassay
ROI	Region of Interest
Ru-O/CN-Ru	Mixed valent ruthenium oxide/cyanoruthenate modified microelectrode
RuOx	Ruthenium oxide modified microelectrode
s.d.	standard deviation
S/N	Signal-to-Noise Ratio
SEM	Standard Error of the Mean
SH2	Src Homology Binding Domain
SI	Stimulation Index
SSCE	Sodium Saturated Calomel (reference) Electrode
SUR1	Sulfonylurea Receptor Subtype 1
TG	Thapsigargin

Abstract of Dissertation Presented to the Graduate School
of the University of Florida in Partial Fulfillment of the
Requirements for the Degree of Doctor of Philosophy

NOVEL REGULATORY MECHANISMS AFFECTING INSULIN SECRETION FROM SINGLE PANCREATIC BETA-CELLS

By

Craig Alan Aspinwall

August 1999

Chairman: Robert T. Kennedy
Major Department: Chemistry

Insulin is produced by β-cells within the pancreas and secreted in response to external stimuli, most notably changes in serum glucose concentrations. Significant progress has been achieved in elucidating the intracellular mechanisms by which glucose elicits exocytosis of insulin; however, regulation of insulin secretion through autocrine and post-vesicle fusion mechanisms remains largely unexplored. In this work, amperometric detection of insulin and 5-hydroxytryptamine (5-HT) was used to investigate novel chemical and physiological mechanisms regulating insulin secretion from single pancreatic β-cells.

Changes in the chemical environment of the β-cell reveal that extracellular Zn^{2+} and H^+, as well as intravesicular H^+, via different mechanisms, alter the concentration of free insulin at the cell surface during exocytosis. Exposure to high pH, whether intravesicular or extracellular, accelerated the rate of insulin release from single vesicles during exocytosis without affecting the absolute amount of insulin released. Increasing extracellular Zn^{2+} concentration through the physiological range decreased the rate of extrusion and the quanta of free insulin through a common ion-effect. In contrast, the rate and quanta of accumulated 5-HT clearance from the vesicle, serving as an internal control, were unaffected by either condition. It is concluded that intravesicular storage conditions and extracellular ions affect the free insulin concentration at the surface of the β-cell during the time course of single exocytosis events. Thus, environmental control of free insulin concentration following vesicle fusion suggests a novel level of regulation affecting autocrine and paracrine signaling within the islet.

Further characterization of the autocrine feedback pathways within the β-cell revealed that application of exogenous insulin elicits exocytosis in single, primary β-cells. The stimulatory effect of insulin is mediated by a wortmannin-sensitive pathway releasing thapsigargin-sensitive, intracellular calcium stores upon activation of the β-cell insulin receptor. Conditions where the insulin receptor is blocked or cell surface concentration of free insulin is reduced during exocytosis diminishes secretion induced by other secretagogues providing the first direct evidence for autocrine action of insulin upon secretion from the same cell. These results indicate that the β-cell insulin receptor can mediate positive feedback for insulin secretion providing a potential link between impaired insulin secretion and insulin resistance.

CHAPTER 1
INTRODUCTION

Regulated secretion of hormones and neurotransmitters by exocytosis is of critical importance for maintenance of physiological activity in higher organisms. The typical secretory vesicle contains between 0.15 and 10 attomoles of material that is released on the millisecond time scale (Chen et al., 1994; Huang et al., 1995; Paras and Kennedy, 1995; Pihel et al., 1996). Insulin secretion from the pancreatic β-cell is an important example of a hormonal regulatory system exhibiting release via exocytosis (Orci et al., 1988). Insulin is a pluripotent hormone, affecting virtually every cell type within the body (Norman and Litwack, 1997). Most importantly, secretion of insulin is the primary regulator of glucose homeostasis, an essential aspect of life in mammals and higher vertebrates. The inability to maintain blood glucose homeostasis, through insufficient production, secretion or utilization of insulin, results in the onset of diabetes mellitus (Kahn, 1998).

Since the discovery and isolation of insulin in 1921 by Banting and Best (Orci et al., 1988), and the subsequent first successful clinical use in 1922 (Hazelwood, 1989), the secretion and physiological actions of insulin have fascinated researchers. A primary interest of the research has been elucidation of the chemical and physiological messengers comprising the stimulus-secretion coupling pathway by which small fluctuations in blood glucose concentration elicit insulin secretion. Despite the volume of knowledge obtained on insulin secretion and β-cell function, many aspects of the insulin secretory process remain unclear, including the hormonal and neuronal interactions responsible for "fine-tuning" basal and glucose-stimulated insulin secretion. Also of interest is the cascade of events within the β-cell leading to transformation of the diabetic state in non-insulin dependent diabetes mellitus. A constant influx of novel technologies and methodologies are required in order to increase the existing knowledge of normal β-cell physiology and regulation if an understanding of the role of the β-cell in non-insulin dependent diabetes mellitus (NIDDM) is to be obtained.

Pancreatic Islets and β-cells

Insulin is produced by β-cells within the pancreas and is released in response to nutrient stimuli and receptor mediated agonists (Liang and Matschinsky, 1994). The mammalian pancreas is comprised of two major tissue types, the exocrine tissue, which secretes digestive enzymes, and the endocrine tissue responsible for release of hormones required for maintenance of glucose homeostasis (Norman and Litwack, 1997). The endocrine tissue of the pancreas is known as the islets of Langerhans, and is composed of four basic cell types: α-cells which produce glucagon, β-cells which produce insulin, δ-cells responsible for secretion of somatostatin and pp-cells responsible for secretion of pancreatic poly-peptide (Hazelwood, 1989). Of these four cell types, the β-cell accounts for more than 70 % of the ~3000 cells within the islet (Orci et al., 1988). Figure 1-1 shows a fluorescently stained pancreatic islet revealing the composition and distribution of the cell types within the islet. The α and δ-cells within an islet are generally located on the islet periphery and comprise ~ 20% and ~2% of the islet cells, respectively (Norman and Litwack, 1997). In contrast, the β-cells are mainly localized to the core of the islet (Hazelwood, 1989) as seen in Figure 1-1.

Insulin is stored as a complex with zinc within the β-cell in secretory vesicles and is released by exocytosis in response to external stimuli, most notably, glucose. In exocytosis, a secretory vesicle surrounded by membrane lipids and containing the secretory product, fuses with the plasma membrane following generation of a chemical or physiological signal. Secretion by exocytosis can be considered to occur in several distinct steps including vesicle docking, vesicle priming, vesicle fusion, and finally extrusion or clearance of the vesicular contents into the extracellular medium (Zimmerberg, 1987). Upon fusion, the secretory product is exposed to the extracellular environment and then is allowed to escape from the vesicle by diffusion. Figure 1-2 shows an electron micrograph of exocytosis in the β-cell. Two insulin containing secretory vesicles are clearly observed, one that has just fused with the plasma membrane and another in the process of fusing (Orci et al., 1988).

Insulin is stored as a solid hexamer bound with two Zn^{2+} ions per hexamer within the chemical environment of the secretory vesicle and therefore must dissolve before is can diffuse away from the cell (Gold and Grodsky, 1984; Blundell et al., 1972; Emdin et al., 1980; Aspinwall et al., 1997). As seen in Figure 1-2, the insulin granule in the "open" secretory vesicle has begun to expand, presumably due to dissolution of the compound. Following release into the extracellular space, insulin can be transported from the islet by vascular capillaries (Bonner-Weir, 1988) or can interact with other cell types within the islet to "fine-tune" the hormonal balance within the bloodstream (Norman and Litwack, 1997).

The maintenance of hormonal interactions between the islet cell types exerts an important level of control over normal regulation of blood glucose levels. Several lines of evidence support this observation. For example, β-cells within islets secrete more insulin on a per cell basis than purified β-cell preparations (Pipeleers et al., 1982). This is presumable due to paracrine interactions within the islet between β–cells and α-cells as addition of glucagon to the culture media ameliorates this problem. Additionally, somatostatin released from the δ-cells of the islet is a potent inhibitor of both insulin and glucagon secretion (Taborsky, 1983) but is regulated by insulin from the β-cell providing a positive-negative feedback loop.

Physiological Regulation of Insulin Secretion.

While most other endocrine or neuronal cells are stimulated to secrete hormones or neurotransmitters by binding of specific chemicals to surface bound receptors, the β-cell possesses a unique stimulus-secretion coupling which requires a fuel stimulus to be metabolized prior to initiation of insulin secretion (Ashcroft and Rorsman, 1989; Berggren and Larsson, 1994). While the physiological mechanisms responsible for glucose-stimulated insulin secretion are not completely understood, it is generally accepted that metabolism of glucose in response to fluctuations in the blood glucose concentration initiates a chain of chemical events responsible for secretion of insulin (Figure 1-3). Glucose concentrations above ~ 8 mM stimulate exocytosis of insulin in the β-cell of non-diabetic models (Pipeleers, 1994). In order to sense changes in blood glucose levels and hence secrete compensatory amounts of insulin, the β-cell possesses a low K_m (~20 mM), high V_{max} (32 mmol/min) glucose transporter, GLUT2, that allows the glucose concentration in the β-cell interior to rapidly equilibrate with extracellular levels (Liang and Matschinsky, 1994). Following entry of glucose through GLUT2, glucokinase phosphorylates the glucose molecules producing glucose-6-phosphate. The activity of this enzyme is considered to be the rate-limiting step in glucose sensing and signal transduction as glucose transport is at least 100 times faster than glucose phosphorylation by glucokinase (Liang and Matschinsky, 1994). Following phosphorylation, glucose enters the glycolytic pathway to be further metabolized. It is at this step of the process where the chemical signals responsible for glucose-stimulated exocytosis are generated. Interestingly, inhibition of glucose metabolism inhibits both electrical activity (membrane depolarization) and insulin secretion in the β-cell (Arkhammar et al., 1987).

Membrane potential in the β-cell is tightly regulated by ATP dependent potassium channels (K_{ATP}) consisting of one sulphonylurea receptor (SUR1) and one pore-forming (Kir6.2) subunit. The activity of the K_{ATP} channel plays a crucial role in stimulus-secretion coupling of glucose-stimulated insulin secretion primarily through interactions of adenine nucleotides. The resting membrane potential in the β-cell is tightly regulated at ~-70 mV. Upon metabolism of glucose, the K_{ATP} channel is inhibited leading to depolarization of the cell membrane and subsequent entry of Ca^{2+} through voltage-gated, L-type, Ca^{2+} channels (Berggren and Larsson, 1994). The ratio of ATP/ADP, which changes reciprocally during glycolysis, appears to be the most important regulator of β-cell membrane potential (Hopkins et al., 1992) and hence Ca^{2+} entry. Following depolarization, entry of Ca^{2+} triggers exocytosis in the β-cell during glucose stimulated insulin secretion (Berggren and Larsson, 1994). The nature of this interaction however, remains unclear. It is clear however, that a defect at any point in the regulatory pathway between glucose entry and exocytosis could result in defective insulin secretion from the β-cell.

In addition to the chemical and ionic interactions leading to depolarization of the cell membrane and elevations in $[Ca^{2+}]_i$ resulting from direct metabolism of glucose, several other second messenger systems are potentially involved in normal regulation of insulin secretion. These include cAMP, inositol (1,4,5) triphosphate, ryanodine receptor agonists, adenosine triphosphate and protein kinases. Due to the complexity, as well as the cross-reactivity, of these signalling systems the exact nature of the interactions upon normal regulation of insulin secretion is unclear. It is becoming increasing obvious, however, that these signalling molecules play a very large role in physiological regulation of exocytosis in the β-cell.

It is well established that increased in cAMP concentrations within the β-cell potentiate insulin secretion. Activators of adenylate cyclase (AC), such as forskolin, which act through G-protein coupled receptors or inhibitors of phosphodiesterases, such as isobutylmethylxanthine (IBMX) both increase insulin secretion in response to Ca^{2+} dependent stimuli while having little stimulatory action of their own (Gillis and Misler, 1993). Several physiological peptides, such as glucagon, glucagon–like peptide and gastric inhibitory peptide, that are known to potentiate insulin secretion, exhibit their effects through increases in cAMP levels within the cell (Liang and Matschinsky, 1994). Evidence of the importance of cAMP modulators in normal regulation of the β-cell has been demonstrated in studies of purified β-cells. As previously mentioned, in purified preparations secrete less insulin than β-cell in islets; however this condition is reversed by addition of glucagon to the culture media (Pipeleers et al., 1982). Additionally, increases in the cAMP levels of pancreatic islets from GK rats, a rodent model of NIDDM, has been demonstrated to restore normal insulin secretion and to reverse the diabetic state (Abdel-Halim et al., 1996).

It has been hypothesised that cAMP acts to enhance insulin secretion by "permitting" the coupling of Ca^{2+} entry or release from intracellular stores to granule fusion (Barnett et al., 1994). Several recent reports have demonstrated a possible mechanism for such an effect. Cyclic AMP activates protein kinase A (PKA) *in vivo* (Blanpied and Augustine, 1999) leading to granule mobilization in the β-cell. While the substrates for PKA have yet to be identified, the action of PKA on vesicle priming appears to act through ATP dependent and Ca^{2+} dependent phosphorylation of a "sensor" protein responsible for vesicle recruitment and fusion (Takahashi et al., 1999). In addition to the Ca^{2+} dependent mechanism, activation of PKA can also participate in a Ca^{2+} independent potentiation of insulin secretion; however the mechanism of this action is much less clear (Ammala et al., 1993).

Cyclic AMP can also potentiate release of intracellular Ca^{2+} stores through both inositol (1,4,5) triphosphate (IP_3) and ryanodine sensitive stores (Liu et al., 1996; Islam et al., 1998; Holz et al., 1999). While both of these intracellular pools have been demonstrated to be activated in the β-cell upon glucose stimulation, considerable controversy exists over which is the primary regulator of intracellular Ca^{2+} stores (Okamoto, 1999; Webb et al., 1996). It is interesting that many common β-cell stimulants, such as ATP and muscarinic acetylcholine (Ach) agonists exert their effects by activating phospholipase C (Li et al., 1991; Hiriart and Ramirez-Mendeles, 1993). This leads to an increase in the IP_3 concentration within the cell generating the release of

Ca^{2+} from the intracellular stores. It is generally believed that release of Ca^{2+} from the intracellular stores alone is not sufficient to generate insulin secretion, leading to the hypothesis of Ca^{2+} release-activated current generating the stimulatory effects of these classes of compounds (Bertram et al., 1995). This is not strictly the case with ATP, which has been observed to generate insulin secretion in the absence of extracellular Ca^{2+} (Li et al., 1991).

In addition to production of IP_3, PLC activation leads to elevated levels of diacylglycerols (DAG) within the β-cell (Howell, 1994). The main physiological target of DAG is protein kinase C (PKC) (Howell, 1994). PKC can also be activated by phorbol esters and has been implicated in a variety of steps in the secretory process of the β-cell ranging from Ca^{2+} sensitization (Kindmark et al., 1992) to Ca^{2+}-independent exocytosis in combination with elevated PKA activation (Komatsu et al., 1997). Although significant progress has been made in elucidating the physiological pathways important in the regulation of insulin secretion from normal β-cells, the intersection of many of the common messenger pathways has precluded assignment of definitive functions for each of the signals, leading to a great deal of uncertainty.

Role of the β-cell in Diabetes Mellitus

Diabetes mellitus is the most common metabolic disease in Western civilizations (Kahn, 1998). Approximately 5 % of the current US population is affected by some form of the disease leading to a major public health concern (Taylor, 1999). In the United States, diabetes is the leading cause of blindness, renal failure and circulatory problems in the extremities in the adult population as well as a major risk factor associated with cardiovascular disease (Kahn, 1998). While the term diabetes encompasses a heterogeneous group of disorders resulting from differing pathologies and onset of the disease, the unifying characterization is elevated blood glucose levels (Harris, 1995). Current classifications of diabetes can be broken down to five major types with the three most common being: insulin-dependent diabetes mellitus (IDDM); non-insulin-dependent diabetes mellitus (NIDDM), and maturity onset diabetes of the young (MODY) (Harris, 1995; Yamagata et al., 1996).

IDDM, commonly referred to as juvenile diabetes, accounts for ~ 3% of all diabetes cases (Harris, 1995). IDDM results from autoimmune destruction of the pancreatic β-cell leading to reduced β-cell mass (Atkinson and Maclaren, 1994). The resulting pathology is loss of basal, as well as non-glucose and glucose-stimulated insulin secretion (Figure 1-4) (Pfeifer et al., 1981). IDDM is characterized by early onset, most commonly before age 20, and results in an average life expectancy that is reduced by ~ 15 years compared to the general population (Harris, 1995). Due to the near total lack of insulin, patients are treated with insulin injections making regulation of normoglyceamia problematic by leading to major fluctuations in the blood glucose level compared to the smaller, more tightly regulated changes in non-diabetics.

NIDDM, in contrast, accounts for ~ 95% of the reported cases of diabetes in the US and predominantly affects adults over 30 years of age (Harris, 1995). Environmental factors such as age, weight and physical activity greatly affect the likelihood of occurrence. The resulting pathologies vary greatly for NIDDM patients but at least two major classifications exist: insulin resistance in peripheral tissues and impaired insulin secretion from the β-cell, both of which lead to hyperglycemia and are considered hallmarks of Type-II diabetes (Taylor et al., 1994; Kahn, 1997). Considerable controversy surrounds the issue of which of these deficiencies is the primary physiological defect in NIDDM leading to several conflicting results. In some studies, the earliest observed defect is dysfunctional secretion (Cunningham et al., 1996; O'Rahilly et al., 1988) and in others insulin resistance appears to be the first detectable problem (Martin et al., 1992).

Several lines of evidence suggest a role of defective β-cell function in NIDDM (Malaisse, 1994). For example, under normal conditions, glucose challenge results in a biphasic insulin secretory response composed of a rapid first phase followed by a sustained second phase, as seen in Figure 1-4. In some NIDDM patients, the first phase of insulin secretion is lost leading many to predict a loss of β-cell function (Figure 1-4). Additionally, loss of oscillatory insulin release has been shown to be an early symptom of Type-II diabetes (O' Rahilly et al., 1988). More recently, models of NIDDM have been discovered possessing defective GLUT2 transporters (Johnson et al., 1990) and defective glucokinase (Vionnet et al., 1992) suggesting impaired glucose signaling as a cause of some forms of NIDDM. These results also explain the maintenance of arginine-stimulated insulin secretion in many NIDDM cases (Johnson et al., 1990).

MODY is a form of NIDDM characterized by early onset, i.e. before age 25, and an autosomal mode of inheritance (Vionnet et al., 1992). It is estimated that 2-5% of all NIDDM cases result from MODY (Yamagata et al., 1996). In MODY, the primary pathogenic defect resulting in elevated blood glucose levels appears to be due to defective glucose signaling and insulin secretion in the β-cell (Polonsky, 1995; Yamagata et al., 1996)). Several genes have been isolated that correspond to glucokinase and GLUT2 expression (Polonsky, 1995; Vionnet et al., 1992). Hence, a primary defect in normal regulation of insulin secretion from the β-cell leads to clinical onset of diabetes.

Measurement of Insulin Secretion

The development of physiological and chemical methods that allow studies of insulin secretion from single islets and β-cells has greatly contributed to the advancement of knowledge of normal β-cell function. Until recently, the only available methods for monitoring insulin secretion suffered from a lack of sensitivity leading to reduced temporal resolution. To account for this low sensitivity, most studies on insulin secretion were performed on either whole animals or pooled groups of islets, hindering secretion studies on isolated β-cells. The development of single cell assays for monitoring secretory activity in the β-cell has led to rapid advancement in the knowledge of β-cell physiology and stimulus-secretion coupling. While serum and islet assays are fairly mature, single cell assays have only recently been applied to the study of normal regulation of cellular processes, including exocytosis.

The most common method for monitoring insulin secretion from perfused whole pancreas or from populations of islets has been radioimmunoassay (RIA) (Berson and Yalow, 1966). RIA is a mass sensitive technique therefore smaller samples, i.e. fewer islets require longer fraction collecting times, typically > 1 min, impairing temporal resolution. Additionally, studies on groups of islets mask the effects of islet heterogeneity. For example, it has been demonstrated that islets from different regions of the pancreas contain varying percentages of β-cells (Orci, 1985). Due to the use of large numbers of islets, the heterogeneity of the population cannot be observed by RIA.

More recently, automated competitive immunoassays based on capillary electrophoresis have been developed to monitor insulin secretion. Using this method, insulin secretion from single islets has been monitored with 3 s temporal resolution (Tao et al., 1998). Due to the sensitivity and temporal resolution, this method has been particularly useful for monitoring oscillatory insulin secretion in response to glucose stimulation from single islets (Tao et al., 1998).

In addition to directly monitoring insulin secretion from populations of islets and single islets, several indirect methods for monitoring insulin secretion from single β-cells have recently been proposed. Due to the tight coupling between β-cell membrane potential and $[Ca^{2+}]_i$ with secretion of insulin from single islets, these properties have been exploited as a marker for secretory activity in the β-cell (Duchen et al., 1993; Smith et al., 1995; Scott et al., 1981). There are several limitations to extension of these properties to insulin secretion, however. For example, it is well established that insulin secretion from β-cells and islets is highly temperature dependent, and is abolished below ~ 30° C. Changes in membrane potential, glucose metabolism and elevations in $[Ca^{2+}]_i$, however are minimally affected by temperature variations, even below 27° C (Dawson et al., 1986).

As an alternative to association of insulin secretion with physiological properties, several methods have been developed with rely on direct detection of vesicle fusion from single β-cells. The most common methods are electrophysiological, or patch-clamp methods. In patch-clamp techniques, a micropipette is pulled to a very reproducible tip size and is physically attached to the cell membrane, forming a high resistance seal (GΩ) seal allowing electrical properties of the cell to be monitored (Penner, 1995). The two most common electrical properties associated with exocytosis are membrane potential changes, as describe earlier, and cellular capacitance measurements.

Membrane capacitance measurements have recently been applied to the study of exocytosis from single β-cells (Gillis and Misler, 1992). The plasma membrane of a cell can be considered to be a capacitor. Upon addition or removal of new membrane area, as in exocytosis and endocytosis, the membrane capacitance changes proportionally with the surface area of the membrane (Gillis, 1995). Monitoring this process allows detection of exocytosis; however, since the capacitance change monitored is a net change, the absolute number of vesicle fusion events must be interpreted with extreme caution.

Direct detection of exocytosis through detection of marker compounds has been explored recently. The most common endogenous marker of insulin secretion from single cells has been ATP, which is co-released with insulin in the β-cell. One approach has been to culture the β-cells with endothelial cells expressing P_{2y} receptors (Kuromi et al., 1995). When ATP released from the β-cell binds to the receptor, the endothelial cells exhibit increases in $[Ca^{2+}]_i$ that can be monitored by fura-2 microscopy. This technique suffers from several limitations, most importantly the inability to quantify insulin secretion. Another approach has been to place a PC-12 cell attached to a patch-clamp pipette next to a β-cell. Upon stimulation with insulin secretoagogues, the whole-cell current of the PC-12 cell increases due to the co-released ATP binding to surface receptors.

Electrochemical Detection of Insulin Secretion

Due to the limitations of indirect detection of exocytosis in the β-cell, direct detection of insulin would be more desirable. Recently, amperometry with microelectrodes has been applied to the study of exocytosis at a variety of cell types including adrenal chromaffin cells (Chow et al., 1992; Ciolkowski et al., 1992; Leszczyszyn et al., 1990; Wightman et al., 1991), PC12 cells (Chen et al., 1994), mast cells (Alvarez de Toledo et al., 1990), neurons (Zhou and Misler, 1995), and melanotrophs (Paras and Kennedy, 1995; Paras and Kennedy, 1997). In this technique, an amperometric electrode is positioned next to a single cell so that released secretory product can be detected with high sensitivity and temporal resolution. When secretion by vesicle fusion occurs, a rapid concentration change occurs in the volume defined by the cell and the active area of the electrode. This concentration change results in the generation of a current spike corresponding to quantitative detection of molecules released from single secretory vesicles by exocytosis (Wightman et al., 1991; Huang et al., 1995; Aspinwall et al., 1997).

Analysis of the current spikes obtained by this method can reveal subtle details about the secretory process unattainable by other available methods. For example, the area of the current spikes, which is in units of Coulombs, can be used to directly quantitate the moles of detected hormone (or transmitter) released per vesicle fusion event using Faraday's Law (Wightman et al., 1991). Additionally, the dynamics of vesicular release events are reflected in the shape and width of the current spikes. The shape of the current spikes obtained has been used to obtain information about the storage of the secretory product (Navanti and Fernandez, 1993; Schroeder et al., 1996; Jankowski et al., 1993; Aspinwall et al., 1997), as well as the mechanism of release (Chow et al., 1992; Navanti and Fernandez, 1996; Schroeder et al., 1996; Aspinwall et al., 1997). The width of the spikes can be used as a measure of the rate of clearance from the vesicle since the width is determined by any slow kinetic step involved in clearing hormone from the vesicle and diffusional broadening of the secreted packet of molecules (Jankowski et al., 1994; Jankowski et al., 1993; Borges et al., 1997; Walker et al., 1996). Thus, the exquisite spatial and temporal resolution, as well as sensitivity of amperometry for measuring actual secretory products has made it well-suited for monitoring exocytosis at the single vesicle level. This has allowed several novel aspects of the process of vesicular release to be probed, including investigation of post-fusion events in exocytosis (Jankowski et al., 1994; Jankowski et al., 1993; Borges et al., 1997; Fernadez-Chacon and de Toledo, 1995; Oberhauser et al., 1996).

This technique has recently been extended to detection of insulin secretion from pancreatic β-cells (Huang et al., 1995; Kennedy et al., 1993). Schematics of the experimental setup are shown in Figure 1-5 and 1-6. While detection of catecholamines and indoleamines is relatively easy at unmodified microelectrodes due to the ease of oxidation, insulin is unreactive at bare carbon electrodes during the time course of an exocytosis event (Kennedy et al., 1993). Therefore, a carbon-fiber electrode modified with ruthenium oxide/cyanoruthenate (Ru-O/CN-Ru), a catalyst that promotes oxidation of insulin, is used for detection. The microelectrode is positioned ~ 1 μm above the cell and exocytosis is monitored by amperometry. This method has allowed the first direct measurement of exocytosis of insulin from single β-cells with high temporal resolution (Kennedy et al., 1993).

Amperometric detection of insulin possesses several advantages over traditional methods for detecting insulin secretion. First, it is highly sensitive and easily miniaturized, allowing detection of single exocytosis events (Huang et al., 1995). Additionally, it is non-invasive, allowing easy coupling with other techniques, such as microfluorimetry, to maximize information related to stimulus-secretion coupling in the β-cell. Finally, amperometry allows for determination of quantitative and kinetic data from single vesicle release events, allowing novel insight into the regulatory mechanisms affecting normal secretion of insulin from the β-cell

Dissertation Overview

Chapter 2 describes the comparison and characterization of two methods for amperometric detection of exocytosis in single pancreatic β-cells. In the first method, direct detection of insulin was performed using an insulin-sensitive, mixed valent Ru-O/CN-Ru chemically modified electrode as previously described (Kennedy et al., 1993; Huang et al., 1995; Aspinwall et al., 1997). In the second, 5-hydroxytryptamine (5-HT) that had been allowed to accumulate within the β-cell secretory vesicles was detected with a bare carbon electrode. The goal of the comparison was to determine whether secretion of accumulated 5-HT could serve as a valid marker of insulin secretion from the β-cell. The ability to use 5-HT as a quantitative marker for insulin secretion was also investigated by comparing spike areas resulting from detection of 5-HT and insulin under a variety of experimental conditions. The results presented here strongly suggest that 5-

HT is useful as a qualitative, but not quantitative, marker of insulin release at single β-cells.

In additional studies, measurement of insulin and 5-HT secretion from β-cells of different species was performed to determine whether a species dependence exists for the two methods compared here. Detection of 5-HT was determined to be equivalent to detection of insulin in human, porcine and canine β-cells; however, in mouse and INS-1 β-cells, 5-HT is more readily detected than insulin through generation of a higher signal to noise ratio. Finally, the effects of common experimental variables was examined for detection of 5-HT and insulin to determine additional limitations of the 5-HT method.

Chapter 3 describes the effects of extracellular Zn^{2+} and pH as well as intravesicular pH on insulin and 5-HT secretion from single pancreatic β-cells. Insulin is stored as a solid hexamer with zinc within the secretory vesicle of the β-cell and must dissolve and dissociate before becoming biologically active. Exposure to high pH, whether intravesicular or extracellular, accelerated the release of insulin during exocytosis without affecting the amount of insulin released. Increasing extracellular Zn^{2+} concentration from 0 to 25 μM decreased the rate of dissociation and the surface concentration of free insulin monomer following vesicle fusion through a common-ion effect on Zn^{2+}-insulin dissociation. The results indicate that both the intravesicular and extracellular environments can alter the free insulin concentration at the surface of the β-cell during secretion suggesting the existence of a series of novel regulatory mechanisms controlling insulin secretion at the single vesicle level.

Chapter 4 presents the discovery of an autocrine feedback mechanism in the β-cell that exerts positive feedback on insulin secretion. Amperometric measurements at single, primary pancreatic β-cells reveal that application of exogenous insulin in the presence or absence of non-stimulatory concentrations of glucose evokes exocytosis mediated by the β-cell insulin receptor. These results provide the first direct evidence that the β-cell insulin receptor can mediate positive feedback for insulin secretion. Furthermore, evidence is presented for direct autocrine action of insulin upon secretion from the same cell providing a potential link between impaired insulin secretion and insulin resistance.

Chapter 5 describes the intracellular mechanism by which insulin stimulates insulin secretion in the pancreatic β–cell. Through studies on primary mouse β-cells and an IRS-1 gene disrupted β-cell tumor line, it was determined that insulin binding to the β-cell insulin receptor activates insulin receptor substrate-1 and phospatidylinositol 3-kinase leading to activation of phospolipase C. Activation of phospolipase C increases the cellular levels of inositol (1,4,5) triphosphate which releases intracellular calcium stores from the endoplasmic reticulum initiating exocytosis.

Chapter 6 presents the investigation of the effects of cryopreservation on insulin secretion from single β-cells. Amperometric detection of insulin and accumulated 5-HT revealed that cryopreservation of pancreatic islets does not significantly reduce the ability of the β-cell to synthesize, store or release insulin in response to traditional stimuli. Additionally, many elements of the glucose-induced stimulus-secretion coupling pathway remain intact following cryopreservation. The results suggest that cryopreservation of pancreatic islets does not significantly alter the function of insulin secreting β-cells and hence should serve as a useful method of storing islets of Langerhans prior to *in vitro* investigation and/or transplantation into diabetic patients.

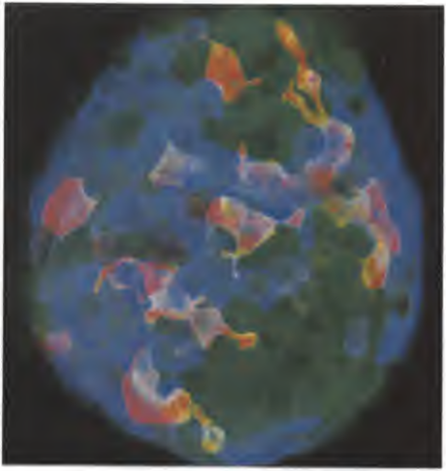

Figure 1-1. Confocal image of fluorescently labeled pancreatic islet of Langerhans. In the image, α-cells are blue, β-cells are green and δ-cells are pink. (Adapted from White, 1995).

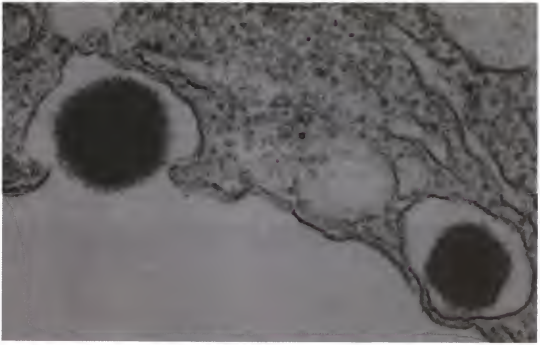

Figure 1-2. Electron micrograph of β-cell secretory vesicles during exocytosis. (Adapted from Orci et al., 1988).

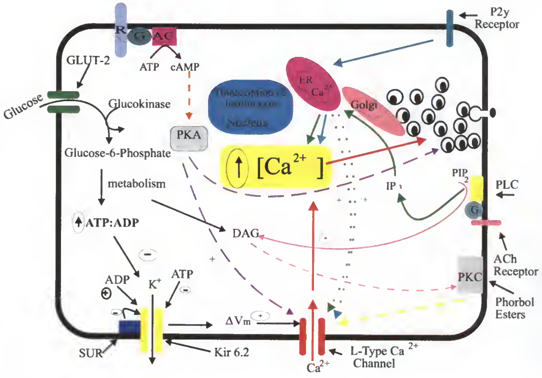

Figure 1-3. Summary of stimulus-secretion coupling pathways in the pancreatic β-cell. Detail description given in text.

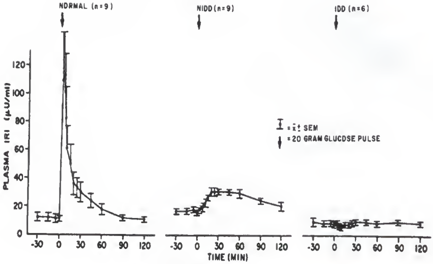

Figure 1-4. Glucose-stimulated insulin response in normal, NIDDM and IDDM patients. (Adapted from Kahn et al., 1997).

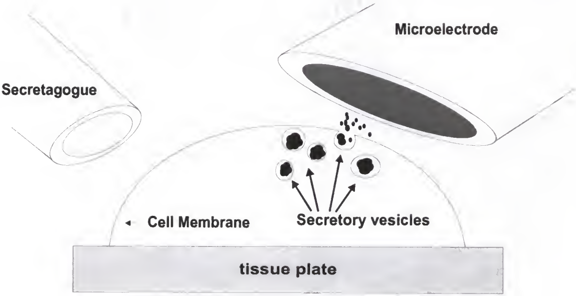

Figure 1-5. Schematic of experimental placement of electrode and stimulant capillary for amperometric detection of exocytosis from single β-cells. Drawing is not to scale.

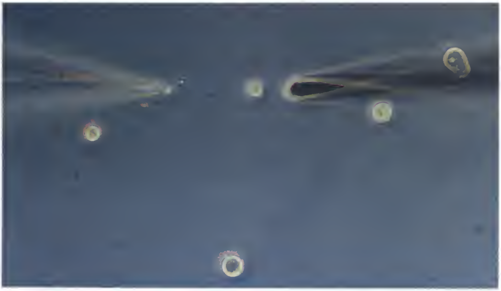

Figure 1-6. Photograph of electrode and pipette placement used for amperometric detection of exocytosis from single β-cells. The electrode, on the right, has an active area of ~ 10 μm diameter as seen by the black surface. The β-cell in the center of the field of view is ~ 9 μm in diameter. The stimulation capillary is shown to the left of the image. The electrode has been moved away from the cell to allow visualization. For amperometric detection of insulin secretion, the electrode would be placed 1 μm immediately above the cell.

CHAPTER 2

AMPEROMETRIC DETECTION OF 5-HYDROXYTRYPTAMINE AS A MARKER OF EXOCYTOSIS FROM SINGLE PANCREATIC BETA CELLS OF DIFFERENT SPECIES

Introduction

Regulated secretion of hormones and neurotransmitters by exocytosis from individual cells is of critical importance for maintenance of physiological activity in higher organisms. The typical secretory vesicle contains between 0.15 and 10 attomoles of material that is released on the millisecond time scale (Chen et al., 1994; Huang et al., 1995; Paras and Kennedy, 1995; Pihel et al., 1996). Amperometry and voltammetry at microelectrodes have recently been demonstrated to possess the sensitivity, as well as the spatial and temporal resolution to detect single exocytosis events (Leszczyszyn et al., 1990; Wightman et al., 1991). These techniques have been successfully applied to quantitative measurement of exocytosis from adrenal chromaffin cells (Leszczyszyn et al., 1990; Wightman et al., 1991; Chow et al., 1992; Ciolkowski et al., 1992), PC12 cells (Chen et al., 1994), mast cells (Tatham et al., 1991; Alvarez de Toledo et al., 1993; Pihel et al., 1996), neurons (Zhou and Misler, 1995), and melanotrophs (Paras and Kennedy, 1995; Paras and Kennedy, 1997). Application of these methods has provided significant new insight into the mechanisms involved in exocytosis and stimulus-secretion coupling (Chow et al., 1992; Alvarez de Toledo et al., 1993; Finnegan and Wightman, 1995; Robinson et al., 1995; Pihel et al., 1996; Borges et al., 1997). In all of these cases, however, the detected species was relatively easy to oxidize and unmodified carbon-fiber microelectrodes could be used for detection.

We have extended this technique to detection of insulin secretion, the primary regulator of glucose homeostasis, from single pancreatic β-cells (Kennedy et al., 1993; Huang et al., 1995; Gorski et al., 1997). For detection of insulin exocytosed from single β-cells, a carbon-fiber electrode chemically modified with ruthenium oxide/cyanoruthenate (Ru-O/CN-Ru) (Kennedy et al., 1993; Huang et al., 1995) or ruthenium oxide (RuOx) (Gorski et al., 1997), catalysts that promote oxidation of insulin, is used. These methods have allowed the first direct and quantitative measurement of insulin release from single β-cells with high temporal resolution (Kennedy et al., 1993; Huang et al., 1995; Gorski et al., 1997). However, experimental issues associated with chemical modification of the microelectrodes to detect insulin have curtailed widespread application of this technique. It may therefore be useful to consider alternative methods for direct detection of exocytosis in the β-cell. Furthermore, it would be useful to establish a marker for secretory activity that would not be affected by the same extracellular chemical events as insulin, therefore serving as a control for investigations of vesicle clearance.

An alternative for detecting secretory activity in β-cells is measurement of a marker compound, i.e. a substance that is co-secreted with insulin. It has been suggested that 5-hydroxytryptamine (5-HT) may serve as a suitable marker for insulin secretion in β-cells (Gylfe, 1978; Smith et al., 1995). A particular advantage of this approach is that 5-HT is easily oxidized at unmodified carbon-fiber microelectrodes, avoiding the need for chemical modification. While native levels of 5-HT present in β-cells are too low to be detected by amperometry (Huang et al., 1995), β-cells will accumulate or "load" 5-HT (or its precursor 5-hydroxytryptophan which is then converted as shown in Figure 2-1), reaching vesicle concentrations approximately 38-fold higher than the extracellular medium (Falck and Hellman, 1963; Hutton et al., 1983). Recently, amperometry has been used to measure accumulated 5-HT released from β-cells of a variety of species (Smith et al., 1995; Willmott et al., 1995; Zhou and Misler, 1996; Kennedy et al., 1996; Aspinwall et al., 1997; Takahashi et al., 1997; Brown et al., 1998; Aspinwall et al., 1999; Takahashi et al., 1999). Application of insulin secretagogues results in detection of 5-HT secretion as a series of current spikes that have many of the characteristics expected of exocytotic release (Smith et al., 1995; Zhou and Misler, 1996). Furthermore, the spikes occur under conditions that are expected to cause insulin secretion. While these studies assume that 5-HT detected is co-released with insulin exclusively, the data do not exclude release from other vesicle populations within the β-cell. Therefore, further characterization of this method is warranted before 5-HT can be confidently used as a marker of insulin secretion.

The primary question which must be addressed is whether 5-HT and insulin are stored and released from the same secretory vesicles, exclusively. Ultrastructural histochemistry, fluorescence microscopy, autoradiography and electron microscopy have provided evidence that accumulated 5-HT is stored in insulin-containing secretory vesicles of the β-cell (Jaim-Etcheverry and Zieher, 1968; Eckholm et al., 1971; Owman et al., 1973; Hellman et al., 1972). Thus, exocytosis should cause release of 5-HT in addition to insulin. Measurements from whole mouse islets (the β-cell containing microorgan) have shown that insulin and accumulated 5-HT are both released following glucose stimulation; however, time-resolved measurements of secretion reveal that the ratio of insulin to 5-HT released changes during stimulation (Gylfe, 1978). Additionally, the stimulation index (ratio of secretion elicited at 20 mM / 3 mM glucose) varies for insulin and 5-HT, which is unexpected if 5-HT and insulin are co-released from the same secretory vesicles by exocytosis (Hellman et al., 1972). Therefore, the data available have not confirmed the reliability of measuring 5-HT as a marker for insulin secretion.

In this work, amperometric detection of insulin and accumulated 5-HT secretion from single pancreatic β-cells of multiple species was compared. The overall goals were to: 1) determine if 5-HT is a valid marker of insulin release, i.e. the two compounds are co-released from the same vesicles exclusively, 2) determine if the species of β-cell affects detection of insulin and 5-HT, and 3) determine optimal conditions and limitations of using 5-HT release as a marker for insulin secretion.

Experimental

Chemicals and Reagents

Type XI collagenase, HEPES, forskolin, muscarine chloride, tolbutamide, 5-hydroxytryptamine·creatine sulfate and 5-hydroxy-*d,l*-tryptophan were obtained from Sigma and used without further purification. Ruthenium chloride and potassium hexacyanoruthenate were from Aldrich and used as received. Fura-2 free acid, fura-2 AM and 4-bromo A23187 were from Molecular Probes. All chemicals for islet and cell culture were obtained from Life Technologies. All other chemicals were from Fisher unless noted and were of highest purity available.

Isolation and *In Vitro* Culture of Mouse β-Cells

Pancreatic islets were isolated from 20-40 g CD-1 mice as described in Appendix A. Briefly, islets were isolated by ductal injection with collagenase type XI and dispersed into single cells by shaking in dilute (0.025%) trypsin/EDTA for 8 minutes at 37° C. Cells were cultured at 37° C, 5% CO_2, pH 7.4 in RPMI 1640 containing 10% fetal bovine serum, 100 U/ml penicillin and 100 μg/ml streptomycin and used on days 2 to 4 following isolation.

Isolation and *In Vitro* Culture of Canine, Porcine, and Human β-Cells

Pancreatic islets were isolated from canine, porcine or human pancreas using controlled collagenase (Boehringer Mannheim) perfusion via the duct, automated dissociation and discontinuous Euro-Ficoll purification using the COBE 2991 blood cell processor as previously described (Ricordi et al., 1988; Warnock et al., 1994a). Islets were cultured overnight at room temperature and dispersed into single cells the following day as described in Appendix A (Huang et al., 1995; Kennedy et al., 1993). Cells were cultured at 37° C, 5% CO_2 in modified CMRL 1066 tissue culture media containing: 10% fetal bovine serum, 26 mM $NaHCO_3$, 25 mM HEPES, 100 U/mL penicillin, and 100 μg/mL streptomycin, pH 7.4.

In vitro Culture of INS-1 Insulin Secreting Tumor Cells

INS-1 cells (Asfari et al., 1992) were graciously provided by Prof. Olof Larsson of the Karolinska Institute. Cells were grown to confluence in tissue culture flasks then trypsinized with 0.025% trypsin/EDTA. A cell suspension was prepared in modified RPMI 1640 media containing 50 μM 2-mercaptoethanol, 10% fetal bovine serum, 25 mM HEPES, 100 U/mL penicillin, 100 μg/mL streptomycin, 2 mM l-glutamine, and 1 mM pyruvate, pH 7.4. Cells were then plated onto 35 mm tissue culture plates and maintained at 37° C, 5% CO_2.

Accumulation of 5-HT into β-cells

For all experiments requiring measurement of 5-HT secretion, dispersed β-cells were allowed to incubate for 16 hours in appropriate tissue culture media containing 0.5 mM 5-HT and 1 mM 5-hydroxytryptophan (5-HTP) at 37° C, 5% CO_2. For some experiments, media contained only 1 mM 5-HT or 0.5 mM 5-HTP where indicated. Cells were used for secretion experiments immediately following 5-HT loading.

Electrode Preparation

Carbon-fiber microelectrodes were constructed as previously described (Kelly and Wightman, 1986; Kawagoe et al., 1993; Huang et al., 1995). A single 9 μm carbon fiber (P-55S, Amoco Performance Products) was aspirated into a filamented glass capillary (0.69 mm i.d. X 1.2 mm o.d. X 4"). The capillary was then pulled on a Narishige PE-2 pipette puller yielding two electrodes. Electrode tips were cut using a scalpel under a dissecting microscope to generate a tip opening of ~ 12-15 μm and the carbon fiber was manipulated to extrude ~ 10 μm from the tip. Cut electrodes were sealed by dipping for 20 s into 3 g of hot epoxy (Epon 828, Miller-Stephenson) containing 0.5 g *m*-phenylenediamine hardener and allowed to cure overnight at room temperature. The following day, electrodes were baked at 100° C for 2 hours then 150° C for 2 hours. Electrodes were then stored at room temperature until use. Prior to use, electrodes were polished for at least 10 minutes on a Sutter BV-10 pipette beveler at an angle of 35° for insulin detection with the Ru-O/CN-Ru modification or 45° for 5-HT detection or insulin detection with the RuOx modification. The electrode was then soaked in electronics grade isopropanol for at least 10 minutes and sonicated in deionized water for 5 minutes immediately prior to use. Electrodes were back filled with mercury to provide electrical connection between the carbon fiber and the current amplifier. This procedure yields electrodes with total tip diameter ~20 µm. For detection of 5-HT, electrodes were used without further treatment immediately following sonication.

For detection of insulin and simultaneous detection of insulin with 5-HT, electrodes were chemically modified as previously described to produce a mixed valent ruthenium oxide/cyanoruthenate (Ru-O/CN-Ru) film (Kennedy et al., 1993) or a ruthenium oxide (RuOx) film (Gorski et al., 1997) as indicated. For preparation of the Ru-O/CN-Ru modified electrode, the potential at the microelectrode was cycled for 25 minutes from 0.46 to 1.06 V vs. sodium saturated calomel electrode (SSCE) at 50 mV/s in a solution of 2 mM $RuCl_3$ and 2 mM $K_2Ru(CN)_6$ dissolved in 0.5 M KCl, pH 2.0. All Ru-O/CN-Ru electrodes were modified in the two-electrode mode using an Ensman EI-400 bipotentiostat and monitored using an oscilloscope. Electrodes were only used if the peak current exceeded 8 nA (typical currents were 10-12 nA). Electrodes were then washed with deionized water and stored in air until use. No more than three electrodes were modified per solution. (Note: Ru-O/CN-Ru modified electrodes may be stored for up to 6 hours and should be discarded if this time is exceeded).

RuOx electrodes were prepared by cycling the electrode potential from –0.85 to 0.65 V vs. SSCE at 100 V/s in 0.20 mM $RuCl_3$ dissolved in 10 mM $HClO_4$ for 15 minutes or until the anodic current reached 3 µA. Electrodes were modified in the 3-electrode configuration with a platinum auxiliary electrode using an Ensman EI-400 bipotentiostat with a modified preamplifier to accommodate the larger current. The microelectrode was connected to the potentiostat *after* initiation of the potential scan. $RuCl_3$ solution was prepared immediately prior to electrode modification and only one electrode was modified per solution. At least 200 ml of $RuCl_3$ solution was prepared for modification to adjust for heterogeneity within the $RuCl_3$. Following modification, RuOx electrodes are stored in deionized water until use. Typically, two electrodes were modified prior to cell experiments. (Note: RuOx electrodes may be stored for at least 1 day prior to loss of activity).

Electrode Testing

Electrode response to 5 μM 5-HT for bare carbon and Ru-O/CN-Ru modified microelectrodes was evaluated by positioning the tip of the electrode approximately 10 μm from a micropipette (30 μm tip diameter) under a KRB solution (see below) on the stage of a microscope. Analyte was pressure ejected from the tip of the pipette at 9 p.s.i. for 5 s while recording the amperometric current. Potential at the working electrode was 0.65 V at bare carbon and 0.85 V at Ru-O/CN-Ru to mimic single cell experiments.

Single Cell Experiments

Single cell measurements were performed similar to those described elsewhere (Huang et al., 1995; Paras and Kennedy, 1995; Wightman et al., 1991; Aspinwall et al., 1997). All amperometric experiments were performed on the stage of a Zeiss Axiovert 100 inverted microscope. Cells were bathed in pH 7.4 Kreb's Ringer Buffer (KRB) containing (in mM): 118 NaCl, 5.4 KCl, 1.2 $MgSO_4$, 2.4 $CaCl_2$, 1.2 KH_2PO_4, 24 $NaHCO_3$ (20 HEPES where indicated), 0.010 forskolin (for canine cells only) (Barnett et al., 1994), and 3.0 *d*-glucose. Prior to single cell experiments, KRB was bubbled with a 5% CO_2/95% air gas mixture for 20 minutes to adjust the buffer pH. Stimulants were prepared in pH adjusted KRB at concentrations indicated. Cells were maintained at 37° C and 5% CO_2 on the stage of the microscope through the use of a microincubator and temperature controller with constant perfusion of 5% CO_2/95% air over the top of the tissue culture plate (Medical Systems, Inc). Amperometry at single β-cells was performed by positioning the sensing tip of the carbon-fiber microelectrode 1 μm from the cell using a piezoelectric micromanipulator (Burleigh PCS-250). Stimulant solutions were applied to individual cells by pressure ejection from a micropipette positioned ~30 μm from the cell using a Narishige MN-153 micromanipulator. Stimulation pipettes were prepared from filamented capillaries (0.58 mm i.d. X 1.0 mm o.d. X 4") and were pulled on a Narishige PE-2 microelectrode puller yielding two pipettes. The tips were hand cut using a scalpel under a dissecting microscope to yield a 5-10 μm diameter opening.

Data Collection

Amperometry was performed using a battery to apply potential to a reference electrode (SSCE) and a current amplifier (Keithley 428 or Axon AI-403) to measure current at the working electrode. For detection of 5-HT with bare carbon microelectrodes and detection of insulin with RuOx modified microelectrodes, the potential at the working electrode was 0.65 V while for detection of insulin the potential at the Ru-O/CN-Ru electrode was 0.85 V. When using the Ru-O/CN-Ru modified electrode, the potential was maintained at 0.40 V between recordings to improve electrode stability as described elsewhere (Kennedy et al., 1993). Data were low pass filtered at 30 Hz, 100 Hz, 300 Hz or 1000 Hz depending on the experiment using an 8-pole Bessel filter (CyberAmp 320, Axon Instruments). For experiments requiring measurement of spike widths, the higher bandwidths were used. For all cases, the data collection rate was at least five times the filter frequency. Data were collected with Axoscope data acquisition software using a personal computer (Gateway 2000 P5-166) via a data acquisition board (Axon DigiData 1200).

$[Ca^{2+}]_i$ Measurements

Measurement of intracellular free calcium $[Ca^{2+}]_i$ was performed as described in Appendix C. Briefly, coverslips containing adherant β-cells were incubated in 2 μM fura-2AM (Molecular Probes) dissolved in KRB at 37° C, 5% CO_2 for 30 minutes. Dye solution was then replaced with KRB and coverslips with adherent cells were placed into a 35 mm coverslip holder for immediate use. Temperature was maintained at 37° C on the stage of a Zeiss Axiovert 100 microscope through use of a microincubator (Medical Systems Corp, Greenvale, NY). Experimental buffers were the same composition used as those for amperometric measurements. The resulting fluorescence from individual cells was collected at 1 Hz through a Fluar 40X oil immersion objective (Zeiss), bandpass filter (510 nm ± 10 nm) and 20 μm pinhole aperture onto a photomultiplier tube using a SPEX CMX cation measurement system and DM3000M data acquisition software (Instruments SA). A two point calibration was performed immediately after experiments as described in Appendix C to allow conversion of ratios to concentration.

Effects of 5-HT on Fura-2 Measurement

For testing the effects of 5-HT on fura-2 ratios *in vitro*, KRB containing 2 mM EGTA, 0 mM Ca^{2+} and 0 μM fura-2 was placed into a tissue culture plate. Solution containing 400 μM free Ca^{2+} buffered with EGTA and 2 μM fura-2 free acid in the presence and absence of 100 μM 5-HT was microinjected into the buffer solution. The fluorescence was collected at 1 Hz through a 20 μm pinhole aperture as for single cell experiments.

Data Analysis

Areas of current spikes were calculated using software provided by Prof. R. M. Wightman (University of North Carolina) as described in Appendix B. For data analysis, spikes were used only if the signal-to-noise ratio was > 10 (3 for detection of insulin from mouse and INS-1 β-cells). For measurements of spike area and spike width, only isolated well-resolved spikes were used. Statistical means were compared using a two-tailed students *t*-test. Results are presented as mean ± 1 standard deviation (s.d.) or mean ± 1 standard error of the mean (SEM) as indicated.

Results

5-HT as a Marker of Insulin Secretion

In order for 5-HT detection to be a valid marker for insulin secretion, it must first be established that 5-HT is released exclusively from insulin containing secretory vesicles. To test the hypothesis that insulin and 5-HT are co-released, we compared results from simultaneous detection of insulin and 5-HT secretion to detection of insulin or 5-HT alone. Figures 2-2 and 2-3 show amperometric recordings obtained from individual canine β-cells stimulated with 17 mM glucose (the primary regulator of insulin secretion *in vivo*) and 200 μM tolbutamide (an oral anti-diabetic), respectively. The data represents recordings made with A) Ru-O/CN-Ru electrode at unloaded cells (measurement of insulin); B) carbon-fiber electrode at 5-HT loaded cells (measurement of 5-HT); and C) recordings with a Ru-O/CN-Ru electrode at 5-HT loaded cells. The latter measurement allows both 5-HT and insulin to be detected simultaneously since the Ru-O/CN-Ru electrode detects both insulin and 5-HT by exhibiting the same sensitivity for 5-HT as the bare carbon microelectrode (Data not shown).

As can be observed by cursory inspection of the traces in Figures 2-2 and 2-3, spikes resulting from detection of 5-HT, insulin or both compounds simultaneously are detected with a similar frequency and temporal distribution which is expected if the two compounds are co-released from the same vesicles. Table 2-1 shows the mean number of current spikes detected per stimulation for insulin, 5-HT and both compounds simultaneously for tolbutamide, muscarine and glucose stimulation. While the only statistically significant difference observed was detection of fewer 5-HT spikes than insulin spikes following tolbutamide stimulation, there is a general trend where the number of 5-HT spikes detected was consistently lower than the number of spikes resulting from detection of insulin or both compounds simultaneously.

Visual inspection of the traces shown in Figures 2-2 and 2-3 reveals that spikes resulting from simultaneous detection of 5-HT and insulin are of larger amplitude than those for insulin or 5-HT alone. Closer analysis of the data confirms these initial observations. Figure 2-4 compares mean spike areas obtained from detection of insulin, 5-HT and both compounds simultaneously following stimulation with muscarine, glucose and tolbutamide, stimulants that elicit exocytosis through different second messenger pathways. In all cases, the area obtained for simultaneous detection of 5-HT and insulin was equal (within experimental error) to the sum of spike areas resulting from detection of 5-HT or insulin alone. The additive area for simultaneous detection of insulin and 5-HT is expected if 5-HT and insulin are exclusively co-released from the same vesicles.

Detection of Insulin and 5-HT from Single β-cells of Multiple Species

The results presented above strongly support the notion that 5-HT and insulin are co-released from canine β-cells; however, given the adequate response of the Ru-O/CN-Ru electrode, there is little advantage to detecting accumulated 5-HT in these cells except as a control for secretory activity in the β-cell. In contrast, in studies of β-cells from other species, we have observed that insulin is much more difficult to detect. This is illustrated in Figure 2-5, which shows detection of insulin current spikes with high frequency and amplitude following stimulation of canine and porcine pancreatic β-cells. Measurement of insulin from mouse β-cells and INS-1 cells (derived from a rodent insulinoma) however, results in detection of current spikes of much lower frequency and amplitude. As the insets demonstrate, spikes resulting from detection of insulin from mouse β-cells and INS-1 cells are much smaller when compared to other species, in many instances being barely distinguished from noise in the baseline. In contrast, measurement of 5-HT consistently generated detectable spikes at β-cells from all species examined as illustrated in Figure 2-6.

Closer analysis is presented in Table 2-2, where the mean area of insulin current spikes and the success rate for detection of insulin are shown to be significantly lower in mouse and INS-1 cells compared to human, canine and porcine β-cells. In contrast, the mean area for 5-HT spikes is only lower for INS-1 cells. In addition to the lower amount of insulin detected per secretory event, a lower frequency of exocytosis events resulting from detection of insulin was also observed in the rodent derived β-cells. The average number of insulin spikes detected per stimulation from canine β-cells was 18 ± 1.4 (Table

2-1) while no more than 2 spikes per stimulation were obtained from comparable stimulation of mouse β-cells (n = 18).

The difficulty of detecting insulin from mouse β-cells can be further illustrated following permeabilization of β-cells with 20 μM digitonin, which leads to entry of calcium followed by massive exocytosis. As shown in Figure 2-7, application of digitonin leads to the detection of current spikes from mouse β-cells that have been allowed to accumulate 5-HT immediately following detection of a large current peak (n = 8 of 8 cells). However, detection of insulin secretion following digitonin treatment did not lead to generation of spikes at either the Ru-O/CN-Ru (0 of 10 cells) or RuOx (0 of 11 cells) modified electrodes, only the large current peak (Figure 2-7 B and C). These results suggest that free insulin monomer is not released at a sufficient concentration to be detected at the electrode following permeablization.

Further analysis of the current spikes obtained from detection of 5-HT and insulin from different species of β-cells reveals additional differences. The mean full width at half-height (FWHH) of insulin and 5-HT spikes is presented in Table 2-3. FWHH is an indicator of the time it takes the secretory product to escape the vesicle, diffuse to the electrode and be detected, hence serving as an indicator of the kinetics of the release event (Schroeder et al., 1992). Significant species variations were observed in the FWHH of spikes resulting from insulin detection while no statistical differences were observed for detection of 5-HT. Additionally, of the 12 current spikes analyzed for insulin detection in mouse β-cells, none possessed a half-width less than 40 ms.

Conditions Affecting 5-HT Detection

The results presented above indicate that 5-HT can serve as a qualitative marker of secretory activity in β-cells, particularly in rodent β-cells where detection of insulin is problematic; however, it is also important to establish whether 5-HT can be used as a quantitative marker of insulin secretion. The area and width of current spikes are commonly used to elucidate quantitative and kinetic data on single vesicle release events (Wightman et al., 1991; Schroeder et al., 1992; Schroeder et al., 1996; Aspinwall et al., 1997). It is therefore necessary to determine if these characteristics are the same (or equally affected) for 5-HT and insulin detection, thus allowing experimental factors that affect the area and kinetics of 5-HT spikes to be directly related to insulin secretion.

There is considerable dependence of loading time and conditions upon 5-HT mean spike area. In rodent β-cells loaded with 1 mM 5-HT, increasing the loading time from 2 to 16 hours leads to a statistically significant increase in 5-HT mean spike area as seen in Table 2-4. Another variable investigated was the composition of the loading solution upon 5-HT mean spike area. As seen in Table 2-4, solutions containing 5-HTP, either with or without 5-HT, result in the largest mean spike area. Based on the data presented in the table, it seems likely that 5-HTP is the major component of the loading solution responsible for vesicular accumulation of 5-HT. Additionally, the maximal concentration of 5-HTP necessary for vesicle loading is 0.5 mM or less, suggesting that equilibrium is reached within the vesicle during the extended loading times. In addition to the loading time and solution composition, slight variations in concentrations of the loading solution or the enantiomeric ratio of 5-hydroxytryptophan lead to differences of 5-HT concentration within the vesicle (data not shown).

While variations in mean 5-HT spike area due to loading conditions can be controlled with reasonable caution, variations in 5-HT accumulation between preparations of β-cells could be more problematic. To investigate this possibility, we compared mean spike areas for detection of 5-HT and insulin in four consecutive canine β-cell preparations. We observed that even under closely controlled loading conditions, the mean 5-HT spike area varied significantly between preparations (Table 2-5); however, the spike area for insulin remained constant, making quantitative comparison of mean spike areas obtained from detection of insulin and 5-HT impossible. Hence, 5-HT cannot be used as a marker for the amount of insulin released during single exocytosis events.

In additional investigations, we compared detection of 5-HT in various biological buffer systems. While bicarbonate is the primary physiological buffer *in vivo*, the use of zwitterionic biological buffers, particularly HEPES, is common in experiments with β-cells. While the buffer composition does not affect the area of 5-HT detected by amperometry (data not shown), it does affect the kinetics of release. As seen in Table 2-6, detection of accumlated 5-HT in 25 mM HCO_3^- buffer results in no significant differences in FWHH at pH 6.4 or 7.4, conditions known to affect FWHH of insulin spikes (Chapter 3, Aspinwall et al., 1997). More interesting however, is the difference obtained at each pH from detection in HCO_3^- or HEPES buffer. Bicarbonate buffer generated spikes that are significantly narrower than those obtained in HEPES at each pH tested ($p < 0.0005$). Therefore, since 5-HT spike widths and areas are affected by a variety of experimental factors, it is unlikely that variations in 5-HT would accurately reflect changes in insulin release.

Effects of 5-HT on $[Ca^{2+}]_i$ Measurement

In an attempt to characterize stimulus-secretion coupling of 5-HT and insulin secretion, and further validate release from the same vesicle pool, we combined intracellular calcium measurements, $[Ca^{2+}]_i$, with amperometric detection of exocytosis in canine β-cells. These techniques are easily coupled because of the non-invasive, non-destructive nature of each. Figure 2-8 shows an example of such an experiment for cells from the same islet preparation. We consistently observed smaller $[Ca^{2+}]_i$ changes following 10 s stimulation with 200 μM tolbutamide for detection of 5-HT compared to insulin but the number of current spikes detected were not statistically different. To further examine this phenomenon we measured the $[Ca^{2+}]_i$ levels in mouse β-cells from the same preparation which were loaded with 0.5 mM 5-HTP compared to unloaded cells. As seen in Figure 2-9 and 2-10, cells loaded with 5-HT exhibited smaller $[Ca^{2+}]_i$ changes upon application of 30 mM K^+ or 10 μM 4-bromo A-23187, a calcium ionophore. The average $[Ca^{2+}]_i$ following application of the ionophore was 710 ± 240 nM (n = 5) for the unloaded cells and 230 ± 140 nM (n = 7) for 5-HTP loaded cells ($p < 0.005$; mean ± s.d.). A further example of the effect of 5-HT on fura-2 binding can be seen in Figure 2-11. When buffer containing fura-2, Ca^{2+} and 5-HT was injected into buffer solution containing only EGTA, the $[Ca^{2+}]$ measured was lower than when the same solution containing no 5-HT was injected. The average $[Ca^{2+}]$ measured was 633 ± 57 nM (n=3) in the presence of 5-HT and 916 ± 175 (n=3) in the absence of 5-HT ($p < 0.01$).

Discussion

Co-release of 5-HT and Insulin

The results presented here provide the most conclusive evidence to date that insulin and 5-HT are co-released from the same secretory vesicles. The additive area for simultaneous detection of insulin and 5-HT strongly suggests that 5-HT is released exclusively from the same vesicles as insulin. Release of 5-HT from a second vesicle population such as the smaller synaptic-like microvesicles (SLMVs) present in the β-cell, would generate detection of some spikes resulting only from oxidation of 5-HT. Assuming a fixed vesicular 5-HT concentration, as implied by the 38 fold increase over the extracellular concentration previously reported (Hutton et al., 1983), SLMVs would contain fewer moles of 5-HT as they are smaller than secretory vesicles. This effect would result in a lower mean spike area for simultaneous detection of insulin and 5-HT than the addition of the individual areas. Further supporting co-release of 5-HT and insulin is the independence of stimulant on mean spike area. This is expected even though different stimulus-secretion coupling pathways are invoked by the stimuli chosen since all produce the same end result, release of product from pre-assembled secretory vesicles. Together, these results strongly suggest the co-release of 5-HT and insulin from the same secretory vesicles and indicate that detection of accumulated 5-HT can serve as a qualitative marker of insulin secretion from the β-cell.

Detection of 5-HT as a Marker for Secretory Activity in Mouse β-cells

While direct detection of insulin at the single cell level is preferred, the results presented here demonstrate that it is not reliable with the available electrodes in mouse β-cells. This may relate to differences in storage of insulin within the secretory vesicle. Insulin is stored within the secretory vesicle as a hexamer bound with 2 zinc ions which dissociates upon exocytosis (Blundell et al., 1972). We have recently shown that an increase in extracellular Zn^{2+} hinders the release of free insulin, the electrochemically detectable form, from the secretory vesicle through a common ion effect (Aspinwall et al., 1997). In mouse and rat β-cells, vesicular zinc levels are 2.4 and 1.5 fold higher, respectively than in canine β-cells (Toroptsev et al., 1974). Thus, it is possible that the zinc-insulin complex released from rodent β-cells dissociates more slowly due to an excess of zinc in the secretory vesicle as indicated by the increased FWHH for insulin spikes generating a lower concentration of free insulin monomer at the cell surface. The result would be fewer spikes generating a concentration above the detection limit, lowering signal-to-noise and leading to detection of fewer and smaller current spikes. Because of the difficulty in detecting insulin, it was impossible to validate the use of 5-HT as a marker for insulin secretion in rodent β-cells.

It was particularly surprising that even the RuOx electrode, which has previously been demonstrated to be ~ 20 times more sensitive to insulin than the Ru-O/CN-Ru electrode (Gorski et al, 1997), is not sensitive enough to detect exocytosis events in the permeabilized mouse β-cells. These results strongly support the hypothesis that the concentration of free insulin in the detection volume defined by the cell and the electrode is not high enough to be detected at either modified electrode following permeablization of mouse β-cells.

Detection of Exocytosis in INS-1 Cells

In this work we also found lower success rates and significantly reduced spike areas from INS-1 cells. The use of tumor cells for studies of insulin secretion is popular because of the ease of culture and the ability to genetically alter the immortalized lines. Therefore, it is important to determine the validity of using amperometry on these lines for future studies of insulin secretion. It has been reported that the insulin content per INS-1 cell is ~ 5 times lower than that of rat and mouse β-cells, although electron microscopy of INS-1 cells has revealed secretory vesicles of similar size to the parental rat β-cells (Asfari et al., 1992). Assuming a similar number of vesicles per cell and an equal distribution of insulin within the vesicle, the mean area obtained per insulin spike from an INS-1 cell should be 5 times lower than that from mouse β-cells. The mean spike area obtained here for detection of insulin is 10 times lower for INS-1 cells, agreeing reasonably well with the prediction. Additionally, while detection of 5-HT generates a signal-to-noise that makes it easily observed, the mean 5-HT area is significantly lower for INS-1 cells compared to all of the other cell types investigated. Several possibilities could explain these observations, including increased pH within the secretory vesicles, higher Zn^{2+} or increased vesicle turnover/recycling.

Taken together, the above data indicate that 5-HT may serve as a suitable marker for secretory activity in a variety of cell types. This is especially true of the rodent β-cell models where detection of accumulated 5-HT consistently generates much higher signal-to-noise and successful stimulation rates compared to insulin detection. The ability to monitor secretion from rodent β-cells is of particular importance because most β-cell and islet studies are conducted on tissue of rodent origin due to availability and the ability to genetically modify strains with relative ease. Additionally, with the increased use of β-cell tumor lines, it is important to develop a method, even one that is indirect, for detecting insulin secretion at the single cell level. Since most of these lines have a lower insulin content than even the INS-1 cells used in this work (Ishihara et al., 1993), it would be impossible to directly detect insulin secretion from single cells thereby hindering stimulus secretion coupling studies.

Limitations to Using 5-HT as a Quantitative Marker of Insulin Secretion

While 5-HT appears to be a useful marker for secretory activity in β-cells, particularly when detection of insulin is not possible, there are several limitations that hinder quantitative comparisons. The most important limitation is the variability of 5-HT accumulation between preparations. Variations in 5-HT accumulation based on time and loading compositions can be avoided by loading for longer times at higher concentrations of 5-HTP so that equilibrium is apparently reached within the vesicle. However, variations in preparations are not easily adjusted.

Additionally, differences in the kinetic parameters of 5-HT and insulin secretion were observed and indicate the need for caution in interpretation of results. As illustrated in the FWHH data from different species, detection of 5-HT secretion led to a consistent spike width across all of the species investigated while detection of insulin resulted in marked differences in spike widths. Furthermore, the effect of extracellular (Aspinwall et al., 1997) and vesicular zinc concentration does not appear to be manifested in the width of the 5-HT spikes, an important difference from insulin secretion. In contrast, the experimental buffer does affect the width of 5-HT spikes detected. Therefore, since the chemical environments that affect FWHH of insulin and 5-HT are quite different, detection of 5-HT does not provide a sufficient marker for the kinetics of insulin extrusion from the vesicle.

Finally, the inability the accurately monitor $[Ca^{2+}]_i$ in 5-HT loaded β-cells severely limits stimulus secretion coupling studies in rodent β-cells and β-cell tumor lines. The nature of the interference between 5-HT and $[Ca^{2+}]_i$ measurement is not immediately apparent but it is not a consequence of less fura-2 accumulating into the cell as the absolute fluorescence for the 340 and 380 nm excitation wavelengths was not significantly different for 5-HT loaded cells compared to unloaded controls (data not shown). Additionally, measurement of basal levels of $[Ca^{2+}]_i$ are unaffected by the presence of 5-HT suggesting the possibility of an interference at the point of calcium entry. This seems unlikely however, as the number of spikes elicited by stimulants dependent upon elevation of $[Ca^{2+}]_i$ is not statistically different for detection of insulin or 5-HT during the simultaneous $[Ca^{2+}]_i$ and amperometry experiments. More likely, 5-HT interferes with the kinetics of fura-2:Ca^{2+} binding and thereby the Stokes shift required for quantitation of rapid $[Ca^{2+}]_i$ changes.

Table 2-1. Comparison of spike frequency resulting from detection of 5-HT, insulin or both insulin and 5-HT under different stimulation conditions from canine β-cells. Data represent the number of current spikes detected per stimulation. Detailed stimulation and analysis conditions given in text. Data presented as mean ± 1 SEM.

Stimulant	**Analyte**		
	Insulin	**5-HT**	**Both**
Tolbutamide	18 ± 1.5 n = 17	12 ± 1.2[a] n = 18	17 ± 2.1 n = 27
Muscarine	23 ± 6.4 n = 8	19 ± 2.0 n = 36	21 ± 2.9 n = 12
Glucose	19 ± 3.6 n = 13	12 ± 1.9 n = 18	19 ± 3.9 n = 12

a Statistically significant difference from the number of spikes per stimulation for insulin ($p < 0.01$)

Table 2-2. Mean spike area and success rates for detection of insulin and accumulated 5-HT from single canine, porcine, human, and mouse pancreatic β-cells and INS-1 cells. Areas were calculated from well-resolved current spikes following stimulation with 30 mM K^+ or 200 μM tolbutamide. Data presented as mean ± s.d.

Species	**Insulin**		**5-HT**	
	Area (pC)	**Success Rate**[a]	**Area (pC)**	**Success Rate**[a]
Canine	0.29 ± 0.20 n = 571	~ 40 %	0.31 ± 0.23 n = 942	~ 40 %
Porcine	0.27 ± 0.18 n = 110	~ 40 %	0.26 ± 0.20 n = 573	~ 40 %
Human	0.29 ± 0.10 n = 216	~ 40 %	0.29 ± 0.20 n = 100	~ 40 %
Mouse	0.20 ± 0.13[b] n = 12	< 10 %	0.27 ± 0.20 n = 505	~ 40 %
INS-1	0.021 ± 0.014[c] n = 24	<10 %	0.15 ± 0.14[d] n=528	~ 40 %

[a] Success Rate is defined as percentage of cells that result in detection of at least 1 current spike following application of stimulant.

[b] Statistically significant difference compared to insulin mean spike area from canine, human, and porcine β-cells ($p < 0.0025$ or lower).

[c] Statistically significant difference compared to insulin mean spike area from mouse, canine, human, and porcine β-cells with ($p < 0.0005$).

[d] Statistically significant difference compared to 5-HT mean spike area from mouse, canine, human, and porcine β-cells ($p < 0.0005$).

Table 2-3. Mean full width half-height (FWHH) for detection of insulin and accumulated 5-HT from single canine and rat pancreatic β-cells. FWHH were calculated from well-resolved current spikes following stimulation with 200 μM tolbutamide. Data presented as mean ± SEM.

Species	**Insulin (ms)**	**5-HT[b] (ms)**
Rat	37 ± 2.9 n = 78	6.0 ± 0.31 n = 98
Canine	30 ± 1.3[a] n = 123	6.1 ± 0.28 n = 345

a Statistically significant difference from FWHH of rat insulin spikes ($p < 0.005$).

b In all cases, spikes resulting from detection of 5-HT were significantly narrower ($p < 0.0005$) that those from insulin detection.

Table 2-4. Effects of loading time and solution composition on 5-HT mean spike area. Data obtained from rodent β-cells. Analysis conditions given in text. Data presented as mean ± s.d.

Loading Solution (Time)	**Spike Area (pC)**
1 mM 5-HT[a] **(2 hours)**	0.031 ± 0.014[c] n = 107
1 mM 5-HT[a] **(16 Hours)**	0.058 ± 0.042[d] n = 142
0.5 mM 5-HT/1 mM 5-HTP[b] **(16 Hours)**	0.27 ± 0.21 n = 505
0.5 mM 5-HTP[b] **(16 Hours)**	0.28 ± 0.21 n = 661

a Data obtained from rat β-cells.

b Data obtained from mouse β-cells.

c Statistically significant difference compared to all 16 hour incubations ($p < 0.0005$).

d Statistically significant difference compared to solutions containing 5-HTP ($p < 0.0005$).

Table 2-5. Difference in mean insulin and 5-HT spike area in 4 consecutive batches of canine β-cells. Areas were calculated from well-resolved current spikes with signal-to-noise greater than 10 following stimulation with 200 μM tolbutamide. Data presented as mean ± s.d.

Batch Number	**Insulin Area (pC)**	**5-HT area (pC)**
1	0.30 ± 0.19 n = 49	0.26 ± 0.19[a] n = 427
2	0.29 ± 0.24 n = 145	0.34 ± 0.25 n = 803
3	0.30 ± 0.23 n = 230	0.33 ± 0.25 n = 503
4	0.31 ± 0.22 n = 84	0.30 ± 0.23[b] n = 250

[a] Statistically significant difference compared to 5-HT mean spike area from batches 2 and 3, ($p < 0.0005$) and from batch 4 ($p < 0.01$).

[b] Statistically significant difference compared to 5-HT mean spike area from batch 2 ($p < 0.025$).

Table 2-6. Effect of buffer composition on mean spike FWHH (ms) for 5-HT detection from canine β-cells. FWHH were calculated from well-resolved current spikes with signal-to-noise greater than 10 following stimulation with 200 μM tolbutamide. Data presented as mean ± SEM.

Buffer	**pH**	
	7.4	**6.4**
20 mM HEPES	$12 \pm 0.9^{a,c}$ n = 90	$14 \pm 0.7^{a,b}$ n = 159
25 mM HCO_3^-	6 ± 0.3 n = 349	5 ± 0.4 n = 139

a Statistically significant difference ($p < 0.0005$) compared to HCO_3^- pH 7.4.

b Statistically significant difference ($p < 0.0005$) compared to HCO_3^- pH 6.4.

c Statistically significant difference ($p < 0.05$) compared to HEPES pH 6.4.

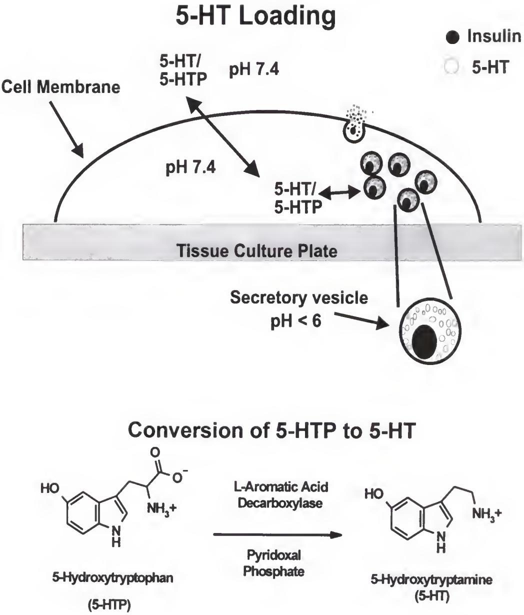

5-HT Loading

Conversion of 5-HTP to 5-HT

Figure 2-1. Loading and conversion of 5-hydroxytryptophan (5-HTP) to 5-hydroxytryptamine (5-HT).

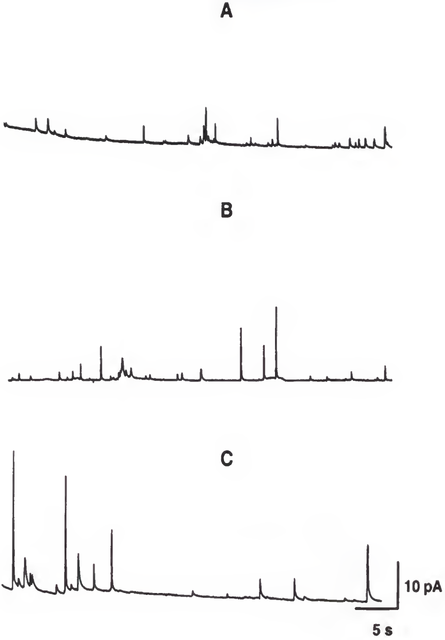

Figure 2-2. Current recordings following stimulation of canine β-cells with 17 mM glucose. Recordings began immediately following 30 s application of stimulant. Detection of A) insulin using Ru-O/CN-Ru modified microelectrode from an unloaded cell, B) accumulated 5-HT using a bare carbon-fiber microelectrode and C) insulin and 5-HT using a Ru-O/CN-Ru electrode. Recordings are from different cells.

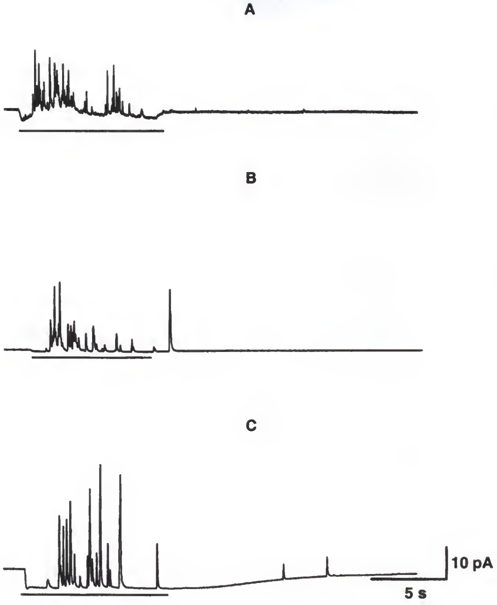

Figure 2-3. Current recordings of canine β-cells stimulated with 200 μM tolbutamide. Detection of A) insulin using Ru-O/CN-Ru modified microelectrode from an unloaded cell, B) accumulated 5-HT using a bare carbon-fiber microelectrode and C) insulin and 5-HT using a Ru-O/CN-Ru electrode. Recordings are from different cells. Bars underneath current traces represent application of stimulant.

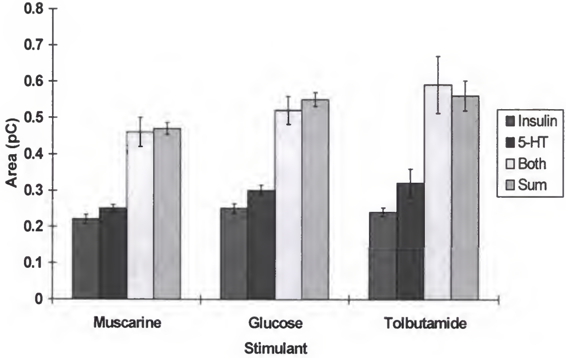

Figure 2-4. Mean spike areas from stimulation of canine β-cells with 20 μM muscarine, 17 mM glucose or 200 μM tolbutamide. Bars labeled insulin were obtained using Ru-O/CN-Ru modified microelectrode from an unloaded β-cell. Bars labeled 5-HT are detection of accumulated 5-HT using a bare carbon-fiber microelectrode. Bars labeled both are simultaneous detection of insulin and 5-HT using a Ru-O/CN-Ru electrode. Bars labeled sum are the addition of insulin and 5-HT areas for a given stimulant. Data presented as mean ± SEM. In all cases detection of both compounds simultaneously was statistically different from detection of insulin or 5-HT alone ($p < 0.0005$).

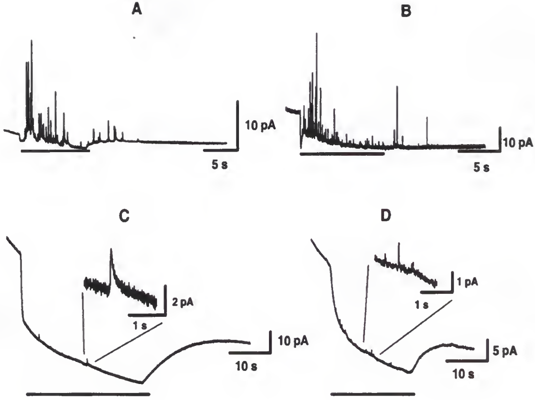

Figure 2-5. Detection of insulin secretion from single pancreatic β-cell of different species. Detection of insulin with Ru-O/CN-Ru electrode from A) canine β-cells stimulated with 200 μM tolbutamide, B) porcine β-cells stimulated with 200 μM tolbutamide, C) mouse β-cells stimulated with 30 mM K^+ and D) INS-1 cells stimulated with 30 mM K^+. Insets in C) and D) are individual spikes from their respective traces. Bars under traces represent application of stimulant.

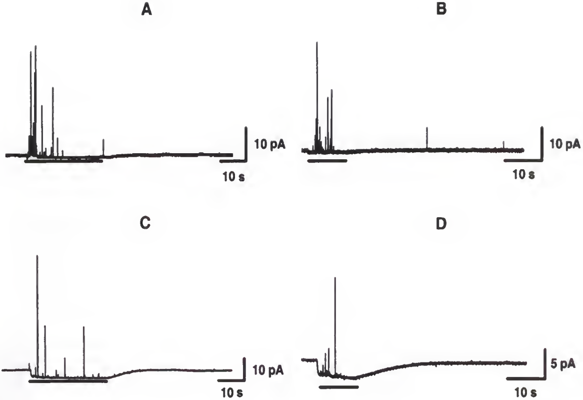

Figure 2-6. Detection of accumulated 5-HT secretion from single pancreatic β-cells of different species. Detection of 5-HT with bare carbon electrode from A) canine β-cells stimulated with 200 μM tolbutamide, B) porcine β-cells stimulated with 200 μM tolbutamide, C) mouse β-cells stimulated with 30 mM K^+ and D) INS-1 cells stimulated with 30 mM K^+. Bars under traces represent application of stimulant.

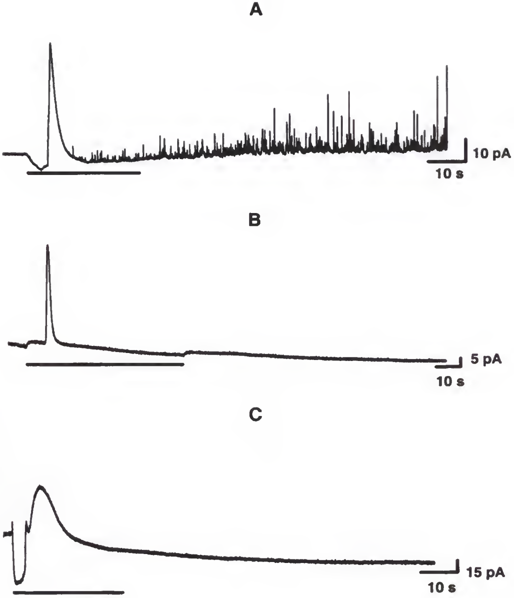

Figure 2-7. Detection of exocytosis from single mouse β-cells permeabilized with 20 μM digitonin. Detection of A) 5-HT with bare carbon electrode, B) insulin with Ru-O/CN-Ru modified electrode and C) insulin with RuOx modified microelectrode. Bars under current trace represent application of digitonin. Recordings are from different cells.

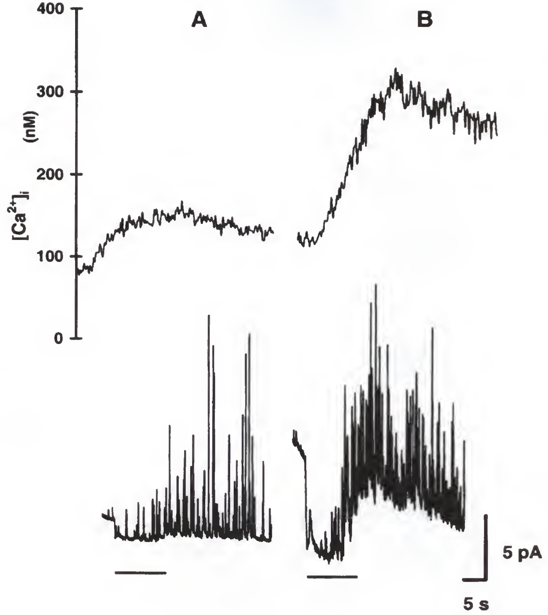

Figure 2-8. Simultaneous detection of $[Ca^{2+}]_i$ and exocytosis from single β-cells upon application of 200 μM tolbutamide. Current traces are amperometric detection of A) 5-HT and B) insulin. Traces representative of 10 and 6 cells for A) and B), respectively. Bars under traces represent application of stimulant. Recordings are from different cells.

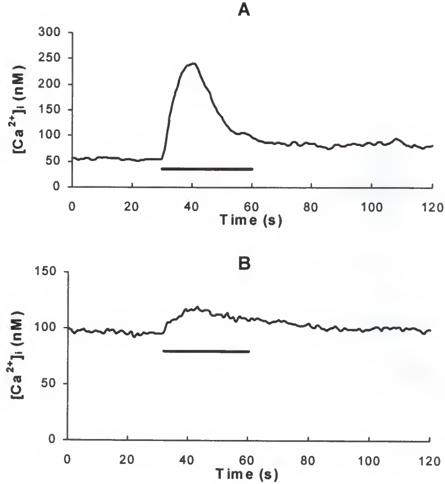

Figure 2-9. Detection of $[Ca^{2+}]_i$ from single β-cells upon application of 30 mM K^+. Representative $[Ca^{2+}]_i$ measurements from single β-cells cultured overnight in A) absence and B) presence of 5-HTP. Traces representative of 7 and 5 cells for A) and B), respectively. Bars under traces represent application of stimulant. Recordings are from different cells.

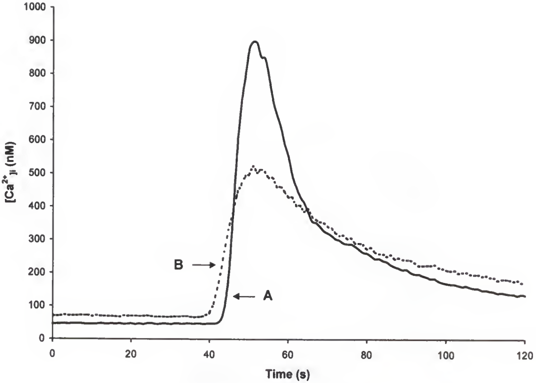

Figure 2-10. Detection of $[Ca^{2+}]_i$ from single β-cells upon application of Ca^{2+} ionophore. Representative $[Ca^{2+}]_i$ measurements from single β-cells cultured overnight in the absence (A) and presence (B) of 5-HTP. Recordings represent data obtained upon 10 s application of 4-bromo A-23187, a non-fluorescent calcium ionophore. Recordings are from different cells.

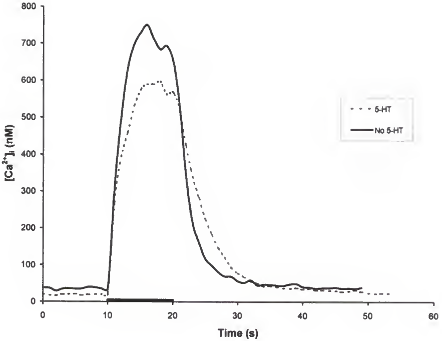

Figure 2-11. Effects of 5-HT on detection of Ca^{2+} by fura-2 microfluorimetry. Traces obtained by microinjection of Ca^{2+} and fura-2 in the A) presence and B) absence of 100 mM 5-HT as described in the text. Each trace is representative of 3 separate experiments. Bars under current trace represent injection.

CHAPTER 3
EFFECTS OF INTRAVESICULAR H^+ AND EXTRACELLULAR H^+ AND ZN^{2+} ON INSULIN SECRETION IN PANCREATIC BETA-CELLS

Introduction

Insulin is synthesized and stored in pancreatic β-cells prior to release by exocytosis in response to external stimuli. A greater understanding of exocytosis of insulin from the β-cell is of intense interest because of the possible role of defective insulin secretion in Type II diabetes (Unger, 1991; Rajan et al., 1990). Secretion by exocytosis can be considered to occur in several distinct steps including vesicle docking, vesicle priming, vesicle fusion, and finally extrusion or clearance of the vesicular contents into the extracellular medium (Zimmerberg, 1987). In this work, we examine the post-fusion clearance of insulin from β-cell secretory vesicles during exocytosis.

Clearance of insulin from secretory vesicles is intimately related to the storage of insulin within the vesicle. Insulin is generally accepted to be stored inside secretory vesicles as a solid hexamer bound with two Zn^{2+} ions per hexamer (Gold and Grodsky, 1984; Blundell et al., 1972; Emdin et al., 1980). This belief is supported by a broad spectrum of evidence. For example, it is known that in the presence of Zn^{2+}, insulin will form tetramers and hexamers that bind Zn^{2+} in an insulin:Zn^{2+} ratio of 4:1 and 6:2, respectively (Blundell et al., 1972). X-ray microprobe studies have revealed that insulin containing secretory vesicles also contain Zn^{2+} in a 1-1.5 fold excess necessary to form

Zn^{2+}-insulin hexamer (Foster et al., 1993). Furthermore, Zn^{2+}-insulin hexamers are insoluble below pH 7 (Blundell et al., 1972; Emdin et al., 1980; Tanford and Epstein, 1954; Epand et al., 1985) and β-cell secretory vesicles possess a V-type H^+-ATPase that maintains the vesicle interior at or below pH 6 (Orci et al., 1986; Hutton, 1982). Electron microscopy and immunohistology also suggest the presence of solid insulin inside vesicles (Orci, 1985; Coore et al., 1969).

Figure 3-1 shows an electron micrograph of a stimulated β-cell. Clearly visible are the secretory granules, some of which contain a dense core that has been shown to be the Zn^{2+}-insulin complex (Orci et al., 1986). During exocytosis, secretory vesicles fuse with the plasma membrane exposing the vesicular interior to the extracellular milieu, allowing release of stored insulin granules. Under normal circumstances, insulin must dissolve in order to escape the vesicle. In addition, insulin must dissociate from the Zn^{2+} complex since insulin monomer is the biologically active form (Berson and Yalow, 1966; Helmerhorst and Stokes, 1986). It is interesting that the intact granule appears to have escaped from the vesicle in Figure 3-1, in contrast to most electron micrographs of exocytosis in the β-cell, such as the one in Chapter 1. Little is known about the mechanism or time scale of dissolution and dissociation of the granule, although one study has demonstrated that insulin is free from Zn^{2+} within 60 s of release (Gold and Grodsky, 1984). Additional investigation of this phenomenon has been hindered by the lack of methods for monitoring insulin secretion with sufficient temporal resolution to observe such effects.

Recently, amperometry with microelectrodes has been applied to the study of exocytosis at a variety of cell types including adrenal chromaffin cells (Chow et al., 1992;

Ciolkowski et al., 1992; Leszczyszyn et al., 1990; Wightman et al., 1991), PC12 cells (Chen et al., 1994), mast cells (Alvarez de Toledo et al., 1993), neurons (Zhou and Misler, 1995), and melanotrophs (Paras and Kennedy, 1995; Paras and Kennedy, 1997). Secretion is detected as a series of current spikes that correspond to detection of concentration pulses generated by exocytosis. Analysis of current spikes can reveal subtle details about the secretory process. The area of current spikes, which is in units of coulombs, can be used to quantitate the moles of detected hormone (or transmitter) released per vesicle fusion event using Faraday's Law (Wightman et al., 1991). The dynamics of vesicular release are reflected in the shape of current spikes. Specifically, the width of spikes can be used as a measure of the rate of clearance from the vesicle since the width is determined by any slow kinetic step involved in clearing hormone from the vesicle and diffusional broadening of the secreted packet of molecules (Jankowski et al., 1994; Jankowski et al., 1993; Borges et al., 1997; Walker et al., 1996). Thus, the exquisite temporal resolution and sensitivity of amperometry for measuring actual secretory products has made it well-suited for probing post-fusion events in exocytosis (Jankowski et al., 1994; Jankowski et al., 1993; Borges et al., 1997; Fernadez-Chacon and de Toledo, 1995; Oberhauser et al., 1996).

We have extended amperometry to detection of insulin exocytosed from pancreatic β-cells (Huang et al., 1995; Kennedy et al., 1993). For this application, a carbon-fiber electrode modified with ruthenium oxide/cyanoruthenate (Ru-O/CN-Ru), a catalyst that promotes oxidation of insulin, is used for detection. This method has allowed the first direct measurement of exocytosis of insulin from single β-cells with high temporal resolution (Kennedy et al., 1993). In using amperometry to study post-fusion events in insulin release, we have found it useful to measure 5-HT release as a control. 5-HT can be "loaded" into β-cells by incubating the cells in media containing 5-HT and/or 5-HTP. Substantial evidence now exists that demonstrates that 5-HT is loaded primarily into β-cell secretory vesicles and that 5-HT is co-secreted with insulin by exocytosis (Chapter 2). 5-HT can be detected at bare carbon electrodes and insulin can be detected only at Ru-O/CN-Ru modified electrodes. Thus, it is possible to measure, in separate experiments, secretion of 5-HT from loaded cells and secretion of insulin from cells which have not been allowed to accumulate 5-HT.

In an initial study on post-fusion clearance of insulin, we found that exposure to a pH gradient between the vesicle and the extracellular environment is required to achieve rapid release of free insulin from solid Zn^{2+}-insulin granules (Kennedy et al., 1996). In the present work, we have extended this investigation to a variety of extracellular pH's. In addition, we examine the effect of intravesicular pH and extracellular Zn^{2+} on insulin secretion. The study reveals strong effects of the extracellular and intravesicular environments on the rate and amount of free insulin released during exocytosis.

Experimental

Chemicals and Reagents

Bafilomycin A_1, *n*-ethylmaleimide, forskolin and tolbutamide were obtained from Sigma and used without further purification. Ruthenium chloride and potassium hexacyanoruthenate were from Aldrich and used as received. All chemicals for islet and cell culture were obtained from Life Technologies. All other chemicals were from Fisher unless noted and were of highest purity available.

Isolation of Canine Islets and *In Vitro* Culture

Pancreatic islets were isolated from mongrel dogs using controlled collagenase (Boehringer Mannheim) perfusion via the duct as previously described (Ricordi et al., 1988; Warnock et al., 1994a). Following isolation, groups of islets were placed in modified CMRL 1066 tissue culture solution (G-100) containing: 10% Fetal calf serum, 25 mM HEPES, 100 U/mL penicillin, and 100 μg/mL streptomycin and cultured at room temperature overnight. The following day, islets were dispersed into single cells according to the procedure described in Appendix A. Cells were plated onto tissue culture dishes (Corning) and incubated at 37° C, 5% CO_2 in G-100, pH 7.4.

Accumulation of 5-Hydroxytryptamine into β-Cells

For experiments requiring measurement of 5-HT secretion, dispersed β-cells were allowed to incubate in G-100 containing 0.5 mM 5-HT and 1 mM 5-hydroxytryptophan for 16 hours at 37° C, 5% CO_2. Cells were used for secretion experiments immediately after loading.

Electrode Preparation and Testing

Carbon fiber microelectrodes were constructed as previously described (Chapter 2; Kawagoe et al., 1993; Kelly and Wightman, 1986). Finished electrodes consisted of a 9 μm carbon fiber (P-55S, Amoco Performance Products) sealed with epoxy (Miller Stephenson, Danbury CT) in the tip of a glass pipette. The total electrode diameter at the tip was ~30 μm and the electrode was polished at a 30-45° angle using a pipette beveler (Sutter Instruments, BV-10). For detection of insulin, electrodes were chemically modified as previously described to produce a mixed valent Ru-O/CN-Ru film (Chapter 2; Kennedy et al., 1993) while 5-HT detection was performed with bare carbon fiber microelectrodes (Chapter 2; Aspinwall et al., 1997). Tests of the electrode response to insulin and 5-HT were performed by positioning the tips of electrode approximately 10 μm from micropipette tips (30 μm outer diameter) under a KRB solution on the stage of a microscope. Solutions were pressure ejected from the tips of the pipettes at 9 p.s.i. for 5 s while recording the amperometric current.

Single Cell Experiments

Single cell measurements were performed similar to those described elsewhere (Chapter 2; Wightman et al., 1991; Paras and Kennedy, 1995; Huang et al., 1995). All amperometric experiments were performed on the stage of a Zeiss Axiovert 100 inverted microscope. Cells were bathed in pH 7.4 Kreb's Ringer Buffer (KRB) containing (in mM): 118 NaCl, 5.4 KCl, 2.4 $CaCl_2$, 1.2 $MgSO_4$, 1.2 KH_2PO_4, 25 $NaHCO_3$, 0.010 forskolin (Barnett et al., 1994), and 3.0 *d*-glucose and maintained at 37° C and 5% CO_2 on the stage of the microscope by a microincubator (Medical Systems, Inc.). Buffer pH was adjusted by varying bicarbonate concentration to achieve the desired pH after bubbling with 5% CO_2. Extracellular Zn^{2+} concentration was adjusted by adding $ZnCl_2$ to the desired concentration. Ionic strength was held constant for all solutions. When appropriate, cells were incubated in G-100 containing either 50 μM *n*-ethylmaleimide or 1 μM Bafilomycin A_1 for 30 minutes prior to experiments. Amperometry was performed at isolated single cells by positioning the sensing tip of the microelectrode 1 μm from the cell using a micromanipulator (Burleigh PCS-250). Stimulant solution (200 μM tolbutamide in bicarbonate buffer) was applied to individual cells by pressure ejection for 10 s from a micropipette positioned ~30 μm from the cell.

Data Collection and Analysis

Amperometry was performed using a battery to apply potential to a sodium saturated calomel electrode (SSCE). Currents were monitored at the working electrode using an AI-403 current amplifier and Cyberamp 320 signal conditioner (Axon, Foster City, CA). For detection of 5-HT the potential at the working electrode was 0.65 V while for detection of insulin the potential was 0.85 V. All voltages are versus SSCE. When using the modified electrode, the potential was held at 0.40 V between recordings to improve electrode stability as described elsewhere (Kennedy et al., 1993). Data were low pass filtered at 300 Hz for insulin measurements and 1000 Hz for 5-HT. These filter settings were found to not affect the peak widths relative to higher settings. Data was collected at a rate which was three to five times the filter frequency using a personal computer (Gateway 2000 P5-166) via a data acquisition board (Axon, DigiData 1200B). The area and half-width of current spikes were calculated using software provided by Prof. R. Mark Wightman (University of North Carolina). For data analysis, spikes were used only if the signal-to-noise ratio was greater than 10. All means are reported ± 1 standard error of the mean. Statistical differences between means were evaluated using a two-tailed Student's *t*-test.

Simulation of Spike Shape

A random-walk model was used to simulate diffusion-limited current spikes obtained from exocytosis as demonstrated in Figure 3-2 (Schroeder et al., 1992). In the model, the cell was considered a hemisphere with 5 μm radius and the electrode was centered directly over the apex of the cell with a 1.0 μm gap between the cell and electrode. An exocytosis event was modeled as a point source of 50,000 molecules diffusing from a location on the cell surface to the electrode. Thus, exocytosis events originating at the base of the cell travel farther to the electrode than exocytosis events originating at the apex of the cell where the distance to the electrode is minimized. Molecules encountering the electrode were counted as detected and removed from the system. Molecules encountering the cell membrane or the insulating portions of the electrode were reflected back to their previous position. The simulation was ended when all molecules were detected or after 3,000 steps had been made in the walk. Longer random walks did not affect the results. For the model, 5-HT was considered to have a diffusion coefficient of 6.0 x 10^{-6} cm^2/s and insulin 2.0 x 10^{-6} cm^2/s (Huang et al., 1995).

Results

Effect of Zn^{2+} on Insulin Detection

We have previously used the Ru-O/CN-Ru electrode to detect insulin and insulin secretion (Huang et al., 1995; Kennedy et al., 1993). An issue that has not been addressed, but which is important in the interpretation of this data, is the effect of Zn^{2+} complexation on insulin detection. Figure 3-3 illustrates current recorded during injection of KRB solutions that contained either A) 30 μM insulin or B) 30 μM insulin with 15 μM added Zn^{2+}, which promotes the formation of Zn^{2+}-insulin complexes (Blundell et al., 1972). As the data show, addition of Zn^{2+} abolishes the signal obtained from detection of insulin. The presence of Zn^{2+} does not affect the detection of other, non-Zn^{2+} binding compounds such as 5-HT (Figure 3-3). These results strongly suggest that the electrode detects only free insulin and not insulin complexed with Zn^{2+}.

Analysis of Spike Width and Shape

Figure 3-4 compares high-resolution recordings of spikes obtained from detection of insulin and 5-HT. Several differences in spike shape were observed following detection of 5-HT and insulin. The most marked difference in shape of the current spikes was that the average width at half height (FWHH) of 5-HT spikes was 5.3 ± 0.4 ms which is significantly lower ($p < 0.0005$) than the 30 ± 2.1 ms obtained for insulin spikes. As previously mentioned, the width at half-height of a current spike is a measure of the average time required for detected material to extrude from a vesicle, diffuse to the electrode and be detected. Thus, some of the difference in width could be attributed to the difference in diffusion coefficient for 5-HT and insulin. The random walk model, which predicts widths based solely on diffusion, indicates that spikes obtained from detection of insulin should be 3 times wider than those from detection of 5-HT, yet we observed a 6-fold difference. As summarized in Table 3-1, the model also predicts that the widest diffusion-limited spikes, which would occur for a release site that is the maximum possible distance from the electrode, would be 22 ms for 5-HT and 58 ms for insulin. Experimentally, we found that none of the 5-HT spikes were broader than this maximum value. In contrast, 10% of the insulin spikes were over the maximum diffusion-limited width. Also striking is the percentage of insulin and 5-HT spikes that fall between the limits predicted for 1-3.5 μm from the electrode. Within this range, 78% of 5-HT spikes but only 35% of insulin spikes are observed. This distance is most likely the best indicator of physiological conditions to compare the data as β-cells tend to "flatten" out when plated onto tissue dishes making it rare to observe a truly hemispherical cell. Taken together, these results indicate that: 1) release of 5-HT is indistinguishable from diffusion control, and 2) a factor other than diffusion contributes to slowed dynamics of insulin release.

Another difference in shape was that 14% of the 5-HT spikes had a small current increase or "foot" prior to the rapid increase to the spike apex as shown in Figure 3-4C. In contrast, such features were not observed on spikes due to detection of insulin at physiological pH. Pre-spike features like those seen in Figure 3-4 for 5-HT detection have also been observed in the detection of catecholamine release from adrenal chromaffin cells (Chow et al., 1992; Jankowski et al., 1993) and 5-HT release from mast cells (Alvarez de Toledo et al., 1993). This shape has been attributed to leakage of material from a fusion pore which forms between the secretory vesicle and the plasma membrane prior to complete opening of the secretory vesicle (Alvarez de Toledo et al., 1993; Chow et al., 1992; Jankowski et al., 1993). The lack of a foot for detection of insulin suggests that insulin does not leak from a fusion pore at a fast enough rate to generate quantities of free insulin that are detectable at the electrode.

Effects of Extracellular pH on Insulin Extrusion

To evaluate the effect of extracellular pH on exocytosis, single cell recordings of insulin secretion were made following tolbutamide stimulation when the extracellular pH was 6.40, 6.90, 7.05, 7.20, 7.40 and 7.90. Similar experiments were performed for detection of 5-HT secretion from loaded cells at pH 6.40, 7.10 and 7.40. Figure 3-5 summarizes the spike widths and areas that were recorded in these different experiments. As described earlier, the area of isolated current spikes is considered a direct measure of the amount of product (insulin or 5-HT in this case) detected due to release from a single secretory vesicle (Wightman et al., 1991, Huang et al., 1995). Spike area for insulin detection is not significantly affected by increasing extracellular pH above 6.9 as seen in Figure 3-5; however, in agreement with previous results (Kennedy et al., 1996), no spikes were detected at pH 6.4. In contrast, the width at half-height of spikes decreased with increasing pH for insulin detection. The constant area combined with decreasing width caused an increase in amplitude with increasing pH for spikes resulting from insulin detection. This resulted in an increase in the S/N ratio, thereby increasing the number of insulin spikes detected per stimulation (Figure 3-6). In contrast, the area and width at half-height for 5-HT current spike detection was unaffected at any pH tested as demonstrated in Figure 3-5.

Effects of Intravesicular pH on Insulin and 5-HT Extrusion

Effects of the vesicular proton pump activity and thereby vesicular pH on insulin and 5-HT secretion, were investigated using Bafilomycin A_1 and *n*-ethylmaleimide. Both compounds are known to inhibit V-type H^+-ATPase activity and thereby elevate vesicular pH until it is in equilibrium with cytoplasmic pH (Bowman et al., 1988; Yoshimori et al., 1991). Figure 3-7 compares typical current traces recorded at untreated cells, and cells incubated with 1 μM Bafilomycin A_1 or 50 μM *n*-ethylmaleimide. As observed from an inspection of these plots, the number of spikes per stimulation, duration of secretory activity and area of the spikes are not significantly different for either of these treatments.

Although overall secretory activity for insulin was unaffected by inhibition of the V-type H^+-ATPase, insulin spike shape was affected as illustrated and summarized in Figure 3-8. The spike width was significantly decreased ($p < 0.001$) by treatment with both agents. Furthermore, after treatment with Bafilomycin A_1, 10% of the detected spikes exhibited a foot and after treatment with *n*-ethylmaleimide 18% of spikes possessed this feature. Spike samples shown in Figure 3-8 are typical of those that possessed a foot. As stated above, no spikes obtained from untreated cells had such pre-spike features. In contrast, the spike width for 5-HT summarized in Figure 3-8D was unaffected by either treatment and there was no effect on the percentage 5-HT spikes displaying feet.

Effects of Extracellular Zn^{2+} Concentration on Insulin and 5-HT Extrusion

In addition to the effects of pH, the effects of 0, 5, 15, and 25 μM extracellular Zn^{2+} on secretion measurements were examined. Figure 3-9 illustrates typical secretion measurements of insulin and 5-HT under these different conditions. As extracellular Zn^{2+} concentration increases, the area of insulin spikes decreases while the half-width increases as summarized in Figure 3-10. These combined effects cause spike amplitudes to decrease and result in detection of smaller numbers of spikes as observed in Figure 3-9. The smaller number of spikes is presumed to result from fewer vesicles liberating a concentration of free insulin above the noise level resulting in fewer spikes of decreased amplitude. This effect is maximized at 25 μM Zn^{2+} where no insulin spikes are detected (data not shown). In contrast, when measuring 5-HT release, the area and half-width of the spikes are not significantly different at any given Zn^{2+} concentration (see Figures 3-9 and 3-10).

Discussion

Dynamics of Exocytosis Events

Although 5-HT is released simultaneously with insulin (Chapter 2), it escapes from the vesicle at a significantly higher rate as evidenced by the narrower spikes and the presence of feet, both of which suggest leakage out of vesicles during fusion pore formation. 5-HT release is indistinguishable from simple diffusion from the vesicle while insulin release is slower suggesting that a factor other than diffusion controls post-fusion release. These results may be explained by considering differences in storage of the two secretory products. While the exact form that 5-HT is stored within the vesicles is unknown, it is reasonable to expect that it is stored in solution since 5-HT is soluble at the vesicular pH. In contrast, insulin is stored as a solid complex of Zn^{2+}-insulin (Gold and Grodsky, 1984; Blundell et al., 1972; Orci, 1985). In addition, the electrode only detects free insulin and not Zn^{2+}-bound insulin as illustrated by Figure 3-3. Therefore, it seems likely from these considerations that the dissolution and dissociation of Zn^{2+}-insulin complex controls the rate of insulin extrusion during exocytosis.

Effects of Extracellular and Intravesicular pH

In initial work, we demonstrated that a change in extracellular pH from 7.4 to 6.4 could hinder insulin clearance to such an extent as to make it undetectable by amperometry while having no effect on 5-HT secretion (Kennedy et al., 1996). The data in Figure 3-5, obtained over a wider pH range, show that decreasing extracellular pH from 7.9 to 6.9 increases the time required for insulin clearance (increasing spike width), but does not affect the amount of insulin released during an exocytosis event (no change in area). Furthermore, increasing extracellular pH increases the rate of extrusion resulting in detection of more current spikes at the electrode (Figure 3-6). In contrast, 5-HT secretion is unaffected in this pH range as seen in Figure 3-5 proving that this effect is specific to insulin extrusion and is not an effect on vesicular fusion.

Further investigation has revealed that increasing vesicular pH with V-type H^+-ATPase inhibitors, which is expected to change the storage conditions for insulin, causes insulin to be more rapidly extruded (narrower spikes) and even leak out of fusion pores (presence of feet). This effect suggests that some dissolution of the insulin granule occurs within the vesicle when the vesicular pH has been raised. Therefore, under normal conditions, low pH inside the vesicle maintains the Zn^{2+}-insulin complex in a solid state that does not escape as readily during fusion pore formation or vesicle fusion. These results further emphasize the importance of the pH gradient between the vesicle and extracellular media in rapidly changing insulin from a solid, storage state to a dissolved, releasable form. These results also highlight the difference between post-fusion release of other hormones and insulin. For example, in catecholamine release from adrenal chromaffin cells, increasing the pH has the effect of increasing the time course of post-fusion extrusion (Jankowski et al., 1993). Furthermore, the effects of pH on catecholamine release are not nearly as dramatic as what was observed here. These differences can be attributed to differences in storage of the compounds. In the catecholamine case, release requires the expansion of a protein gel that encapsulates the catecholamine while extrusion of free, biologically active insulin requires dissolution of a solid-state hormone complex (Jankowski et al., 1993).

Effect of Zn^{2+} on Insulin Extrusion

In addition to dissolving, the insulin-Zn^{2+} complex must ultimately dissociate after vesicle fusion since the biologically active form of insulin is monomer (Berson and Yalow, 1966; Helmerhorst and Stokes, 1986). We have postulated that availability of extracellular Zn^{2+} may affect release of free insulin from β-cells through a common-ion effect. Extracellular Zn^{2+} concentrations in the range of 5-25 μM markedly decreased area and increased width of insulin spikes without affecting detection of 5-HT spikes. The lack of an effect on 5-HT detection demonstrates that the effect is specific to extrusion from the vesicle and not earlier steps in exocytosis. Unlike pH manipulations, extracellular Zn^{2+} not only increased the time course of release of free insulin, but also decreased the amount of free insulin detected from an exocytosis event. Decreases in amount of free insulin detected occurred even though half-widths of detected spikes suggest that a release event is occurring at a rate which is fast enough to yield a detectable spike. A possible explanation for this result is that after vesicle fusion, the Zn^{2+}-insulin hexamer dissolves, but does not dissociate because of the high extracellular Zn^{2+} concentration, allowing most of the insulin to escape from the detection area in the undetectable Zn^{2+}-insulin complex form (Figure 3-3). Interestingly, the effects of Zn^{2+} on insulin secretion are similar to those observed for catecholamine secretion from adrenal chromaffin cells (Pihel et al., 1996). Although Zn^{2+} decreased the quanta in both cases, the chemical mechanisms are markedly different. Rather than a common ion effect on hormone complex, the Zn^{2+} effect on catecholamine secretion was due to the ability of Zn^{2+} to cross-link the protein matrix in chromaffin secretory vesicles hindering escape of catecholamines (Pihel et al., 1996).

The results presented here demonstrate that micromolar Zn^{2+} concentrations can affect free insulin concentration in the immediate vicinity of a β-cell during secretion. The possible physiological significance of the Zn^{2+} effect is not clear since the actual concentration of Zn^{2+} in the interstitial space of an islet is not known; however, Zn^{2+} concentration in serum is approximately 15-25 μM (Hurley, 1969; Chen et al., 1995;

Zalewski et al., 1993; Bonner et al., 1979). It has previously been demonstrated that *in vivo* insulin is available as free monomer within a few seconds of entering the portal vein, presumably because the large dilution of insulin drives dissociation (Gold and Grodsky, 1984). Therefore, it seems unlikely that extracellular Zn^{2+} could affect the endocrine function of free insulin.

Regulation of Insulin Extrusion during Exocytosis

Our observations show that free insulin concentrations in the vicinity of β-cells are affected by the intravesicular pH and extracellular pH and Zn^{2+} concentration. Figure 3-11 presents a summary of the processes involved in regulating concentration of free insulin at the surface of the β-cell. These results have been interpreted as effects on the rate of dissolution and dissociation of Zn^{2+}-insulin hexamers during exocytosis. This interpretation ignores the possible role of vesicle matrix proteins, such as chromagranin, in storing and extruding free insulin. In adrenal chromaffin cells and mast cells, glycoproteins like chromagranin in the vesicle matrix have been shown to be critical in storing and then extruding the secretory products (Nanavati and Fernandez, 1993; Rahamimoff and Fernandez, 1997; Wightman et al., 1995; Schroeder et al., 1996). These studies have shown that matrix proteins help release the secretory products in a pH-dependent mechanism that involves ion-exchange and phase transition of the storage proteins (Nanavati and Fernandez, 1993; Rahamimoff and Fernandez, 1997; Wightman et al., 1995; Schroeder et al., 1996). Chromagranin is found in the secretory vesicles of β-cells (Ehrhart et al., 1986; Hutton et al., 1988; Guest et al., 1989) and therefore could play a similar role for extruding insulin. Our data cannot exclude such a possibility; however, it seems unlikely given the differences in storage of insulin in β-cells and histamine or catecholamines in the other cells types. First of all, insulin is stored as a solid (Gold and Grodsky, 1984; Blundell et al., 1972, Emdin et al., 1980) and therefore is not associated with the chromagranin. Furthermore, histochemical evidence shows that chromagranin in β-cell secretory vesicles is concentrated in the halo region (Figure 3-1) separate from insulin in the dense core (Guest et al., 1989). Finally, in β-cell vesicles, insulin and C-peptide comprise 80% of the protein content and membrane bound proteins 10%, leaving just 10% of the protein as matrix proteins (Hutton, 1989). Such a distribution would seem to preclude a dominant role for chromagranin in storing and dispersing insulin, especially given the importance of Zn^{2+}-insulin complexation in storage.

Post-Fusional Regulation of Insulin Secretion

This study has revealed some of the chemical events involved in driving post-fusion release of insulin from β-cells. The effects of H^+ and Zn^{2+} on insulin release that were observed are a natural manifestation of the complex mechanism of insulin synthesis and storage. The fact that the quanta of insulin release and the rate of insulin release can be altered also raises the possibility that the intravesicular and extracellular ionic environment can regulate insulin secretion. Such post-fusion control of release has recently been proposed as a novel regulatory mechanism in a variety of cell types (Rahamimoff and Fernandez, 1997). Post-fusion regulation of insulin release would seem to hold little relevance to the endocrine action of insulin given the large distance between the release site and site of action. However, several lines of evidence support the notion of an autocrine and/or paracrine role for insulin within the islet.

Specifically, insulin has been demonstrated to: 1) bind to islet cells (Patel et al., 1982), 2) affect insulin secretion (Xu et al., 1996; Hazelwood, 1989) and 3) activate insulin receptors in β-cell lines (Rothenberg et al., 1995; Gazzano et al., 1985). It has also been demonstrated that β-cells within an islet secrete more insulin per cell than purified β-cell preparations suggesting the importance of intra-islet communication (Pipeleers et al., 1982). The concentrations of insulin at the surface of cells within an islet can easily exceed 10 nM, a concentration well above the EC_{50} for β-cell insulin receptor activation (Rothenberg et al., 1995; Aspinwall et al., 1999). Assuming a mean islet radius of 75 μm (Appendix A), only 8 exocytosis events would be required to generate a 10 nM concentration of insulin within the islet based on the value of 2.4 amol of insulin per vesicle fusion event (Huang et al., 1995). The concentration of insulin at the cell membrane could therefore be considered to be even higher during the time course of granule release suggesting that slight variations in the extracellular or intravesicular environment could play a marked role in modulating the activation of β-cell insulin receptors during exocytosis. Therefore, if the intravesicular or extracellular ionic environment does mediate post-fusion regulation of insulin release, then the effects would likely be exerted at the level of autocrine or paracrine signaling of insulin within the islet.

Table 3-1. Comparison of simulated spike width to experimental mean spike widhs. Predicted width of spikes are generated through a random walk model of diffusion as described in the text. Upper limits are defined as the widest spike predicted for the given distance. Electrode distance is defined as 1 μm added to the distance of release event from cell apex (apex = 0).

	5-HT		**Insulin**	
Electrode Distance (μM)	**Predicted Width of Upper Limit (ms)**	**Percentage of Spikes Below Upper Limit**	**Predicted Width of Upper Limit (ms)**	**Percentage of Spikes Below Upper Limit**
1	0.51	0	1.4	0
3.5	7.4	78	21	35
6	22	100	58	90

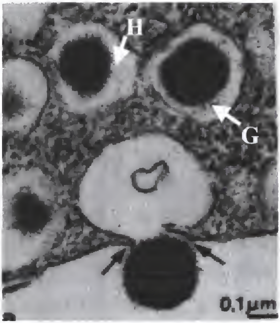

Figure 3-1. Electron micrograph of insulin containing secretory vesicles. Dark granules (G) within the secretory vesicle are precipitated Zn^{2+}-insulin complex. The clear halo (H) surrounding the Zn^{2+}-insulin granule contains soluble material within the vesicle. (Adapted from Norman and Litwack, 1997.)

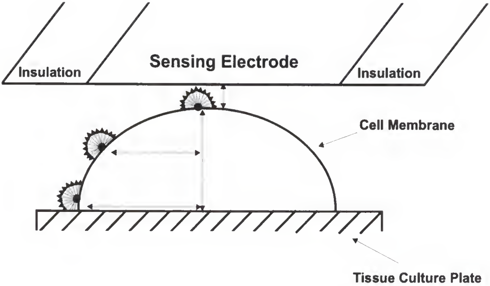

Figure 3-2. Schematic of random walk simulation conditions. Cell was assumed to be hemisphere of 5 μm radius. Electrode was positioned 1 μm above the apex of cell. Secreted product diffusing from the apex travels1 μm to electrode surface while vesicle fusion at the base of the cell requires 6 μm diffusion before detection. Detailed conditions of simulation are given in the text.

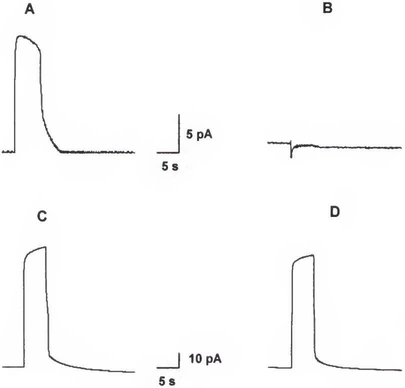

Figure 3-3. Amperometric detection of free and Zn^{2+}-complexed insulin. Current traces are recording of: A) 30 μM insulin, B) 30 μM insulin with 15 μM zinc, C) 5 μM 5-hydroxytryptamine, and D) 5 μM 5-hydroxytryptamine with 15 μM zinc. All analytes were dissolved in KRB and applied to a Ru-O/CN-Ru modified microelectrode by pressure ejection as described in the text. Current scale in B) is the same as A) and in D) is the same as C).

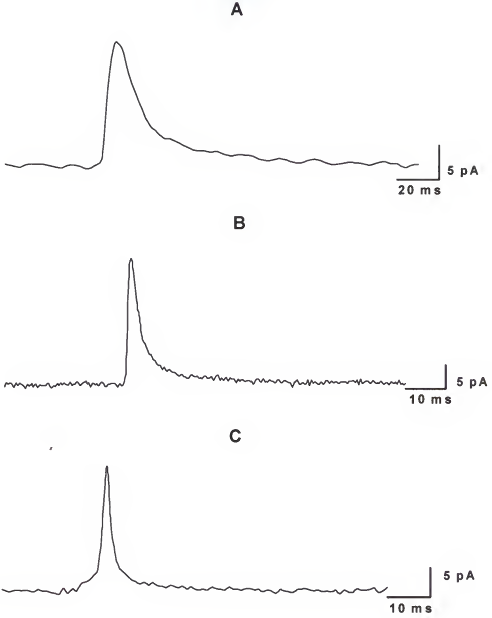

Figure 3-4. Comparison of isolated spike shapes for insulin and 5-HT detection. Spikes are due to detection of A) insulin, B) 5-HT with no prespike feature, and C) 5-HT with a prespike feature, or “foot.”.

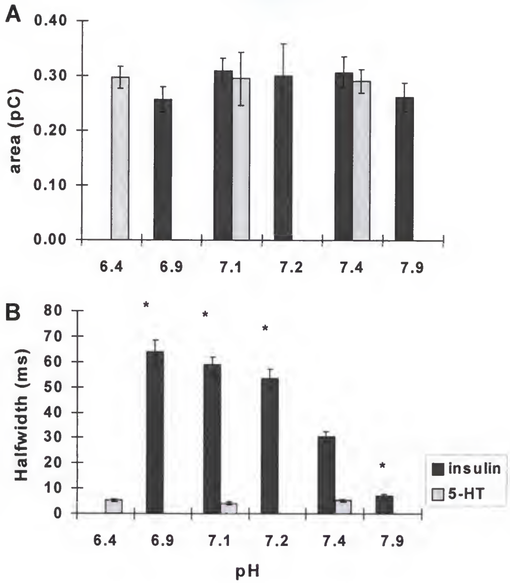

Figure 3-5. Comparison of insulin and 5-HT secretory area and width at half height at different extracellular pH. A) Mean spike area obtained versus extracellular pH for insulin and 5-HT and B) mean half-width of spikes obtained versus extracellular pH for insulin and 5-HT. The asterisk (*) indicates that the difference from pH 7.4 had $p < 0.0005$. For insulin detection, number of spikes (n) was 53, 84, 15, 50, and 80 for pH 6.90, 7.05, 7.20, 7.40 and 7.90 respectively. For 5-HT detection, number of spikes (n) was 130, 84, and 107 for pH 6.40, 7.10, and 7.40, respectively. In all cases, at least 4 different cells were used to collect the spikes used.

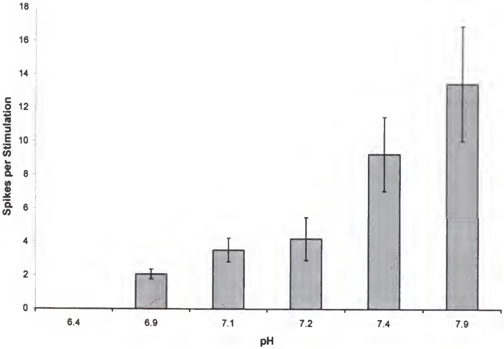

Figure 3-6. Effects of extracellular pH on detection of insulin from single pancreatic β-cells. Data obtained from 10 s stimulation of single β-cells with 200 mM tolbutamide. Spikes were counted only if S/N exceeded 5 (to allow for lower S/N at lower pH).

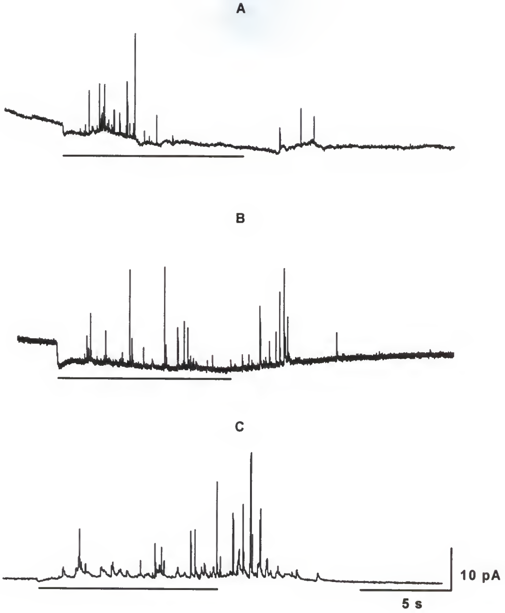

Figure 3-7. Effect of Bafilomycin A_1 and *n*-ethylmaleimide incubation on β-cell secretory activity. Current recordings obtained from detection of insulin following treatment with A) Control, B) 1 μM Bafilomycin A_1 and C) 50 μM *n*-ethylmaleimide as described in text. Bars under current trace represent application of stimulant. Dips in the current traces are a result of nonfaradaic processes due to stimulation. Recordings are from different cells.

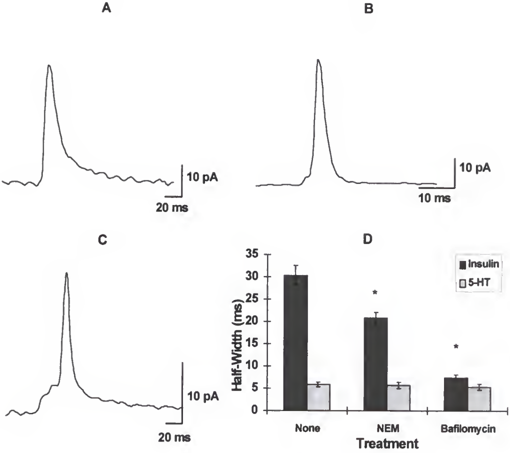

Figure 3-8. Effect of intravesicular pH on insulin spike shape. Detection of insulin following treatment with: A) control, B) 1 µM Bafilomycin A_1 and C) 50 µM *n*-ethylmaleimide. Spikes in B) and C) are examples that display a "foot". D) Comparison of spike half-widths for insulin and 5-HT spikes following treatment with V-type H^+-ATPase blockers. Asterisk (*) indicates that half-width was different from control with $p < 0.001$. For insulin detection number of spikes (n) was 49, 230, and 145 for no treatment, 50 µM *n*-ethylmaleimide, and 1 µM Bafilomycin A_1, respectively. For 5-HT detection, n was 132, 65, and 140 for no treatment, 50 µM *n*-ethylmaleimide, and 1 µM Bafilomycin A_1, respectively. Spikes were obtained from at least 6 different cells for each experiment.

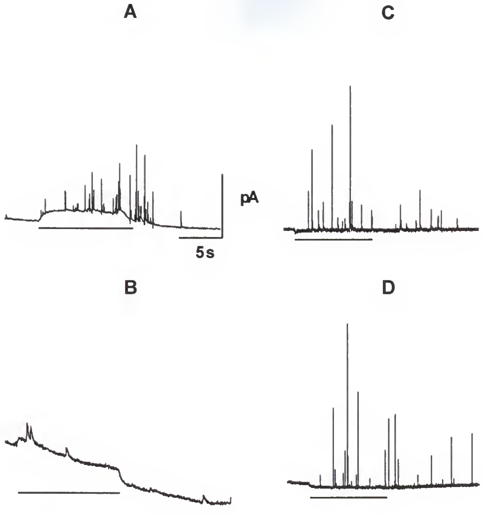

Figure 3-9. Effect of extracellular Zn^{2+} on insulin and 5-HT secretion from single β-cells. Current recordings obtained from detection of: A) insulin with 0 μM extracellular Zn^{2+}, B) insulin with 15 μM extracellular Zn^{2+}, C) 5-HT with 0 μM extracellular Zn^{2+} and D) 5-HT with 15 μM extracellular Zn^{2+}. Bars under current trace represent application of stimulant. Recordings are from different cells. Scale represents: A) 10 pA, B) 5 pA and C and D) 20 pA. Traces A and B were digitally lowpass filtered at 30 Hz for presentation purposes.

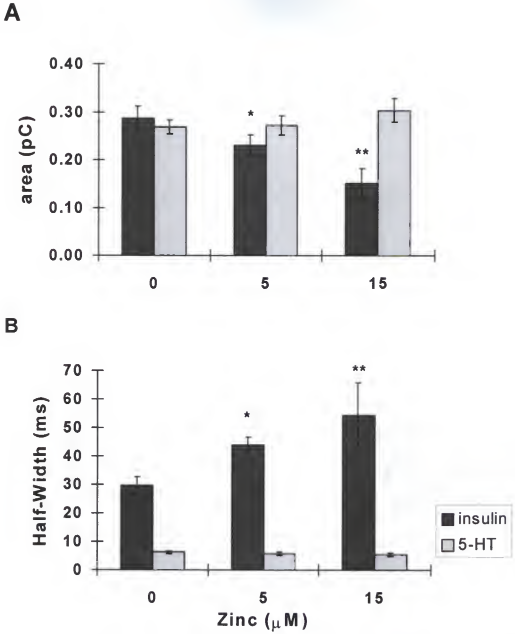

Figure 3-10. Comparison of insulin and 5-HT secretory area and width at half height at different extracellular [Zn^{2+}]. A) Effect of extracellular [Zn^{2+}] on mean spike area for insulin and 5-HT. Asterisk (*) indicates different from 0 μM [Zn^{2+}] at $p < 0.10$ and ** indicates different at $p < 0.02$. B) Effect of extracellular [Zn^{2+}] on mean half-width of spikes for insulin and 5-HT. Asterisk (*) indicates different from 0 μM [Zn^{2+}] at $p < 0.001$ and ** indicates different at $p < 0.01$. For detection of insulin, number of spikes (n) was 76, 68, and 22, while for detection of 5-HT, n was 198, 75, and 70 for 0, 5 and 15 μM extracellular zinc, respectively. For all experiments, at least five different cells were used.

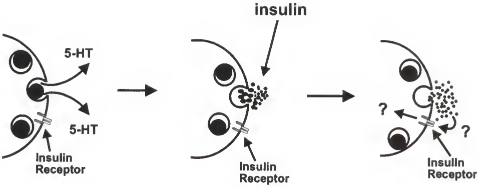

$$(INS_6Zn_2)_{solid} \xrightarrow{-H^+} (INS_6Zn_2)_{soln.} \longrightarrow INS_x + 2\ Zn^{2+}$$

Figure 3-11. Proposed mechanism of insulin clearance from individual secretory vesicles.

CHAPTER 4
INSULIN-STIMULATED INSULIN SECRETION IN SINGLE PANCREATIC BETA-CELLS

Introduction

Glucose is the principal regulator of insulin secretion from pancreatic β-cells in the islets of Langerhans (Komatsu et al., 1997; Prentki et al., 1997); however, recent discoveries suggest that intraislet communication through paracrine interactions may also exert an important level of control over insulin secretion and ultimately glucose homeostasis. For example, glucagon secreted from islet α-cells potentiates insulin secretion (Moens et al., 1996) whereas somatostatin secreted from δ-cells is a potent inhibitor of glucose-stimulated insulin secretion (Schuit et al., 1989). Although these paracrine interactions are well established, the potential autocrine action of insulin upon insulin secretion remains unclear.

Several lines of evidence support the possibility of an autocrine action of insulin on β-cells. Insulin binds to the surface of β-cells (Patel et al., 1982; Verspohl and Ammon, 1980) and functional insulin receptors and receptor substrates identical to those found in peripheral tissues have been identified in both clonal and primary β-cells (Verspohl and Ammon, 1980; Gazzano et al., 1985; Harbeck et al., 1996; Rothenberg et al., 1995). Glucose stimulation of β-cell lines activates the β-cell insulin receptor in the same way as application of exogenous insulin suggesting that insulin secreted from β-cells binds to the insulin receptor eliciting a physiological response (Rothenberg et al., 1995; Xu et al., 1998b). The complete physiological consequences of insulin receptor activation in the β-cell have yet to be completely elucidated but at least one effect is initiation of protein synthesis at both transcriptional and translational levels (Xu et al., 1998b; Xu and Rothenberg, 1998; Leibiger et al., 1998).

While functional insulin receptors have been identified on β-cells, the possible effects on insulin secretion mediated by β-cell insulin receptors have not been firmly established. Several reports have shown that glucose-stimulated insulin or C-peptide secretion from islets or perfused pancreas is suppressed in the presence of exogenous insulin leading many to believe that insulin inhibits secretion in β-cells (Ammon and Verspohl, 1976; Argoud et al., 1987; Draznin et al., 1986; Iversen and Miles, 1971; Liljenquist et al., 1978; Loreti et al., 1974; Pace et al., 1977; Sodoyez et al., 1969). Under similar conditions however, some reports have shown no effect of insulin on glucose-stimulated insulin secretion (Beischer et al., 1983; Luzi et al., 1992; Malaisse et al., 1967; Marincola et al., 1983; Schatz and Pfieffer, 1977; Stagner et al., 1986; Tanaka et al., 1980; Van Schravendijk et al., 1990). These data are difficult to interpret as direct autocrine action of insulin on secretion from the β-cell however, as intact organs or islets possess neuronal and hormonal regulatory mechanisms that could interact with exogenous insulin. Additionally, maintenance of normoglycemia during the time course of the experiments is often difficult due to the addition of exogenous insulin. Finally, the high glucose levels used to evoke stimulation likely lead to maximal activation of β-cell insulin receptors by secreted endogenous insulin, masking the effect of exogenous insulin.

Experiments with purified β-cells and β-cell lines have also generated conflicting evidence for insulin feedback. Glucose-stimulated insulin secretion from purified rat β-cells was inhibited by 20% at exogenous insulin concentrations above 1 μM; however, lower concentrations (1-100 nM) evoked no effect (Van Schravendijk et al., 1990). In another report, measurements of the effect of insulin on C-peptide secretion in βTC3 cells failed to show direct evidence of secretory regulation by insulin (Rothenberg et al., 1995). Furthermore, transfected βTC6-F7 cells in which the insulin receptor was overexpressed showed enhanced basal and glucose-stimulated insulin secretion, but fractional secretory levels (percentage of total releasable cell insulin secreted) remained unchanged at all glucose concentrations (Xu and Rothenberg, 1998). As a control, cells expressing kinase negative (inactive) insulin receptors exhibited decreased basal and glucose-stimulated insulin secretion (Xu and Rothenberg, 1998). Recent studies have confirmed that manipulation of IRS-1 levels in β-cell lines affect levels of insulin synthesis and secretion (Kulkarni et al., 1998b, Xu et al., 1998a). These results suggest an autocrine pathway regulating one or more of the following: insulin secretion, insulin synthesis, and glucose sensing/utilization.

Given the ambiguities of previous experiments, we have attempted to directly characterize the effect of exogenous insulin upon insulin secretion from single β-cells using amperometry (Wightman et al., 1991; Huang et al., 1995). In this technique, an amperometric electrode is positioned next to a single cell so that released secretory product can be detected with high sensitivity and temporal resolution. When secretion by vesicle fusion occurs, a current spike is recorded that corresponds to quantitative detection of packets of molecules released by exocytosis (Wightman et al., 1991; Huang et al., 1995; Aspinwall et al., 1997). Secreted insulin can be detected directly using a carbon fiber amperometric electrode that is modified with a mixed valent film of cyanoruthenate and ruthenium oxide (Huang et al., 1995). Alternatively, 5-hydroxytryptamine (5-HT) secretion can be detected as a marker of exocytosis in β-cells (Chapter 2; Aspinwall et al., 1997; Kennedy et al., 1996; Smith et al., 1995; Zhou and Misler, 1996). In this approach, 5-HT is allowed to accumulate into insulin containing secretory vesicles of β-cells and 5-HT secretion is detected using an unmodified carbon fiber electrode. An important characteristic of the 5-HT method for these experiments is the lack of interference from exogenous insulin with the secretory measurements. This methodology allowed the measurement of exocytosis from single, isolated cells that were not affected by possible paracrine interactions of neighboring cells thus allowing direct observation of the effect of insulin on regulation of β-cell exocytosis for the first time.

Experimental

Chemicals and Reagents

Bovine insulin, Type XI collagenase, HEPES and tolbutamide were obtained from Sigma and used without further purification. Monoclonal anti-insulin, poly clonal anti-insulin receptor$_\alpha$ and IgG were obtained from BioDesign International (Kennebunk, ME) and were of rabbit origin. All chemicals for islet and cell culture were obtained from Life Technologies. All other chemicals were from Fisher unless noted and were of highest purity available.

Isolation and *In Vitro* Culture of Mouse Islets and β-Cells

Islets were isolated from 20-30 g CD-1 mice following ductal injection with collagenase and dispersed into single cells by shaking in dilute trypsin for 10 minutes at 37° C (Appendix A; Aspinwall et al., 1999; Pralong et al., 1990). Cells were cultured in pH 7.4 RPMI 1640 containing: 10% fetal bovine serum, 100 U/ml penicillin and 100 μg/ml streptomycin at 37° C, 5% CO_2. Dispersed β-cells were used on days 2 to 4 after isolation.

Isolation and *In Vitro* Culture of Canine, Porcine, and Human Islets and β-Cells

Pancreatic islets were isolated from canine, porcine or human pancreas using controlled collagenase (Boehringer Mannheim) perfusion via the duct, automated dissociation and discontinuous Euro-Ficoll purification using the COBE 2991 blood cell processor as previously described (Ricordi et al, 1988; Warnock et al., 1994a). Islets were dispersed into single cells the next day using a previously described procedure (Appendix A; Huang et al., 1995). Cells were cultured at 37° C, 5% CO_2 in modified CMRL 1066 tissue culture media containing: 10% fetal bovine serum, 25 mM HEPES, 100 U/mL penicillin, and 100 μg/mL streptomycin, pH 7.4.

Data Collection and Analysis

Microelectrodes were constructed as described in Chapter 2. Amperometry was performed using a battery to apply potential to a sodium saturated calomel electrode (SSCE) as previously described (Chapter 2; Aspinwall et al., 1997). For measurements of 5-HT secretion, dispersed β-cells were incubated in tissue culture media containing 0.5 mM 5-hydroxytryptamine and 1 mM 5-hydroxytryptophan for 16 hours at 37° C, 5% CO_2, pH 7.4 (Chapter 2; Aspinwall et al., 1997). Cells were used for secretion experiments immediately after loading. Measurements requiring direct detection of insulin were performed on β-cells which were not allowed to accumulate 5-HT prior to experimentation and the microelectrode was chemically modified with a film of mixed valent cyanoruthenate and ruthenium oxide as described in Chapter 2. For detection of 5-HT the potential at the working electrode was 0.65 V while for detection of insulin the potential was 0.85 V. Data were low pass filtered at 100 Hz and collected at 500 Hz using a personal computer (Gateway 2000 P5-166) via a data acquisition board (Axon Instruments, DigiData 1200B). For direct measurement of insulin using chemically modified microelectrodes, data was further high pass filtered following collection to remove the slow component of the background current associated with detection of the insulin stimulant, leaving the rapid current spikes unaffected (Moore and Jorgenson, 1993).

Amperometric measurements were made by positioning microelectrodes ~1 μm from a cell and applying stimulant from a micropipette ~ 30 μm from the cell as described in Chapter 2 (Huang et al., 1995; Aspinwall et al., 1997). All experiments were performed with cells at 37° C, incubated in pH 7.4 Kreb's Ringer buffer (KRB) containing (in mM): 118 NaCl, 5.4 KCl, 2.4 $CaCl_2$ (unless noted otherwise), 1.2 $MgSO_4$, 1.2 KH_2PO_4, 3 *d*-glucose (unless noted otherwise) and 25 HEPES (24 $NaHCO_3$ for insulin measurements). Stimulant solutions (1 nM-1 μM insulin, 200 μM tolbutamide, 17 mM glucose) were prepared by dissolving the desired concentration of stimulant in KRB. K^+ stimulant, 30 mM, was prepared in the same composition as KRB but by replacing 30 mM NaCl with KCl to maintain ionic strength. All means are reported ± 1 standard error of the mean (SEM). Statistical differences between means were evaluated using a two-tailed Student's *t*-test.

Anti-Insulin Receptor Antibody Experiments

Mouse β-cells were stimulated with 100 nM insulin and exocytosis of 5-HT detected by amperometry to establish viability. Following successful stimulation with 100 nM insulin, 10 nM anti-insulin receptor$_\alpha$ was added to the buffer and allowed to incubate for 5 minutes. The same cell was then stimulated again with 100 nM insulin in the presence of the antibody. Following insulin stimulations, the cell was stimulated with 30 mM K^+ in the presence of antibody to confirm cell viability.

Investigation of Autocrine Activation of β-Cells

Direct autocrine activation of 5-HT loaded β–cells was investigated by first establishing cells to be responsive to 100 nM insulin stimulation by amperometric detection of 5-HT exocytosis. Following establishment of viability, cells were stimulated with 30 mM K^+. Following K^+ stimulation, 25 nM anti-insulin receptor$_\alpha$ was added to the buffer and allowed to incubate for 5 minutes. Cells were again stimulated with 30 mM K^+ and the number of exocytosis events detected in the presence and absence of antibody was compared.

In a second series of experiments, 5-HT loaded canine β-cells were bathed in KRB of varying H^+ and Zn^{2+} concentration. Buffer pH was adjusted by varying bicarbonate concentration to achieve the desired pH after bubbling with 5% CO_2. Extracellular Zn^{2+} concentration was adjusted by adding Zn^{2+} to the desired concentration and ionic strength was held constant for all solutions. Cells were then stimulated with 200 μM tolbutamide dissolved in KRB of matching pH and Zn^{2+} concentration and 5-HT secretion detected by amperometry. The number of 5-HT spikes detected per stimulation was then compared at the various pH and Zn^{2+} concentrations.

Membrane Potential Measurements

Membrane potential measurements were made in the whole-cell perforated patch configuration at room temperature. Pipettes were pulled from borosilicate glass and had resistances between 4 and 6 MΩ. Pipette solutions contained (in mM): 10 KCl, 76 K_2SO_4, 10 NaCl, 1 $MgCl_2$, 10 HEPES and 200 μg/ml amphotericin B, pH 7.35. Data was low pass filtered at 100 Hz and collected at 500 Hz using Axopatch 200A patch-clamp amplifier and DigiData digitizer (Axon Instruments, Foster City, CA).

Extracellular Calcium Dependence of Insulin Stimulation

The extracellular calcium requirement for insulin stimulation was investigated using amperometry at 5-HT loaded mouse β-cells. Cells were bathed in KRB containing 0 mM Ca^{2+} and stimulated with 100 nM insulin dissolved in KRB containing either 0 or 5 mM Ca^{2+}. All data is from paired experiments of cells stimulated with both 0 and 5 mM Ca^{2+} containing stimulants.

$[Ca^{2+}]_i$ Measurements

Intracellular free calcium ($[Ca^{2+}]_i$) was monitored using fura-2 fluorescence microscopy as described in Appendix C. Briefly, 25 mm coverslips containing mouse β-cells were incubated in 2 μM fura-2AM (Molecular Probes) dissolved in KRB at 37° C, 5% CO_2 for 30 minutes. Dye solution was then replaced with KRB and coverslips with adherent cells were placed into a coverslip dish for immediate use. The resulting fluorescence ratios from individual cells were collected at 1 Hz through a Fluar 40X oil immersion objective (Zeiss), band pass filter (510 nm ± 10 nm) and 20 μm pinhole aperture onto a photomultiplier tube using a SPEX CMX cation measurement system and DM3000M data acquisition software (Instruments SA).

Results

Insulin Stimulated Insulin Secretion in Single β-Cells

In view of the majority of prior results suggesting negative feedback of insulin on insulin secretion, it was surprising to find that application of bovine insulin to isolated mouse β-cells at non-stimulatory (3 mM) glucose concentrations stimulated exocytosis (Figure 4-1A). This result was confined to β-cells as the cells that responded to insulin also exhibited exocytosis when stimulated with 17 mM glucose or 200 μM tolbutamide, stimulants known to act exclusively (of the islet cell types) at β-cells (n = 8) (Figure 4-1B). Furthermore, the effect did not result from a contaminant in the insulin stimulatory solution as addition of an anti-insulin antibody to the stimulant solution abolished the secretory response elicited by insulin stimulation in all cases (n = 7) (Figure 4-1C). Finally, the stimulatory effect is not an artifact of measuring accumulated 5-HT instead of insulin, as it was possible to directly measure insulin secretion at single β-cells that had not been allowed to accumulate 5-HT (n = 5) (Figure 4-1D). The observation of insulin-stimulated insulin secretion is not unique to mouse cells as we observed similar stimulatory effects on insulin secretion following stimulation with exogenous insulin in human (n = 10), porcine (n = 7), and canine β-cells (n = 21) (Figure 4-2).

Requirement of β-Cell Insulin Receptor for Insulin Stimulated Exocytosis

To determine if insulin-stimulated insulin secretion was mediated by the β-cell insulin receptor, we examined the antagonistic effect of anti-insulin receptor$_\alpha$ on insulin-stimulated insulin secretion (Figure 4-3). For these experiments, cells were stimulated with 100 nM insulin to establish responsiveness, then incubated with 10 nM polyclonal anti-insulin receptor$_\alpha$ to block the insulin receptor, and stimulated again with 100 nM insulin. In no case was secretion detected following application of antibody ($n = 4$). Subsequent stimulation with 30 mM K^+ in the presence of anti-insulin receptor$_\alpha$ evoked secretion in all cases establishing cell viability following antibody treatment. In control experiments, addition of immunoglobulins had no detectable effect on insulin-stimulated exocytosis (data not shown). We also found that the insulin-stimulated insulin secretion was dependent upon the concentration of applied insulin in the range of 1-100 nM as illustrated in Figure 4-4 for canine and mouse β-cells. It was found that higher concentrations of insulin (1 μM) did not induce a significantly different number of exocytosis events in either species observed. (In evaluating the concentrations used to elicit secretion, it is important to realize that the concentrations reported are those present in the pipette. During stimulation, the solution is diluted by ill-defined amount as it is applied to the cell).

Direct Autocrine Stimulation of Single β-Cells

We next investigated the possibility of direct autocrine action of insulin at single β-cells. Cells which had been established as insulin responsive by detection of 5-HT secretion following insulin stimulation, were stimulated with 30 mM K^+ in the presence and absence of 25 nM anti-insulin receptor$_\alpha$ in order to prevent autocrine activation of the β-cell insulin receptor. As shown in Figure 4-5, stimulation resulted in 20.2 ± 4.5 spikes per stimulation preceding addition of antibody and was reduced to 9.6 ± 2.4 spikes per stimulation ($n = 13$) upon addition of antibody ($p < 0.05$). This result suggests that the antibody blocks released insulin from binding to the β-cell insulin receptor and further enhancing release.

As further confirmation that insulin could contribute to direct positive feedback, we investigated the effects of conditions that reduce the free insulin concentration at the cell surface. We have previously shown that increasing H^+ and Zn^{2+} in the extracellular media significantly decreases the extrusion rate of insulin from single secretory vesicles following vesicle fusion. This leads to a decrease in the concentration of free insulin, the biologically active form, at the cell surface (Chapter 3; Aspinwall et al., 1997). Table 4-1 summarizes the effects of hindered vesicle extrusion of insulin on exocytosis from the β-cell. The data are presented as the number exocytosis events detected follwing stimulation with 200 μM tolbutamide from cells incubated in control buffers and buffers containing varying H^+ and Zn^{2+} concentrations as indicated in Table 4-1. The number of spikes detected following stimulation is significantly reduced at higher H^+ ($p < 0.01$) and Zn^{2+} ($p < 0.005$) concentrations. Thus, under conditions where the concentration of free insulin at the cell surface is reduced following vesicle fusion, the number of exocytosis events detected is significantly lower. These results are consistent with the hypothesis that secreted free insulin activates further insulin secretion.

Glucose Dependence of Insulin-Stimulated Insulin Secretion

The primary physiological action of insulin is to stimulate glucose uptake and utilization. Therefore we examined the interaction between exogenous insulin stimulation and extracellular glucose concentration by measuring the effect of insulin stimulation upon insulin secretion of β-cells bathed in 0, 3, and 20 mM glucose. At 0 and 3 mM glucose, application of 100 nM insulin evoked a comparable amount of secretory activity as shown in Figure 4-6A and B. While the number exocytosis events elicited per stimulation is lower for cells bathed in 3 mM glucose, the results are not statistically different (Figure 4-6C).

As a further indicator of the glucose dependence of the insulin stimulatory effect, we investigated the frequency of secretion at 0, 3 and 17 mM glucose. The data is shown in Figure 4-6D and is represented as the change in frequency (Delta F; spikes s^{-1}) of exocytosis before and during addition of 100 nM insulin. Cells incubated in the lower glucose concentrations underwent the largest frequency change of exocytosis due to the lack of basal secretion from these cells. More interestingly, cells that were bathed in 20 mM glucose further increased the frequency of detected exocytosis events from $0.17 \pm 0.051\ s^{-1}$ to $0.22 \pm 0.084\ s^{-1}$ ($n = 5$) upon application of 100 nM exogenous insulin. This increase however was not statistically significant, indicating that insulin receptors on the β-cell membrane are probably maximally activated from exogenous insulin released during glucose-stimulated exocytosis.

Effects of Insulin on Membrane Potential and Intracellular $[Ca^{2+}]_i$

The novelty of insulin as an insulin secretagogue prompted us to explore other effects of insulin on common second messenger pathways. Many insulin secretagogues such as glucose, sulfonylureas, and K^+ depolarize the plasma membrane leading to opening of L-type voltage-gated Ca^{2+} channels, thereby allowing Ca^{2+} entry into the cell and initiation of exocytosis. Insulin however, did not depolarize the membrane in β-cells that could be depolarized by 200 μM tolbutamide (Figure 4-7). The average change in membrane potential from baseline to plateau (not including action potential) following tolbutamide stimulation was 32.5 ± 1.58 mV, with the occurrence of action potentials while the average change following insulin stimulation was 1.47 ± 1.52 mV (n = 13). As illustrated in Figure 4-7, while some cells showed a small depolarization, others were unaffected or slightly hyperpolarized.

In agreement with the minimal effect on membrane potential, insulin-stimulated secretion was not dependent upon extracellular Ca^{2+}. Figure 4-8 illustrates paired experiments where β-cells bathed in Ca^{2+}-free KRB were stimulated with 100 nM insulin containing either 5 mM or 0 mM Ca^{2+} (n = 10). The numbers of exocytosis events were not significantly different for insulin stimulant containing either Ca^{2+} concentration. This result is not an artifact of low levels of Ca^{2+} in the media as we have used similar protocols to demonstrate the Ca^{2+} dependence of glucose, tolbutamide and K^+ stimulation (Huang et al., 1995). Although the presence, and therefore entry, of extracellular Ca^{2+} was not required to initiate secretion, stimulation with insulin did elicit increases in intracellular free calcium levels within the cell (n = 5) as seen in Figure 4-9. Also seen in Figure 4-9, the insulin-evoked $[Ca^{2+}]_i$ changes were of smaller magnitude than those caused by K^+ but were of longer duration.

Discussion

The data presented above demonstrates, for the first time, that insulin can stimulate insulin secretion in single pancreatic β-cells (Figure 4-1). The stimulatory effect of insulin is mediated by the β-cell insulin receptor as evidenced by the antagonistic effect of anti-insulin receptor (Figure 4-3). Furthermore, the insulin concentrations necessary for this effect are in the nanomolar range which is reasonable since the EC_{50} for activation of the β-cell insulin receptor is ~4 nM (Rothenberg et al., 1995). Additionally, concentrations of insulin at the surface of β–cells within the islet can easily reach the concentrations tested in this work. Assuming a mean islet radius of 75 μm (Appendix A), only 8 exocytosis events would be required to generate a 10 nM concentration of insulin within the islet assuming 2.4 amol of insulin per vesicle fusion event (Huang et al., 1995).

The data presented here leads us to propose a novel regulatory mechanism whereby insulin released from a single cell can modulate secretory activity from that cell and neighboring cells within the islet. Figure 4-10 illustrates this proposed mechanism, where insulin secreted from the cell must first dissolve and dissociate from the zinc-insulin storage complex. Since the concentration of insulin at the cell surface is quite high upon vesicle fusion, the rate of dissociation of the zinc insulin complex likely plays an important role in controlling the free insulin concentration at the cell membrane. This suggests that slight variations in the extracellular environment affects the autocrine activity exerted by insulin upon the β-cell (Chapter 3;Aspinwall et al., 1997.) Additionally, this hypothesis is in agreement with previous results that demonstrated that β-cell insulin receptors are activated by glucose (Rothenberg et al., 1995).

Experimental evidence for this proposed regulatory mechanism consists of the following. Insulin released from a single β-cell is present at a sufficient concentration to activate the β-cell insulin receptor and enhance secretion. Decreased K^+ stimulated secretion is detected when the insulin receptor is blocked by anti-insulin receptor. Tolbutamide induced secretion was significantly lowered when the cell surface concentration of free insulin was reduced by increasing the extracellular concentration of H^+ and Zn^{2+}. A relatively minor enhancement of secretion is observed upon application of exogenous insulin during stimulation with 20 mM glucose, a condition in which released endogenous insulin may be expected to activate receptors to near maximal levels. Taken together, these results suggest that a portion of secretion that is normally observed from single β–cells is due to positive autocrine feedback upon β-cell exocytosis acting through the β-cell insulin receptor.

Although insulin evokes secretion, it does not evoke membrane depolarization and subsequent Ca^{2+} entry to cause secretion as evidenced by the minimal effect on membrane potential (Figure 4-7) and independence of the insulin-stimulatory effect on extracellular Ca^{2+} (Figure 4-8). Insulin-stimulated insulin secretion is not mediated by glucose or increases in glucose utilization as the effect occurs even at 0 mM glucose. Insulin does however, evoke increases in $[Ca^{2+}]_i$. These results are consistent with a mechanism of stimulation in which insulin evokes release of intracellular calcium stores to initiate exocytosis, reminiscent of ATP binding to P_{2y} receptors in β-cells (Li et al., 1991; Tang et al., 1996).

Autoreceptor effects on hormone or neurotransmitter secretion are well-known; however, most autoreceptors mediate negative feedback on secretion. The β-cell-insulin system appears to be a rare example of positive feedback on secretion. The interplay of this positive feedback effect with other regulatory mechanisms to control insulin secretion and glucose homeostasis *in vivo* is likely complex. It is reasonable to speculate that positive feedback would cause augmented secretion during the initial stages of elevated glucose levels giving rise to a greater bolus of insulin release; however, other mechanisms must eventually take over to suppress release. Such a sequence could contribute to the rapid increase observed in first phase insulin secretion and the sustained, lower secretion during second phase (See Chapter 1). The possibility that insulin has a local effect on secretion also raises the possibility of novel regulatory mechanisms that might occur within islets. For example, since Zn^{2+} and H^+ can control the cell-surface concentration of insulin after vesicular fusion (Aspinwall et al., 1997), these ions could play a role in regulating insulin secretion by affecting positive feedback. Serum concentrations of Zn^{2+} are in the range of 15-25 μM (Hurley, 1969) which would be sufficient to have a large effect on the free insulin concentration around the β-cell.

The existence of positive feedback may allow explanation of several phenomena in β-cells. For example, cultured β-cells in contact with other β-cells have been shown to secrete more insulin than isolated cells (Bosco et al., 1989; Maes and Pipeleers 1984). This result has not been explained, but could be mediated by insulin from one cell stimulating further release in neighboring cells. In addition, insulin secretion from islets has been demonstrated to be oscillatory in nature and many models for oscillation have assumed some form of positive feedback by a diffusible factor released from β-cells (Cunningham et al., 1996; Maki and Keizer 1995). No compound has been satisfactorily identified that could serve this role; however, these results indicate insulin as a possible candidate. Oscillations in insulin release are of significant interest since loss of oscillatory release is an early symptom of Type-II diabetes (O' Rahilly et al., 1988). Finally, it has been demonstrated that many Type II diabetics have a marked reduction in first phase insulin secretion (Polonsky, 1995), which to date has remained unexplained but could be envisioned as involving lack of positive feedback from the β-cell insulin receptor. Supporting the possibility that autocrine activation of the β-cell insulin receptor is involved in early secretory responses is recent work in which mice with knock-outs of the β-cell insulin receptor have impaired early insulin secretion and concomitant glucose intolerance (Kulkarni et al., 1998a; Kulkarni et al., 1999).

Perhaps most importantly, these results suggest a possible link between impaired insulin secretion and insulin resistance, both of which can lead to hyperglycemia and are considered hallmarks of Type-II diabetes (Taylor et al., 1994). Considerable controversy surrounds the issue of which of these deficiencies is the primary cause of diabetes. In some studies, the earliest observed defect is dysfunctional secretion (Cunningham et al., 1996; O'Rahilly et al., 1988) and in others insulin resistance appears to be the first detectable problem (Martin et al., 1992). The observation that insulin receptors on β-cells mediate insulin secretion and synthesis (Xu et al., 1998b; Xu and Rothenberg, 1998; Leibiger et al., 1998), in addition to the well-known role in activating glucose utilization, leads to the possibility of a direct link between dysfunctional insulin secretion and insulin resistance. Such a link is supported by evidence that disruption of the β-cell insulin receptor (Kulkarni et al., 1999) or β-cell receptor substrates (Kulkarni et al., 1998b; Xu et al., 1998a) induces defects in secretion while disruption in insulin receptor substrates in peripheral tissues induces insulin resistance (Withers et al., 1998; Tamemoto et al., 1994).

Table 4-1. Effect of insulin complexation on autocrine feedback at β-cell insulin receptor. The number of stimulations is given as n. Detailed conditions given in text. Data presented as mean ± SEM.

pH	**$[Zn^{2+}]$ (μM)**	**Spikes per stimulation**
7.4	0	15 ± 2.6 n = 24
7.4[a]	15	5.5 ± 0.78 n = 40
6.4[b]	0	7.2 ± 1.2 n = 25

[a] Statistically different from control (pH = 7.4 and $[Zn^{2+}] = 0$ μM) with $p < 0.005$.

[b] Statistically different from control (pH = 7.4 and $[Zn^{2+}] = 0$ μM) with $p < 0.01$.

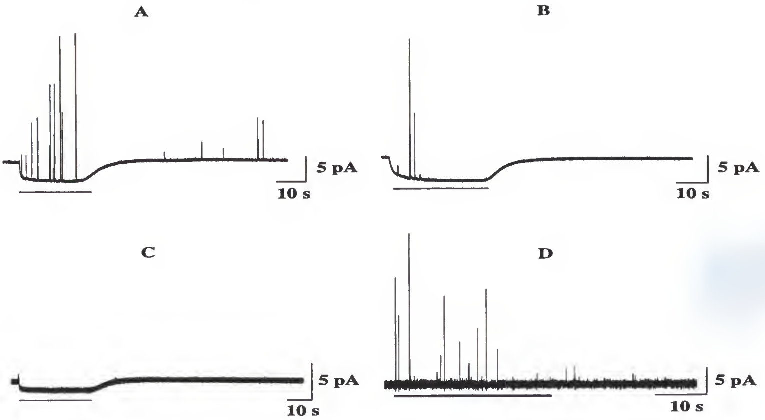

Figure 4-1. Detection of exocytosis elicited by insulin stimulation at single mouse β-cells. Detection of 5-HT upon application of A) 100 nM insulin and B) 200 μM tolbutamide (same cell as A). C) Detection of 5-HT upon stimulation with 100 nM insulin with 100 nM anti-insulin. D) Detection of insulin upon stimulation with 100 nM insulin with chemically modified microelectrode. Data in D) has been high-pass filtered to remove background response to insulin stimulant (Moore and Jorgenson, 1993). In all cases, bar under current traces represents application of stimulant.

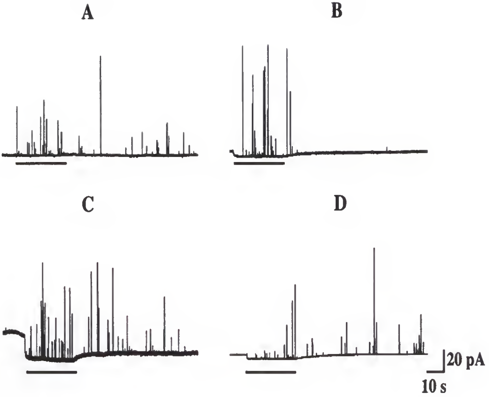

Figure 4-2. Insulin-stimulated exocytosis in β-cells from different species. Detection is from A) canine, B) porcine, C) human and D) mouse β-cells upon application of 100 nM insulin. Bars under current traces represent application of stimulant.

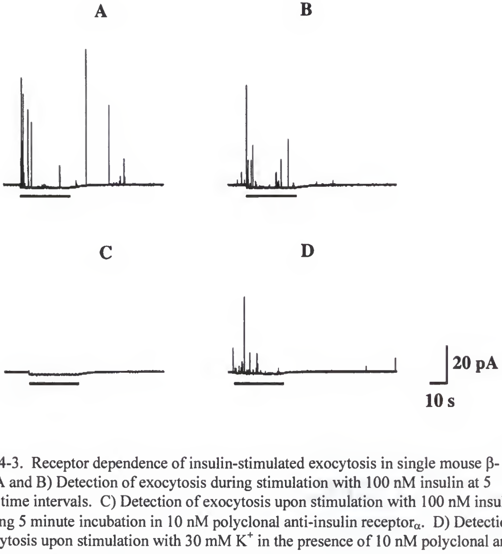

Figure 4-3. Receptor dependence of insulin-stimulated exocytosis in single mouse β-cells. A and B) Detection of exocytosis during stimulation with 100 nM insulin at 5 minute time intervals. C) Detection of exocytosis upon stimulation with 100 nM insulin following 5 minute incubation in 10 nM polyclonal anti-insulin receptor$_{\alpha}$. D) Detection of exocytosis upon stimulation with 30 mM K^+ in the presence of 10 nM polyclonal anti-insulin receptor$_{\alpha}$. All data is detection of accumulated 5-HT from same cell. Bars underneath traces represent application of stimulant.

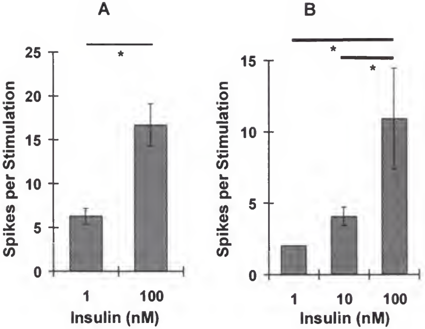

Figure 4-4. Concentration dependence of insulin-stimulated exocytosis in single β-cells. A) Frequency of exocytosis events detected following insulin stimulation in mouse β-cells ($n = 7$ and 8 for 1 and 100 nM insulin, respectively). B) Frequency of exocytosis events detected, following insulin stimulation in canine β-cells ($n = 4$, 14 and 12 for 1, 10 and 100 nM insulin, respectively). Higher concentrations of insulin (1 μM) did not evoke a significantly different number of exocytosis events for either species. A) Statistical significance for * is $p < 0.05$. B) Statistical significance for * is $p < 0.025$.

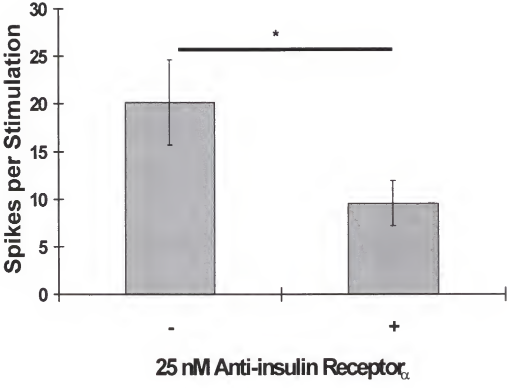

Figure 4-5. Autocrine feedback on exocytosis at single β-cells. Data is the number of exocytosis events detected in the presence (+) and absence (-) of 25 nM anti-insulin receptor$_\alpha$ upon stimulation with 30 mM K^+. Statistical significance for asterisk (*) is $p < 0.05$.

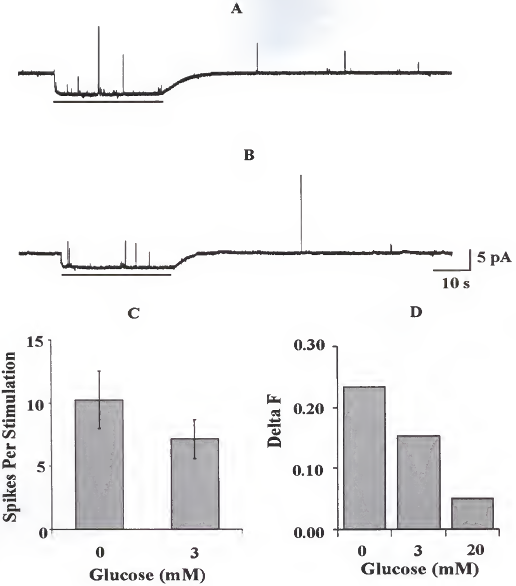

Figure 4-6. Glucose dependence of insulin-stimulated insulin secretion. Detection of exocytosis from single mouse β-ells during stimulation with 100 nM insulin dissolved in KRB with 2.4 mM Ca^{2+}. Buffer contains 2.4 mM Ca^{2+} with A) 0 mM glucose and B) 3 mMglucose. Bars underneath current traces represent application of stimulant. C) Summary of effect of glucose concentration on secretory activity at 0 and 3 mM glucose as measured by number of spikes per stimulation. Difference is not statistically significant. D) Change in frequency of secretion (spikes per second) following application of insulin to β-cells in KRB containing various glucose concentrations.

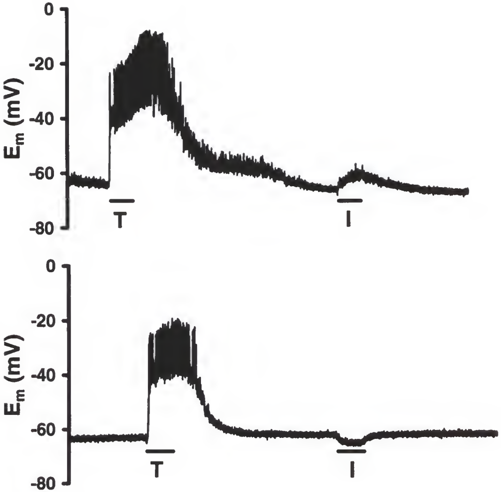

Figure 4-7. Effect of insulin on membrane potential in single mouse β-cells. Membrane potential measurements following stimulation with 200 μM tolbutamide (T) and 100 nM insulin (I) at a single β-cell. Trace shown in A) demonstrates a slight depolarization upon insulin stimulation while trace in B) demonstrates a slight hyperpolarization following stimulation with insulin. Bars under traces represent 30 s application of stimulant.

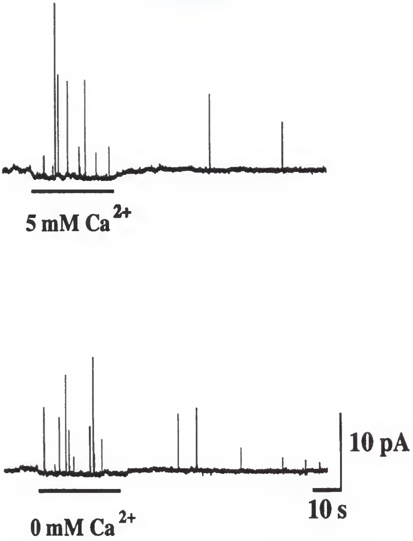

Figure 4-8. Extracellular calcium dependence of insulin-stimulated exocytosis. Detection of exocytosis during application of 100 nM insulin to cells incubated in Ca^{2+}-free KRB. Stimulant contained 5 mM $CaCl_2$ or 0 mM $CaCl_2$ as indicated. Data is from same cell. Bar represents application of stimulant for 30 s.

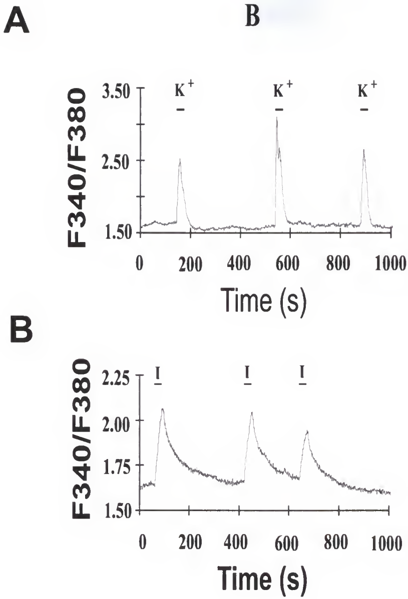

Figure 4-9. Effect of insulin on $[Ca^{2+}]_i$ in single mouse β-cells. Fura-2 microfluorimetry measurements of $[Ca^{2+}]_i$ changes following application of A) 30 mM K^+ (K) or B) 200 nM insulin (I) dissolved in KRB containing 2.4 mM Ca^{2+}. Bar above traces represents application of stimulant for 30 s.

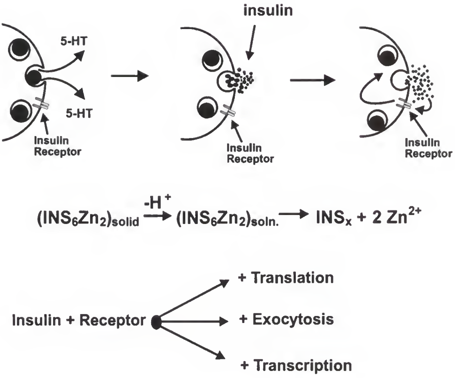

Figure 4-10. Proposed mechanism of autocrine feedback. Insulin released from a single exocytosis event dissolves and dissociates from the zinc complex. Upon dissociation, insulin can bind to β-cell insulin receptors to increase secretion, transcription or translation (see text). An added level of control is induced by alterations in the extracellular environment, affecting the concentration of free insulin monomer at the cell surface.

CHAPTER 5
INSULIN-STIMULATED INSULIN SECRETION IS MEDIATED BY RELEASE OF INTRACELLULAR CALCIUM STORES THROUGH A WORTMANNIN-SENSITIVE PATHWAY

Introduction

Insulin secreted by the pancreatic β-cell is the primary regulator of serum glucose concentrations in mammals. While substantial progress has been made elucidating the underlying physiological mechanisms responsible for normal regulation of insulin secretion from the β-cell, many aspects of this process remain unclear. In particular, chemical and physiological interactions between cells within the islet exert an important level of control in the physiological regulation of insulin secretion. Both hormonal and neuronal interactions within the islets modulate β-cell activity and insulin secretion *in vitro* and *in vivo* (Norman and Litwack, 1997). While several paracrine interactions affecting insulin secretion within the islet have been characterized, including the effects of glucagon and somatostatin (Moens et al., 1996; Schuit et al., 1989), the physiological consequences of autocrine activation of the β-cell by insulin are beginning to be investigated.

Past investigation of the effect of insulin on insulin secretion from the β-cell has led to conflicting results. While several reports have shown that glucose-stimulated insulin or C-peptide secretion from islets or perfused pancreas is suppressed in the presence of exogenous insulin (Ammon and Verspohl, 1976; Argoud et al., 1987;

Draznin et al., 1986; Iversen and Miles, 1971; Liljenquist et al., 1978; Loreti et al., 1974; Pace et al., 1977; Sodoyez et al., 1969), others have shown no effect of insulin on glucose-stimulated insulin secretion (Beischer et al., 1983; Luzi et al., 1992; Malaisse et al., 1967; Marincola et al., 1983; Schatz and Pfieffer, 1977; Stagner et al., 1986; Tanaka et al., 1980; Van Schravendijk et al., 1990). These data are difficult to interpret as a direct autocrine interaction with the β-cell, as all of these studies were performed on intact pancreas or islets possessing neuronal and hormonal regulatory mechanisms that could also interact with exogenous insulin.

Fueling the debate on the physiological action of insulin upon β-cell function is the recent discovery that β-cells possess many elements of the insulin-receptor signaling pathway. These include expression of functional insulin receptors on the β-cell surface (Verspohl and Ammon, 1980; Gazzano et al., 1985; Rothenberg et al., 1995) as well as the presence of insulin receptor substrates (IRS-1 and IRS-2) (Harbeck et al., 1996; Velloso et al., 1995; Sun et al., 1997). In addition, phosphatidylinositol 3-kinase (PI-3K) has been observed in β-cells and islets and is activated following stimulation with glucose (Alter and Wolf, 1995; Gao et al., 1996). More recently, protein kinase B (PKB), a key element in insulin-stimulated signal transduction has been identified in the β-cell (Holst et al., 1998). While the presence of functional components of the insulin signaling pathway in the β-cell strongly suggests the presence of an autocrine regulatory action, the physiological consequences of insulin receptor signaling in the β-cell have remained largely uncharacterized.

Several lines of evidence support the notion that insulin secreted from the β-cell can be involved in autocrine regulation of β-cell function. Insulin binds to receptors on the surface of β-cells (Patel et al., 1982; Verspohl and Ammon, 1980) and activates tyrosine phosphorylation of insulin receptors (Rothenberg et al., 1995) and receptor substrates (Velloso et al., 1995) as in peripheral tissues. Additionally, glucose stimulation of β-cell lines activates the β-cell insulin receptor (Rothenberg et al., 1995) and IRS-1 (Velloso et al., 1995) in the same way as application of exogenous insulin. Furthermore, maximal glucose-stimulated production of phosphatidylinositol 3,4,5-triphosphate (PIP_3), a major product of PI-3K activity, coincides with the peak early phase insulin secretion in islets and clonal β-cells (Alter and Wolf, 1995). Thus autocrine activation of the β-cell insulin receptor by secreted insulin occurs with physiological stimuli.

Recent studies have begun to characterize the physiological consequence of insulin receptor activation in the β-cell. For example, it has been clearly demonstrated that activation of the insulin signaling pathway in β-cells leads to initiation of insulin synthesis at both transcriptional and translational levels, increasing the cellular content of releasable hormone in primary and clonal β-cell cultures (Xu et al., 1998b; Xu and Rothenberg, 1998; Leibiger et al., 1998). Furthermore, the use of genetically modified β-cell lines has provided evidence for an autocrine mechanism of positive feedback in the β-cell. In βTC6-F7 cells transfected to overexpress the insulin receptor, basal and glucose-stimulated insulin secretion was enhanced compared to kinase negative controls (Xu and Rothenberg, 1998). In another report, clonal cells lacking the IRS-1 protein showed both decreased insulin content and glucose-stimulated secretion, further suggesting autocrine control of insulin synthesis and/or secretion (Kulkarni et al., 1998b).

While enhanced secretion through an autocrine feedback loop is clearly observed in clonal cells (Xu and Rothenberg, 1998), the degree of interaction *in vivo* is unclear from these studies. The strongest evidence for a physiologically important autocrine pathway comes from studies with genetically modified mice. Construction of mice containing tissue specific deletions of the β-cell insulin receptor (βIRKO) exhibited impaired glucose tolerance and insulin secretion characteristic of diabetes (Kulkarni et al., 1998a; Kulkarni et al., 1999). However, the βIRKO mice exhibited reduced insulin content within the β-cell as well, making it unclear if the diminished secretion was due to reduced synthesis of insulin or a defect in the exocytosis mechanism.

We have recently shown that application of exogenous insulin results in direct stimulation of insulin secretion in the β-cell (Aspinwall et al., 1999). Moreover, we were able to demonstrate that insulin secreted from a single β-cell could exert positive feedback at the same cell, directly increasing the amount of secretion. Application of insulin to single mouse β-cells leads to increases in intracellular free Ca^{2+} ($[Ca^{2+}]_i$) but the stimulatory effect of insulin on β-cell secretory activity was independent of extracellular Ca^{2+} (Aspinwall et al., 1999). While mechanism for autocrine activation of β-cell transcription has been investigated, the mechanism by which insulin stimulates the increase in $[Ca^{2+}]_i$, and the relationship of the Ca^{2+} changes with insulin-stimulated secretion remains obscure. In the current work, we extend investigation of insulin-stimulated insulin secretion to identify crucial elements in the signaling pathway as well as the nature of the intracellular Ca^{2+} changes previously observed.

Experimental

Chemicals and Reagents

Type XI collagenase, HEPES, thapsigargin, wortmannin, nifedipine and bovine insulin were obtained from Sigma and used without further purification. Fluo-4AM was from Molecular Probes. Unless otherwise stated, all chemicals for islet and cell culture were obtained from Life Technologies. All other chemicals were from Fisher unless noted and were of highest purity available.

Stock solution of 100 μM insulin was prepared by dissolving bovine insulin in 20 ml of 5 mM HCl and discarded after 2 days. Stock solutions of thapsigargin and wortmannin were prepared at 5 mM and 1 mM in DMSO while 20 mM nifedipine stock solution was prepared in absolute ethanol. Fluo-4AM was prepared at 1 mM in DMSO. All stock solutions were stored at 4° C.

Isolation and *In Vitro* Culture of Mouse β-Cells

Islets were isolated from 20-30 g CD-1 mice as described in Appendix A. Briefly, islets were isolated by ductal injection with collagenase type XI and dispersed into single cells by shaking in dilute (0.025%) trypsin/EDTA for 8 min at 37° C (Appendix A). Cells were cultured on 35 mm tissue culture dishes (Nunclon) or 25 mm glass coverslips at 37° C, 5% CO_2, pH 7.4 in RPMI 1640 containing 10% fetal bovine serum, 100 U/ml penicillin and 100 μg/ml streptomycin and used on days 2 to 4 following isolation.

Culture of βTC3 (IRS-1^+/IRS-$1^?$) and (IRS-1^-/IRS-1^-) Cells

βTC3 cells expressing the IRS-1 protein and IRS-1 specific knockouts were graciously obtained from Dr. Rohit Kulkarni of Harvard Medical School. βTC3 cells were cultured in 200 ml tissue culture flasks in Dulbecco's Modified Eagle Media (DMEM) containing 25 mM d-glucose, 10% fetal bovine serum, 100 U/ml penicillin and 100 μg/ml streptomycin at 37° C, 5 % CO_2. Cells were passaged with 0.025 % trypsin/EDTA at 70 % confluence and plated onto 35 mm tissue culture plates (Nunclon) for single cell experiments. Cells were used on days 2-5 following passage.

Amperometric Detection of Exocytosis

Microelectrodes were constructed consisting of carbon fiber disks sealed in glass micropipettes and were polished to a 45° angle and cleaned prior to use (Chapter 2; Huang et al., 1995; Aspinwall et al., 1997). Amperometric measurements were made by positioning microelectrodes ~1 μm from a cell and applying stimulant from a micropipette ~ 30 μm from the cell as described elsewhere (Chapter 2; Huang et al., 1995; Aspinwall et al., 1997). All experiments were performed with cells at 37° C incubated in pH 7.4 Kreb's Ringer buffer (KRB) containing (in mM): 118 NaCl, 5.4 KCl, 2.4 $CaCl_2$, 1.2 $MgSO_4$, 1.2 KH_2PO_4, 3 *d*-glucose and 20 HEPES. Stimulant solutions (50 or 100 nM insulin and 17 mM glucose) were prepared by diluting insulin stock solution or dissolving *d*-glucose to the desired concentration of stimulant in KRB. KCl, 30 mM, was prepared as above but by removing an equal concentration of NaCl to maintain ionic strength.

Amperometry was performed using a battery to apply potential to a silver-silver chloride (Ag/AgCl) reference electrode as previously described (Chapter 2; Aspinwall et al., 1997). For measurements of 5-HT secretion, dispersed β-cells were incubated in tissue culture media containing 0.5 mM 5-hydroxytryptophan for 16 hours at 37° C, 5% CO_2, pH 7.4. Cells were used for secretion experiments immediately after loading. For detection of 5-HT the potential at the working electrode was 0.65 V vs. Ag/AgCl. Data were low pass filtered at 100 Hz and collected at 500 Hz using a personal computer (Gateway 2000 P5-166) via a data acquisition board (Axon Instruments, DigiData 1200B).

Thapsigargin, Wortmannin, and Nifedipine Treatments

Mouse β-cells were stimulated with 100 nM insulin and exocytosis of 5-HT detected by amperometry to establish viability. Following successful stimulation with 100 nM insulin, 1 μM wortmannin, 1 μM thapsigargin or 20 μM nifedipine was added to the buffer and allowed to incubate for 5 minutes. The same cell was then stimulated again with 100 nM insulin in the presence of the chemical added.

Confocal Imaging of $[Ca^{2+}]_i$

All imaging experiments were performed in collaboration with Mr. Weijun Qian on a Nikon RCM 8000 laser scanning confocal microscope, consisting of a Nikon Diaphot 300 invert microscope, an argon-ion laser (INNOVA Enterprise 622, Coherent), associated optics and mechanical and computer control units. Prior to imaging experiments, 25 mm coverslips containing adherent cells were loaded with 1 μM fluo-4AM in DMSO for 30 min at 37° C.

Dye solution was then replaced with KRB and coverslips with adherent cells were placed into a 35 mm coverslip holder for immediate use. Temperature was maintained at 37° C on the stage of a Nikon Diaphot 300 microscope through use of a microincubator (Medical Systems, Corp, Greenvale, NY) and temperature controller (Warner Instruments, Hamden, CT). Experimental buffers were the same composition as those used for amperometric measurements. Images were collected using a photomultiplier tube at 1 Hz through a Nikon 40x, (NA 1.15) water-immersion objective and 520 ± 10 nm bandpass filter using the 488 excitation line of the laser. Images were stored on an optical disc cartridge (TQ-FH332, Panasonic) for later analysis.

Image Analysis

The images were played back from the optical disk cartridge, captured and analyzed using Simca image analysis software (C-IMAGING Systems, Cranberry Township, PA) in combination with an 8-bit frame grabber. Regions of interest (ROI) consisting of either the entire cell or localized intracellular regions were drawn by free hand and applied to a series of images. The average intensity of the ROI were measured as a function of frame number.

Data Analysis

Amperometric current spikes were analyzed as described in Appendix B. For data analysis, spikes were used only if the signal-to-noise ratio was > 10. All means are reported ± 1 standard error of the mean (SEM). Statistical differences between means were evaluated using a two-tailed Student's *t*-test.

Results

Insulin-Stimulated Release of Intracellular Ca^{2+} Stores

As shown in Figure 5-1 application of 100 nM insulin, but not buffer solution, results in increased $[Ca^{2+}]_i$ as monitored by fluo-4, a Ca^{2+} sensitive fluorescent indicator. Localization of the $[Ca^{2+}]_i$ changes within the cell appear to initiate inside the cell, not at the cell membrane as observed with depolarizing stimuli such as glucose (Theler et al., 1992). Figure 5-2 shows further analysis of the images shown in Figure 5-1 where the relative intensity change (% basal) was measured by drawing regions of interest (ROI's) around the entire cell. The data shown in Figures 5-1 and 5-2 is representative of 8 of 11 experiments; however in the other 3 repetitions, the localized increase in $[Ca^{2+}]_i$ was followed by large changes over the entire cell (data not shown) following application of 100 nM insulin.

The localization and magnitude of the Ca^{2+} changes observed following application of insulin suggest that the increase in $[Ca^{2+}]_i$ is a result of mobilization from intracellular Ca^{2+} stores. In order to further elucidate the mechanism of $[Ca^{2+}]_i$ increase, thapsigargin, an agent which depletes intracellular Ca^{2+} stores, was applied to the cells. Figure 5-1 shows a representative series of images from 2 separate experiments. Cells were first stimulated with buffer to ensure no membrane damage to the cell (Figure 5-1A). Following buffer stimulation, 100 nM insulin was applied to the cells and Ca^{2+} changes were observed (Figure 5-1B). After successful stimulation with insulin, 5 μM thapsigargin was added to the buffer and allowed 5-10 minutes to equilibrate. Following incubation, stimulation with 100 nM insulin was unable to increase $[Ca^{2+}]_i$ (Figure 5-1C), strongly suggesting the requirement for mobilization from intracellular stores as a requirement for insulin-stimulated $[Ca^{2+}]_i$ changes in the pancreatic β-cell. In a series of control experiments, 100 nM insulin was applied twice with a 5 minute gap between stimulations and $[Ca^{2+}]_i$ changes of similar localization and magnitude were obtained (data not shown).

Requirement of Intracellular Ca^{2+} Mobilization for Insulin-Stimulated Exocytosis

After observing intracellular Ca^{2+} mobilization following insulin stimulation, we investigated the possible requirement of Ca^{2+} mobilization on insulin-stimulated exocytosis. As seen in Figure 5-3, application of 100 nM insulin to a single, dispersed β-cell results in detection of exocytosis at the microelectrode. Previous studies have shown this to be a result of insulin secretion from single β-cells (Aspinwall et al., 1999). Following repetitive stimulation with 100 nM insulin to ensure viability, β-cells were incubated with 5 μM thapsigargin for 5- minutes. As illustrated in Figure 5-3, addition of thapsigargin completely abolished exocytosis from the same cell (n = 4 cells) suggesting the requirement of intracellular Ca^{2+} mobilization for insulin-stimulated insulin secretion.

Effects of Nifedipine on ISIS

In previous studies, removal of extracellular Ca^{2+} resulted in no difference in the ability of insulin to elicit secretory activity from single β-cells. This, combined with the localization of the $[Ca^{2+}]_i$ changes and the suppression of insulin-stimulated $[Ca^{2+}]_i$ changes and secretion by thapsigargin strongly suggest the release of Ca^{2+} from intracellular stores modulates secretory activity in the β-cell. However, a large $[Ca^{2+}]_i$ increase was observed in 3 of 11 cells that appears to result from entry of extracellular Ca^{2+}. Additionally, slight depolarization of the cell membrane was observed in some cases, creating the possibility that voltage gated Ca^{2+} channels could be involved in the pathway. Since no EGTA was used to buffer the Ca^{2+} in the media, it is possible that some residual Ca^{2+} entered the cell through a voltage gated Ca^{2+} channel. Since simultaneous $[Ca^{2+}]_i$ and secretion measurements were not performed due to experimental limitations (see Chapter 2), it is unclear if cells exhibiting this large change in $[Ca^{2+}]_i$ are more likely to undergo exocytosis. To rule out this possibility, cells were stimulated with 100 nM in the presence and absence of 20 μM nifedipine, an inhibitor of L-type Ca^{2+} channels. As demonstrated in Figure 5-4, application of nifedipine did not significantly alter the ability of 100 nM insulin to elict secretory activity in dispersed β-cells. Additional analysis shows that the number of secretory events elicited per insulin stimulation were statistically similar in both cases (Figure 5-5). This data, combined with the Ca^{2+} imaging experiments and thapsigargin strongly suggest a mechanism where insulin activates release of intracellular Ca^{2+} stores thereby generating exocytosis.

Involvement of IRS-1 in Insulin-Stimulated Insulin Secretion

We have previously demonstrated that application of insulin to single β-cells elicits exocytosis of insulin through interaction with the β-cell insulin receptor. Insulin receptor substrates (IRS) proteins are intimately coupled to the insulin receptor and hence the insulin signaling pathway (White, 1997). In order to investigate the pathway involved in autocrine activation of β-cell secretion, we studied insulin stimulation in βTC3 cells lacking IRS-1 through gene disruption. Figure 5-6 shows data from control and IRS-1 knockout cells using amperometric detection of accumulated 5-HT. In previous work, it was demonstrated that 5-HT and insulin are co-released from the same secretory vesicles, hence detection of 5-HT serves as a marker of insulin secretion (Chapter 2; Aspinwall et al., 1997; Aspinwall et al., 1999). As seen in the figure, control cells stimulated with 25 or 100 nM insulin leads to detection of accumulated 5-HT released by exocytosis (n=16 of 33 cells). In the IRS-1 knock out cells, no secretory activity was detected upon application of 100 nM insulin (n=25 of 25 cells) but exocytosis was detected in IRS-1 knockout cells stimulated with 30 mM K^+ (n= 8 of 12 cells). Of IRS-1 knockout cells stimulated with both K^+ and insulin as shown in Figure 5-6, 3 of 4 responded to K^+ but none to insulin.

Wortmannin Sensitivity of ISIS

After observing IRS-1 involvement in insulin stimulation of exocytosis in the β-cell, we investigated the role of phosphotidylinositol 3-kinase (PI-3K) in insulin-stimulated insulin secretion. PI-3K is activated by IRS-1 in many cell types and serves as a mediator between the insulin receptor and many down stream proteins containing SH2 domains. Figure 5-7 shows exocytosis elicited by application of 100 nM insulin to a single, dispersed β-cell. Following repetitive stimulation with 100 nM insulin to ensure viability, β-cells were incubated with 1 μM wortmannin, an inhibitor of PI-3K for 5 minutes. As illustrated in Figure 5-7, addition of wortmannin completely abolished exocytosis from the same cell (n = 4 cells) suggesting the requirement of PI-3K as an important signaling molecule in the insulin-stimulated insulin secretion pathway.

Discussion

Autocrine activation of insulin secretion in the pancreatic β-cell is a novel discovery with potential clinical importance. The discovery that functional insulin receptors on the β-cell play a potential role in normal regulation of insulin secretion provide the first direct link between impaired insulin secretion and insulin resistance in non-insulin dependent diabetes mellitus (NIDDM) (Aspinwall et al., 1999; Kulkarni et al., 1999). Investigation of the physiological mechanisms by which insulin exerts the stimulatory effect on insulin secretion from the β-cell are therefore essential. Recent studies have shown impaired glucose tolerance and insulin secretion in mice genetically altered to abolish the autocrine pathway in the β-cell (Kulkarni et al., 1999; Withers et al., 1998). In order to determine the possible defects in the autocrine pathway that could contribute to impaired insulin secretion seen in NIDDM, the autocrine signaling pathway within the β-cell must be further characterized.

The observation of $[Ca^{2+}]_i$ changes following insulin stimulation was quite surprising considering the independence on extracellular Ca^{2+} of insulin stimulation of exocytosis. This suggests that the increase in $[Ca^{2+}]_i$ is mediated by release of IP_3-sensitive Ca^{2+} stores within the β-cell based on the thapsigargin and imaging experiments. It is likely that the release of Ca^{2+} activates PKC leading to exocytosis. Activation of PKC has previously been demonstrated to elicit exocytosis independent of entry of Ca^{2+} from the extracellular environment (Eliasson et al., 1996). While the exact nature of stimulatory effect of PKC is presently unclear, it is generally believed that PKC is involved in priming and transport of secretory vesicles into a readily releasable position.

Figure 5-8 presents a summary of the proposed mechanism of activation within the β-cell based on the data presented here. Autocrine activation of insulin secretion in the β-cell is mediated by activation of IRS-1 and PI-3K, leading to production of phosphatidylinositol (3,4,5) triphosphate (PIP_3). Increases in cellular PIP_3 lead to activation of PLC, thereby increasing the IP_3 concentration within the cell. This leads to release of Ca^{2+} from the endoplasmic reticulum likely causing activation of PKC. Previous investigations of autocrine activation in the β-cell have suggested the insulin response is mediated by IRS-2 (Leibiger et al., 1998); however, the results presented here and in other reports (Kulkarni et al., 1998a) make it unlikely that IRS-2 is involved in the stimulatory effect of insulin on exocytosis in the β-cell.

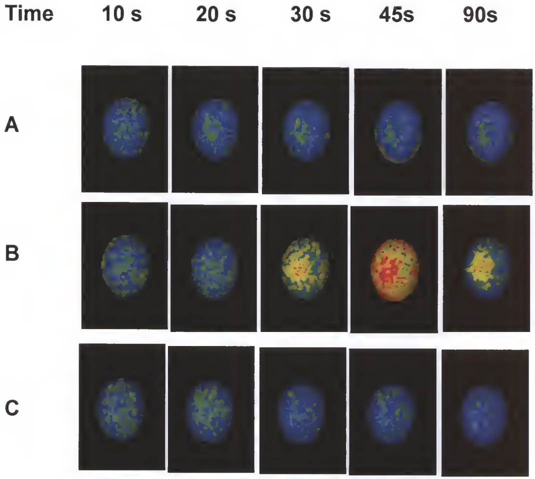

Figure 5-1. Confocal fluorescence microscopy of $[Ca^{2+}]_i$ in response to insulin stimulation. Images were collected at 1 Hz using the fluorescent Ca^{2+} indicator, fluo-4 and ratioed against the first image in the series as described in text. Image series are A) control stimulation, B) stimulation with 100 nM insulin and C) 100 nM insulin following addition of 5 μM thapsigargin. Stimulant was applied from 25-55 s. Scale is indicated as ratio values where blue = 1 to red = 1.5.

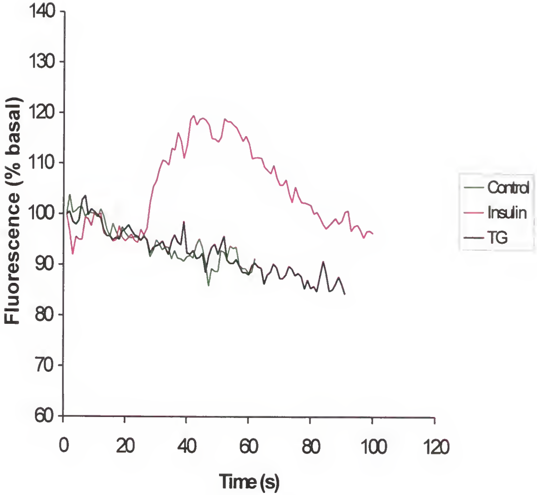

Figure 5-2. Whole cell Ca^{2+} changes in response to insulin stimulation. Whole cell fluorescence was obtained by drawing regions of interest around the entire cell and applying the ROI to the entire series. Data series presented is the same series shown in Figure 5-1. Stimulant was applied from 25 to 55 s. Thapsigargin (TG) was applied as indicated in text. Detailed experimental conditions given in text.

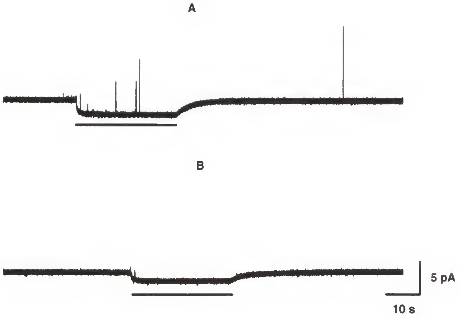

Figure 5-3. Effects of thapsigargin on insulin-stimulated insulin secretion. Data represents amperometric detection of 5-HTfrom single β-cell upon stimulation with 100 nM insulin in the A) absence and B) presence of 5 μM thapsigargin. Data is from same cell. Bars under current trace indicate application of stimulant.

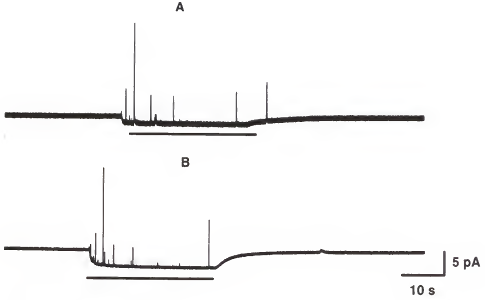

Figure 5-4. Effect of nifedipine on insulin-stimulated insulin secretion. Detection of accumulated 5-HT from single β-cells in the A) absence and B) presence of 20 μM nifedipine upon stimulation with 100 nM insulin. Bars under current trace indicate application of stimulant.

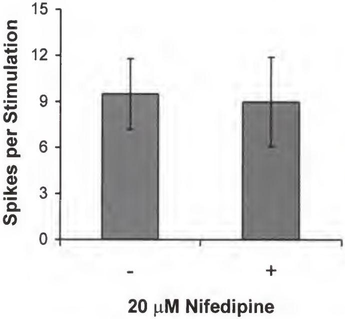

Figure 5-5. Effects of nifedipine on frequency of secretory activity elicited by application of 100 nM insulin from single β-cells. There is no statistical difference in the average number of spikes obtained per stimulation in the presence or absence of 20 μM nifedipine.

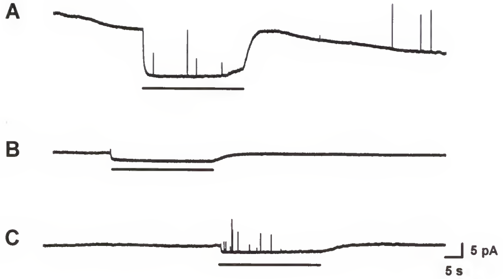

Figure 5-6. Detection of insulin-stimulated exocytosis in control and IRS-1 knockout βTC3 cells. Detection of accumulated 5-HT from A) control βTC3 cell stimulated with 100 nM insulin B) IRS-1 knockout cell stimulated with 100 nM insulin and C) IRS-1 knockout cell stimulated with 30 mM K^+. Data in B) and C) are from same cell. Bars under current traces indicate application of stimulant.

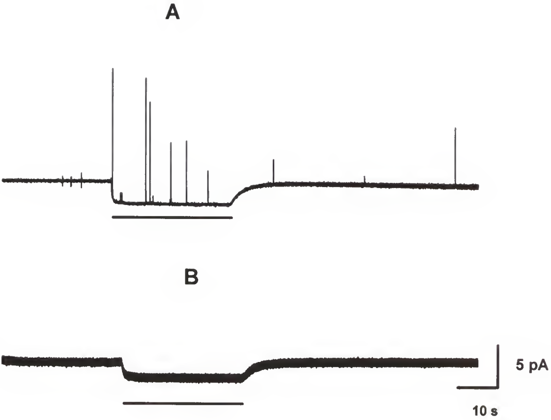

Figure 5-7. Effect of wortmannin on insulin-stimulated insulin secretion. Amperometric detection of 5-HT secretion upon stimulation of single β-cells with 100 nM insulin A) before and B) after addition of 1 μM wortmannin. Data is from same cell. Bars under current traces represent application of stimulant.

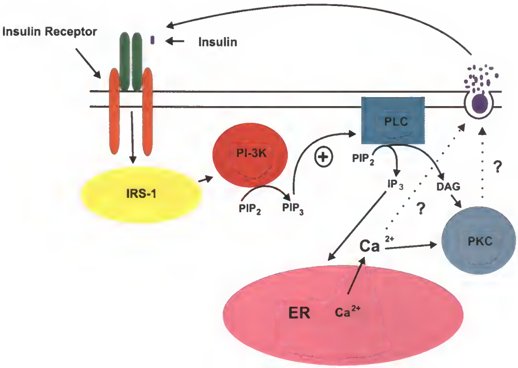

Figure 5-8. Summary of insulin signaling pathway involved in autocrine activation of pancreatic β-cell.

CHAPTER 6
COMPARISON OF SECRETORY ACTIVITY FROM FRESH AND CRYOPRESERVED PANCREATIC ISLETS AND BETA-CELLS

Introduction

The study of pancreatic islets and β-cells is of great interest due to the role of insulin secretion in both insulin-dependent (IDDM) and non-insulin dependent (NIDDM) diabetes mellitus. IDDM is a disease associated with loss of islet mass through autoimmune destruction of the pancreatic β-cell (Atkinson and Maclaren, 1994). The resulting pathology is loss of basal, as well as non-glucose and glucose-stimulated insulin secretion due to reduction of functional β-cells (Pfeifer et al., 1981). NIDDM, in contrast, results in elevated blood glucose levels through either defective insulin secretion from the β-cell or insulin resistance in the peripheral tissues (Taylor, 1999). Due to the complications and impact of both forms of the disease, development of novel research and treatment methodologies are of great importance.

Due to variations in the pathology of the diseases, treatments for IDDM and NIDDM cases vary considerably. NIDDM can most often be controlled through careful monitoring of dietary intake along with moderate physical activity (Kahn, 1998). Patients with IDDM however, are generally treated with intravenous injections of insulin at predetermined times. Since injection of insulin occurs in large doses instead of the smaller, tightly regulated physiological insulin changes in non-diabetics, maintenance of normoglycemia is quite difficult leading to long term health problems (Taylor, 1999). Furthermore, blood glucose levels must be closely monitored following injection to prevent onset of hypoglycemia; however, this is undesirable due to the physical discomfort of available testing methods and the reliance upon patient compliance. The net result of the complications associated with IDDM is a life expectancy that is ~ 15 years shorter than that of non-diabetics (Harris, 1995). Therefore, alternative treatment pathways leading to normal regulation of glucose homeostasis in IDDM are highly desirable.

A possible treatment for IDDM would be to replace the lost β-cell mass through islet transplantation, thereby restoring physiologically regulated insulin secretion. Clinical transplantation of pancreatic islets has, in fact, been used with limited success to induce insulin independence in some IDDM patients (Scharp et al., 1990; Scharp et al., 1991). A major obstacle to successful treatment of IDDM by islet transplantation has resulted from the inability to isolate sufficient numbers of viable islets from the human cadaveric donor pancreas. To circumvent this problem, cryopreservation and low temperature banking of isolated islets has been developed, allowing islets from multiple donors to be pooled prior to transplantation (Hering et al., 1993; Warnock et al., 1991; Warnock et al., 1992). Additionally, cryopreservation allows storage of islets until donor specific tolerance is established, greatly diminishing the occurrence of transplant rejection (Bretzel et al., 1986; Gray et al., 1984; Lakey et al., 1996; Rajotte et al., 1995). Low temperature banking of islets also allows assessment of both sterility and viability prior to transplantation, thus improving the safety and success of the procedure (Rajotte et al., 1995).

While treatment IDDM is the primary driving force for cryopreservation studies on pancreatic islets, research efforts focusing on NIDDM could also potentially benefit from these studies. The ability to obtain pancreatic islets and β-cells is a necessity for studies of physiological regulation of insulin secretion. In large animal and human islet isolations, typical yields are in excess of 1 million islets (Warnock et al, 1994a; Ricordi et al., 1988). Typical studies of insulin secretion involve the use of fewer than 10,000 islets during the *in vitro* culture time, which is limited to less than two weeks in most cases. This results in considerable waste of islet tissue that is difficult and expensive to obtain. The ability to cryopreserve islets for future use would markedly reduce the islet waste, research costs and the number of animals sacrificed.

While cryopreservation of pancreatic islets introduces several potential advantages to research and transplantation studies, there are many limitations. For example, previous studies have reported a loss of islet mass and reduction in insulin secretion following cryopreservation, thawing and the subsequent period of tissue culture (Moser and Warnock, 1991; Warnock et al., 1994b). These losses are highly variable depending on the species of islets cryopreserved and the condition of the islets following isolation . A further complication is the limited availability of human cadaveric pancreas donors, severely limiting the ability to successfully cryopreserve human islet tissue for both transplantation and research purposes.

The physiological mechanism for the loss of insulin secretion following cryopreservation has yet to be elucidated, making it unclear if the observations are produced by defects in the β-cell, defects in intraislet communication or simply from the loss of islet mass. It has been demonstrated that β-cells in islets secrete more insulin per cell than purified β-cell preparations (Pipeleers et al., 1982). Due to the high level of functional dependence of the β-cell on other cell types within the islet, it is feasible that the reduced insulin secretion observed following cryopreservation could result from losses or damage to non-β-cells as well as a loss in β-cell function. Analysis of insulin secretion from single β-cells prior to and following cryopreservation of isolated islets would provide unique information that would greatly advance the understanding of the nature of these defects, as well as validate the use of cryopreservation as a method of islet storage for fundamental β-cell research. To date, direct analysis of secretory function from single β-cells has not been possible due to the lack of available methods for monitoring the sub-femtomole amounts of insulin released from single β-cells with suitable temporal resolution.

Recently, amperometry has been used for detection of insulin secretion from individual β-cells, *in vitro* (Kennedy et al., 1993; Huang et al., 1995; Aspinwall et al., 1997; Aspinwall et al., 1999). Amperometric detection of exocytosis has been demonstrated to possess the sensitivity, spatial resolution and temporal resolution necessary to detect single exocytosis events allowing a novel method for the study of individual β-cell function (Huang et al., 1995). For amperometric detection of insulin, a carbon fiber microelectrode chemically modified with a mixed valent film of ruthenium oxide and cyanoruthenate is positioned adjacent to a single β-cell (Kennedy et al., 1993; Huang et al., 1995). Following stimulation of the β-cell, a series of current spikes is observed resulting from oxidation of insulin contained within individual secretory vesicles (Kennedy et al., 1993; Huang et al., 1995). An alternative method for detection of exocytosis from single β-cells is to "load" the β-cells with an electrochemical marker, specifically 5-hydroxytryptamine (5-HT) or its precursor 5-hydroxytryptophan (5-HTP). 5-HT has been demonstrated to accumulate into insulin containing secretory vesicles in the β-cell and is co-released with insulin (Chapter 2; Hellman et al., 1972; Smith et al., 1995; Aspinwall et al., 1997). Therefore, exocytosis of 5-HT can be detected by amperometry with a bare carbon fiber microelectrode and can serve as a marker of insulin secretion from single β-cells.

Amperometric detection of insulin secretion has been used to reveal novel information into the physiological mechanisms of insulin secretion (Kennedy et al., 1996; Aspinwall et al., 1997; Aspinwall et al., 1999). Detection of 5-HT has also been useful in elucidating many details of the stimulus-secretion coupling pathways present in the β-cell (Smith et al., 1995; Takahashi et al., 1999; Aspinwall et al., 1999). Because of the sensitivity and the spatial resolution to detect single exocytosis events, this method is ideal for investigating single cell function. Here, we use amperometry to compare insulin secretion and β-cell function in cell populations from fresh and frozen-thawed pancreatic islets.

It was determined that the amount of insulin released per secretory event is equivalent for both freshly isolated and frozen-thawed canine islets following cryopreservation. Additionally, the observed frequency of secretory events detected from single β-cells following stimulation with tolbutamide and muscarine, known insulin secretagogues, was equivalent in both fresh and frozen thawed canine islets indicating that common elements of stimulus-secretion coupling pathways remain intact following cryopreservation and thawing. Finally, response to glucose in both fresh and frozen-thawed islets was equivalent. Taken together, the results indicate that under appropriate cryopreservation conditions, loss of β-cell function can be minimized suggesting a larger role for cryopreservation in future transplantation studies.

Experimental

Chemicals and Reagents

All reagents used for islet isolation and tissue culture were from Life Technologies. Collagenase (Liberase-CI) and DNAse were supplied by Roche Molecular Biochemicals (Indianapolis, IN). HEPES, tolbutamide, isobutylmethylxanthine (IBMX) and muscarine chloride were from Sigma and were used without further purification. All other chemicals were from Fisher and were of the highest available purity.

Islet Isolation and *In Vitro* Culture

Pancreatic islets were isolated from mongrel dogs using controlled collagenase perfusion via the duct, automated dissociation and discontinuous Euro-Ficoll purification using the COBE 2991 blood cell processor as previously described (Ricordi et al., 1988; Warnock et al., 1994a). Islet mass was quantified by two independent investigators. Recovery of islets following culture and cryopreservation was determined by comparing the yield of thawed, cultured islets to the yield of islets immediately following isolation. Groups of purified islets were placed in CMRL tissue culture medium supplemented with 10% heat inactivated fetal calf serum, and antibiotics (penicillin/streptomycin) and divided into two groups. One group was cultured overnight before dispersion into single cells. The second group of islets was cryopreserved and stored in liquid nitrogen until further use. Aliquots from each experimental group were evaluated for *in vitro* islet survival and functional viability.

Cryopreservation of Islets

The cryopreserved islets were frozen and thawed using established techniques (Rajotte et al., 1995; Rajotte and Mazur, 1981). Briefly, islets were equilibrated with the cryoprotectant dimethylsulfoxide (DMSO) and supercooled to -7.5° C. Tubes containing the islets were then nucleated, and slowly cooled at 0.25° C/minute to -40° C before being plunged into liquid nitrogen for low temperature storage. Islets were rapidly thawed at 200° C/minute to 0° C in a 37° C water bath before the DMSO was removed using a sucrose dilution protocol (Lakey et al., 1997; Rajotte et al., 1995). Following the freeze/thaw process, multiple samples were removed for post isolation recovery, viability assessment and dispersion into single cells.

Islet Dispersion

Islets were dispersed into single cells using a previously described method (Appendix A; Kennedy et al., 1993). Briefly, islets were washed 2 times in Ca^{2+}/Mg^{2+} free HBSS, then exposed to the enzyme blend versene, followed by digestion with 1 mg/mL trypsin (1:250). Cells were plated in 0.1 mL aliquots onto tissue culture dishes and incubated at 37° C, 5 % CO_2 for 1-2 hours. Media was then added and cells were maintained at 37° C, 5% CO_2 until use.

Assessment of Islet Viability

In vitro functional viability of both the freshly isolated and cryopreserved islets was assessed by incubation in RPMI tissue culture medium containing either 2.8 mM glucose or 20 mM glucose supplemented with 50 μM IBMX (Warnock et al., 1994b).

After a two-hour incubation at 37° C, the supernatant was removed and assessed for insulin content using a radioimmunoassay kit and human insulin standards (Coat-a-count). Insulin secretion of the freshly isolated and cryopreserved islets was expressed per islet equivalent and the stimulation index (SI) was calculated by dividing the insulin output during stimulation with high (20 mM) glucose plus IBMX by insulin output during low (2.8 mM) glucose incubation.

Single Cell Experiments

Amperometric detection of exocytosis from isolated, single β-cells was performed with a carbon fiber microelectrode which was positioned 1 μm from the cell using a piezoelectric micropositioner (Burleigh, PCS 250) (Kennedy et al., 1993; Huang et al., 1995). Finished electrodes consisted of a 9 μm carbon fiber sealed with epoxy in the tip of a glass pipette. The electrode was polished at a 35-45° angle using a pipette beveler (Sutter, BV-10) prior to use. For detection of insulin, electrodes were chemically modified to produce a mixed valent ruthenium oxide and cyanoruthenate film as previously described (Chapter 2; Kennedy et al., 1993; Huang et al., 1995). Detection of 5-hydroxytryptamine (5-HT) was performed using bare carbon fiber microelectrodes (Chapter 2; Aspinwall et al., 1997). Electrochemical measurements were made using a battery to apply potential to a sodium saturated calomel electrode (SSCE). Currents were monitored at the working electrode using an AI-403 current amplifier and Cyberamp 320 signal conditioner (Axon Instruments). For detection of 5-HT the potential at the working electrode was 0.65 V vs. SSCE. For detection of insulin, the potential at the working electrode was 0.85 V vs. SSCE and electrode potential was held at 0.40 V between recordings to improve electrode stability (Kennedy et al., 1993). For detection of 5-HT secretion, dispersed β-cells were allowed to incubate in tissue culture media containing 0.5 mM 5-HT and 1 mM 5-hydroxytryptophan for 16 hours at 37°C, 5% CO_2, pH 7.40 (Aspinwall et al., 1997). Cells were used for secretion experiments immediately following 5-HT loading.

Amperometric measurements of exocytosis were performed on the stage of a Zeiss Axiovert 100 inverted microscope. Cells were bathed in pH 7.4 Kreb's Ringer Buffer (KRB) containing (in mM), 118 NaCl, 5.4 KCl, 2.4 $CaCl_2$, 1.2 $MgSO_4$, 1.2 KH_2PO_4, 25 $NaHCO_3$, 0.010 forskolin (Barnett et al., 1994), and 3.0 *d*-glucose. Cells were maintained at 37° C and 5% CO_2 on the microscope stage using a microincubator (Medical Systems, Inc., Greenvale, NY). Stimulant solution (200 μM tolbutamide or 40 μM muscarine chloride dissolved in bicarbonate buffer) was applied to individual cells by pressure ejection for 10 seconds from a glass micropipette positioned approximately 30 μm from the cell.

Data Analysis

For analysis, spikes were only counted if the signal-to-noise ratio was greater than 10. Areas for individual secretory events were calculated as described previously (Appendix B; Huang et al., 1995). For spike area determinations, only single, isolated (well-resolved) current spikes resulting from detection of insulin with the chemically modified microelectrode were compared. Results are expressed as mean ± standard error of the mean (SEM). Differences between the experimental groups were analyzed by paired Student's *t*-tests. The differences between the experimental groups were considered statistically significant for $p < 0.05$.

Results

Glucose-Stimulated Insulin Secretion During Static Incubation

In vitro functional viability of freshly isolated and cryopreserved canine islets is shown in Table 6-1. Islets which had been cryopreserved and then cultured for a period of 48 hours at 37° C prior to viability testing resulted in similar basal and glucose-stimulated insulin levels compared with non-frozen controls from the same islet preparation. During stimulation with RPMI solution containing 20 mM glucose and 50 μM IBMX, no statistically significant differences were observed in stimulated insulin response between freshly isolated and frozen-thawed canine islets (Table 6-1). As an additional indicator, the stimulation index, a ratio of the insulin secreted during high glucose plus IBMX over the insulin output during low basal levels, was 10 ± 1.7 for islets which had been cryopreserved and thawed compared with 12 ± 1.2 for the control non-frozen group of islets ($p = ns$) (Table 6-1).

Single β-cell Function Following Cryopreservation

Analysis of single, dissociated β-cells was performed by amperometric detection of insulin or 5-HT (as a marker for frequency of exocytosis events only) following dissociation and stimulation with tolbutamide or muscarine chloride. Figure 6-1 illustrates an example of current recordings obtained for detection of insulin secretion with a Ru-O/CN-Ru modified microelectrode from freshly isolated and cryopreserved canine β-cells upon stimulation with tolbutamide. Isolated current spikes in the trace have previously been shown to result from detection of insulin from single secretory vesicles (Huang et al., 1995). The area of the current spikes is proportional to the number of analyte molecules released and detected according to Faraday's Law (Wightman et al., 1991; Huang et al., 1995). For detection of insulin, the average area per exocytosis event was 0.29 ± 0.02 pC (n = 152 spikes) for freshly isolated β-cells and 0.31 ± 0.03 pC (n = 51 spikes) for frozen-thawed β-cells corresponding to approximately 2.7 ± 0.2 and 2.9 ± 0.3 amol of insulin, respectively (p = ns).

In addition to the similar mean spike areas, the frequency of exocytosis events recorded per stimulation following application of tolbutamide was equivalent between both freshly isolated and cryopreserved islets from a series of seven paired experiments. For stimulation with tolbutamide, an average of 7.0 ± 1.3 spikes per 10 s stimulation were recorded from dispersed β-cells from the freshly isolated islet group compared with 6.0 ± 1.4 for β-cells from the frozen-thawed preparations of islets (minimum of 10 β-cells per run in each experimental group, Figure 6-2).

The viability of the cryopreserved β-cell preparations was further explored by application of muscarine to freshly isolated and frozen-thawed canine β-cell preparations. Muscarinic activation of insulin secretion proceeds via different second messengers than tolbutamide, allowing dissection of possible defects in the β-cell stimulus-secretion coupling pathways caused by cryopreservation. Figure 6-3 shows stimulation with 40 μM muscarine elicits insulin secretion of similar magnitude and frequency in both frozen-thawed and freshly isolated β-cells. In one paired experiment for this stimulant, 6 of 7 β-cells dispersed from the cryopreserved islet group resulted in detection of insulin using the modified electrode, compared to 12 of 19 β-cells from the freshly isolated islet group. As seen in Figure 6-2, the average number of exocytosis events per 10 s stimulation was

10 ± 2.7 (n = 6) for the frozen-thawed β-cells versus 9.2 ± 2.9 (n = 12) for the freshly isolated β-cells (p = ns).

Discussion

The recent development of amperometric methods for time-resolved detection of insulin secretion has allowed investigation of the many unique aspects of insulin secretion, including storage, stimulus-secretion coupling and autocrine activation of the β-cell (Kennedy et al., 1993; Huang et al., 1995; Smith et al., 1995; Kennedy et al., 1996; Aspinwall et al., 1997; Aspinwall et al., 1999). The data presented here shows, for the first time, the effect of cryopreservation on insulin biosynthesis and secretion from single pancreatic β-cells. Thus, the current study suggests that amperometric detection of exocytosis can be a useful tool in the study of β-cell function and insulin secretion from both fresh and cryopreserved islets of Langerhans.

Recovery of functionally viable islets following cryopreservation is a key prerequisite if cryopreservation of pancreatic islets is to be effectively utilized as a method of islet storage for research and clinical transplantation. Previous studies have reported reduced insulin secretion and islet function following cryopreservation and thawing (Moser and Warnock, 1991; Warnock et al., 1994b). It has been suggested that the reduced insulin secretion observed is due damage to the β-cell, specifically the inability of the β-cell to properly synthesize or package insulin (Sandler and Andersson, 1987). The results presented here suggest that the number of secretory events, as well as the amount of insulin released per secretory event is equivalent for β-cells dissociated from both fresh and frozen-thawed canine islets. This observation suggests that insulin biosynthesis, packaging and storage within the secretory vesicle, as well as the exocytotic mechanism of insulin release in the β-cell remains intact following cryopreservation. Therefore regulation of exocytosis in β-cells appears to be unaffected by the cryopreservation process.

Additionally, the observed rate of secretory events detected from single β-cells by amperometry following tolbutamide and muscarine stimulation, which act via different stimulus-secretion coupling pathways, was equivalent in both fresh and frozen-thawed canine β-cells. The action of both stimulants appears to be unaffected by the cryopreservation process suggesting that many of the metabolic processes and signal transduction pathways required for sustained β-cell functional *in vivo,* such as membrane polarization/depolarization and formation of inositol 1,4,5 triphosphate remain intact. As many elements of the glucose-signaling pathway are represented by the combination of secretion coupling with muscarine and tolbutamide, it is reasonable to assume that many of the key elements of glucose signaling in the β-cell also remain unaffected by the cryopreservation process. This is further supported by the equivalent glucose- stimulated insulin release of fresh and cryopreserved islets.

The results from the present study indicate that under appropriate cryopreservation conditions, loss of islet function cannot be attributed to a loss of β-cell function. As assayed by amperometry, β-cells from cryopreserved islets were shown to be capable of synthesizing and secreting equivalent amounts of insulin at frequencies comparable to those from cultured non-frozen islets. This presents the possibility that previous studies that observed a decrease in insulin secretion following cryopreservation were a result of a loss of β-cell mass and not a loss of the ability of the β-cell to synthesize or secrete insulin. However, it is difficult to compare the data presented here to previous reports where a decrease in islet function was observed as the glucose-stimulated insulin secretion obtained here was equivalent for fresh and cryopreserved islets. Taken together, the present data indicate that β-cell function can be maintained following cryopreservation as observed at the single β-cell level by amperometry.

Table 6-1. Insulin secretion from freshly isolated and frozen-thawed canine islets during static incubation. Results are from seven paired experiments. Stimulation index is the insulin secretion at 20 mM glucose + 50 μM IBMX over insulin secretion at 2.8 mM glucose.

Experimental Islet Group	**Insulin Secretion (μU/IE/h)**		**Stimulation Index**
	2.8 mM Glucose	**20 mM Glucose 50 μM IBMX**	
Fresh	1.3 ± 0.2	15 ± 1.1	12 ± 1.2
Frozen-Thawed	1.4 ± 0.2	14 ± 2.4	10 ± 1.7

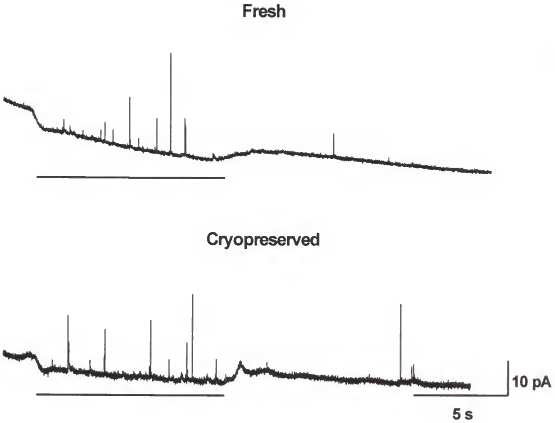

Figure 6-1. Current recordings obtained for detection of insulin secretion from freshly isolated and frozen/thawed canine β-cells. Bars under current trace represent application of 200 μM tolbutamide. Insulin was detected with Ru-O/CN-Ru modified microelectrode as described in text.

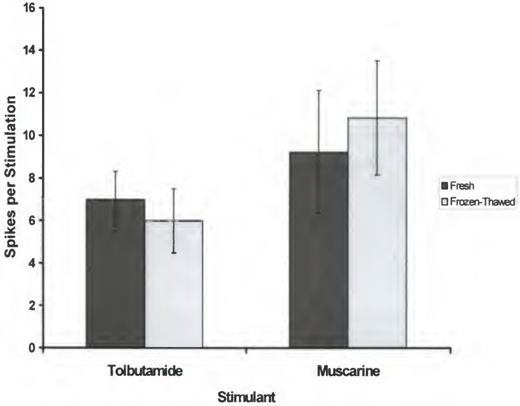

Figure 6-2. Secretory activity from fresh and cryopreserved β-cells upon stimulation with 200 μM tolbutamide or 40 μM muscarine chloride. Stimulation was for 10 s. Spikes were only counted for S/N > 10. Detailed experimental conditions given in text.

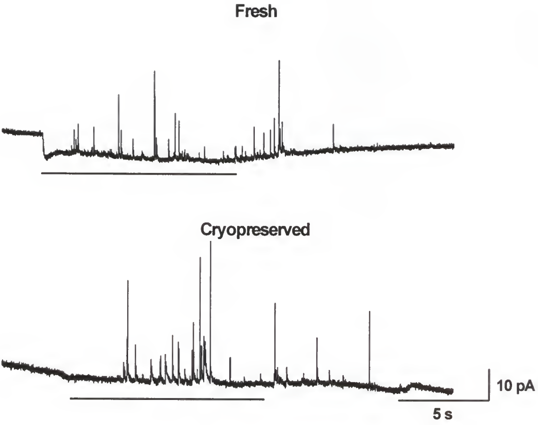

Figure 6-3. Current recordings obtained for detection of insulin secretion from freshly isolated and frozen/thawed canine β-cells. Bars under current trace represent application of 40 μM muscarine chloride. Detailed experimental conditions given in text.

CHAPTER 7
SUMMARY AND FUTURE DIRECTIONS

Summary

Amperometric detection of insulin secretion from single pancreatic β-cells has been used to reveal novel insight into the functionality of single β-cells, as well as the regulation and physiological mechanism of vesicular insulin secretion. Amperometry offers several advantages that make it ideal for these investigations. First, the spatial and temporal resolution achieved has allowed the first direct observation of single granule dissociation kinetics in the β-cell. The sensitivity attained with this method has allowed quantitative study of single-vesicle release events opening new avenues of research from the level of single-vesicle fusion to stimulus-secretion coupling. Due to the ability to investigate the mechanisms of exocytosis at the level of single-vesicle release events, it has been possible to dissect the secretory process from the point of vesicle fusion to the dissociation of insulin to the biologically active form. Furthermore, amperometric detection of exocytosis in the β-cell has allowed the first direct observation and characterization of the physiological effects of autocrine activation of insulin secretion in single β-cells.

Also revealed in this work are some of the chemical events involved in driving post-fusion release of insulin from β-cells. The effects of H^+ and Zn^{2+} on insulin release that were observed are, presumably, a natural manifestation of the complex mechanism of insulin synthesis and storage. However, the nature of insulin storage leads to the unique possibility that environmental control over insulin secretion has led to the evolution of novel regulatory pathways controlling exocytosis of insulin. The fact that the quanta and the rate of insulin release can be altered by variations in the vesicular and extracellular environment raises the possibility that insulin secretion can be regulated by slight fluctuations in the ionic composition, *in vivo*. Such post-fusion control of release has recently been proposed as a novel regulatory mechanism in a variety of cell types (Rahamimoff and Fernandez, 1997) however, few examples have been explored. Post-fusion regulation of insulin release would seem to hold little relevance to the endocrine action of insulin given the large distance between the release site and site of action. Therefore, post-fusion regulation of insulin secretion, likely exerts the physiological effect at the level of autocrine or paracrine signaling within the microenvironment of the islet.

Further investigation of this phenomenon has revealed for the first time, that application of exogenous insulin to single β-cells at physiologically relevant concentrations evokes exocytosis of insulin mediated by the β-cell insulin receptor. Furthermore, activation of the β-cell insulin receptor results in the release of intracellular Ca^{2+} from thapsigargin sensitive stores. The intracellular pathway coupling activation of the insulin receptor to exocytosis and release of Ca^{2+} involves many elements of the traditional insulin signaling cascade including activation of insulin receptor substrate 1, phophatidylinositol 3-kinase and phospholipase C. In addition, factors affecting the concentration of free insulin at the cell membrane have been shown to regulate insulin secretion by post-vesicle fusion control of autocrine feedback providing the first known example of secretory product from one vesicle affecting the secretory activity of the same cell by a positive feedback mechanism.

Perhaps most importantly, these results suggest a possible link between impaired insulin secretion and insulin resistance, both of which can lead to hyperglycemia and are considered hallmarks of Type-II diabetes (Taylor et al., 1994). It is controversial as to which of these events is the underlying cause of the disease. Some reports suggest that impaired β–cell function and hence insulin secretion are the first observable symptoms (Cunningham et al., 1996; O'Rahilly et al., 1988) while others suggest that insulin resistance appears to be the first detectable problem (Martin et al., 1992). The observation that β-cells contain functional insulin receptors and receptor substrates that can mediate autocrine activation in the β-cell strongly suggests that autocrine feedback plays an important role in normal regulation of the pancreatic β-cell (Rothenberg et al., 1995; Xu et al., 1998b; Xu and Rothenberg, 1998; Leibiger et al., 1998; Aspinwall et al., 1999). The participation of insulin receptors on β-cells to increase the amount of insulin secretion and synthesis leads to the possibility of a direct link between dysfunctional insulin secretion and insulin resistance. Such a link is supported by evidence that disruption of the β-cell insulin receptor (Kulkarni et al., 1999) or β-cell receptor substrates (Kulkarni et al., 1998b; Xu et al., 1998a) induces defects in both synthesis and secretion of insulin from the β-cell while disruption the same insulin receptor substrates in the peripheral tissues induces insulin resistance (Withers et al., 1998; Tamemoto et al., 1994).

The data presented here also provide the most conclusive evidence to date that insulin and 5-HT are co-released exclusively from the same secretory vesicles.

Therefore, detection of accumulated 5-HT should serve well as a qualitative marker of vesicle fusion; however, the variability induced by measuring a compound that is not endogenous to the cell excludes quantitative comparisons of 5-HT release to insulin release. These results suggest that detection of accumulated 5-HT can serve as a control for secretory activity in the β-cell; however, interpretation of results obtained using this method should be made with caution, particularly when quantitative or kinetic data for release of insulin are under investigation. Furthermore, in instances where detection of insulin results in low signal-to-noise, particularly rodent β-cells, 5-HT provides a useful marker for secretory activity, allowing direct measurement of exocytosis from single β-cells illustrating the utility of the method for future studies.

The most important limitations to detecting 5-HT as a marker of insulin secretion lie in the inability to quantitatively correlate the amount and rate of insulin and 5-HT released from single secretory vesicles. As different environmental conditions affect both the rate and amount of insulin or 5-HT released per vesicle, it is unlikely that results obtained for 5-HT detection can be accurately applied to release of insulin. Additionally, the interference of 5-HT with fura-2 based $[Ca^{2+}]_i$ measurements in the β-cell severely limit the ability to use detection of 5-HT for simultaneous measurement of $[Ca^{2+}]_i$ and exocytosis. This markedly limits the ability to perform stimulus-secretion coupling experiments, particularly in rodent β-cells and β-cell tumors, the most common experimental models, due to the difficulty of directly detecting insulin.

Future Directions

Investigation of Autocrine Activation of Insulin Secretion

Insulin signaling is an important aspect of survival and normal function in virtually every cell type. However, the mechanisms through which insulin elicits different physiological results using many of the same signaling molecules remains unclear. While several key events in the insulin-stimulated insulin secretion (ISIS) pathway were investigated in the present work, many others remain to be determined. As an example, the effects of insulin signaling of protein kinase C (PKC) remains unclear. PKC is activated by increases in intracellular Ca^{2+}, which was observed following insulin stimulation, as well as diacylglycerol (Howell, 1994). Additionally, PKC can be activated by protein kinase B, which is in turn activated by PI-3K, as well as several other signaling molecules within the cell. It soon becomes clear that the complexity of the intracellular interactions is immense and many additional signaling molecules and pathways need to be investigated before a consolidated picture of normal regulation of insulin secretion can be obtained.

The results presented here demonstrate the importance of autocrine activation of the β-cell *in vitro*. However, the degree of importance in the *in vivo* regulation of insulin secretion is less clear. Mice lacking the β-cell insulin receptor develop symptoms similar to diabetes (Kulkarni et al., 1999); however, several previous studies have suggested that exogenous insulin has no effect on insulin secretion *in vivo*. Further characterization of the physiological consequences of autocrine activation within the islet and whole animal is therefore warranted. The development of techniques to produce tissue-specific gene disrupted mice (Kulkarni et al., 1999; Kulkarni et al., 1998a) should aid in the study of the effects of the autocrine pathway within these models, allowing dissection of the ISIS regulatory pathway both *in vitro* and *in vivo*.

Co-localization of β-cell Insulin Receptors and Exocytosis Sites

One interesting aspect of insulin-stimulated insulin secretion is the localization of insulin receptors on the cell surface in relation to vesicle release sites. Previous data have shown that the β-cell is polarized in both the location of secretory vesicles within the cell (Bonner-Weir, 1988) and the sites of release of insulin at the cell surface (Paras et al., 1999). Since the β-cells contain a very low number of functional insulin receptors (Verspohl and Ammon, 1980), it is likely that the receptors must be co-localized in the vicinity of vesicle release sites in order to achieve maximal autocrine activation. A similar effect has been demonstrated regarding the co-localization of Ca^{2+} channels and insulin-containing secretory vesicles within the β-cell (Bokvist et al., 1995).

Successful determination of this phenomenon will depend on development of novel methodologies that will allow higher spatial resolution and sensitivity, as well as the ability to be easily coupled with other techniques for monitoring changes within the cell and at the cell membrane. While amperometry at carbon fiber microelectrodes can be easily miniaturized to sub-micron levels for localization studies (Paras et al., 1999), the electrodes are inherently single point sensors allowing only one area of the membrane (defined by the size of the electrode) to be monitored at any given time. This leads to several experimental difficulties. For example the localized release sites are less than 2 μm in diameter in many cases making it difficult to find the "hot-spot" (Paras et al., 1999). Techniques that allow determination of secretory activity over the entire membrane simultaneously are therefore desirable.

One such possibility would be the construction of amperometric electrodes that contain multiple sensing elements. Recent advances in microfabrication and nanoparticle technology have allowed construction of carbon micro and nano-structures that could allow miniaturization. This could allow individually addressable micro and nano electrode arrays to be constructed that would be capable of spatially mapping the secretory sites on the cell surface. One potential drawback would be a difficulty in chemically modifying the individual elements of the array to directly detect insulin as the Ru-O/CN-Ru modified electrode (Kennedy et al., 1993) suffers from limited stability. An alternative could be the miniaturization and construction of a sol-gel electrode array based on the recently reported dirhodium catalyst capable of oxidizing cystine at physiological pH (Tess and Cox, 1998).

Another approach is the measurement of Zn^{2+} release by confocal fluorescence microscopy. Zn^{2+} is co-released with insulin from the secretory granules with identical temporal and spatial characteristics. Confocal microscopy offers the ability to image low intensity fluorescent processes due to the ability to reject background fluorescence (Tsien and Bacskai, 1995). When coupled with a Zn^{2+} specific fluorescence indicator, secretory activity would be observed at the cell membrane with spatial resolution near the diffraction limit. More importantly, secretory activity from the entire cell could be observed simultaneously assuming high enough temporal resolution can be achieved. Preliminary investigations using zinquin, a highly specific Zn^{2+} fluorophore that increases its fluorescence intensity upon binding (Zalewski et al., 1993; Mahadevan et al., 1996), have revealed the utility of the confocal imaging technique. Additionally, confocal detection of Zn^{2+} has confirmed observations of localized secretion made by amperometry. In combination, amperometry and Zn^{2+} fluorescence microscopy provide an experimental arsenal suitable for determination of localized insulin secretion.

In addition to localization of secretory sites, methodologies must be developed and employed to localize insulin receptors on the β-cell membrane if correlation is to be achieved. Traditional studies of insulin receptor localization have relied upon immunohistochemistry using electron microscopy (Patel et al., 1982; Orci, 1985) or fluorescence microscopy (Michel and Parsons, 1990). Unfortunately, the majority of available protocols using these methods rely on fixing the cells in order to visualize receptor binding. This is problematic for studies involving detection of exocytosis as the cell must remain functional. While electron microscopy could be used to reveal the location of vesicles in relation to the insulin receptor, it would not correlate to the actual location of release. Therefore, development of confocal microscopy techniques capable of imaging receptors on the surface of living cells is warranted in order to perform localization studies of the ISIS effect on the β-cell.

APPENDIX A
ISOLATION AND PREPARATION OF PANCREATIC ISLETS AND BETA-CELLS

Procurement and Handling of Canine, Porcine, and Human Islets

Canine, porcine and human islets of Langerhans are supplied through ongoing research collaborations with Dr. Jonathan Lakey and Dr. Camillo Ricordi. Islets are isolated and shipped overnight via FedEx following isolation. Several aspects must be considered before islets are used for single cell experiments. First, islet purity is of utmost importance. If the islet preparation contains more than 20% acinar tissue, it is better not to use the islets for single cell experiments. This significantly lowers the probability of finding β-cells and also leads to growth of fibroblasts on the tissue culture plates which cover the plate by the second to third day of culture. As fibroblasts grow on the tissue culture plates, they grow over the top of the β-cells, blocking the detection of insulin with microelectrodes. A second issue that must be considered is the *in vitro* culture time of the islets. Typically, islets are cultured for 1-3 days before being shipped. If the islets have been in culture for more than 2 days total (including the shipping time), it is best to use them only for single-islet experiments. Islets become more fragile in culture leading to increased sensitivity to the dispersion enzymes, thereby increasing the likelihood of cell damage. Finally, sterility in handling must be strictly observed. Islets that have been in culture are much more easily contaminated than freshly isolated islets necessitating strict adherence to sterile procedures.

Upon receipt, islets should be checked for sterility, purity and structural integrity. For this purpose, the exterior of the islet container is sterilized with 70% ethanol followed by 70% isopropanol. After the islets are mixed thoroughly by shaking the centrifuge tube in which they arrive, a 3 ml aliquot is removed and transferred to a 35 mm tissue culture dish. The sample is then observed under both a dissecting microscope at 40X magnification and an inverted, compound microscope at 400X (or greater). Observation under the dissecting microscope allows determination of structural integrity and purity. Islets have a golden color (Figure A-1) while acinar tissue will be gray or black. Also, islets are more dense and have a spherical or oblate spherical shape while acinar tissue is less organized structurally. In many cases, large animal islets will be over-digested, making it more difficult to distinguish between islet tissue and acinar tissue. Experience will help aid in purity determinations. Finally, the sample should be observed under the higher magnification to check for bacterial contamination. Typical bacteria can be seen as 1-2 μm rod shapes that move randomly in tissue culture media, if present. If bacteria are present in this initial stage, islets should be discarded immediately.

Isolation of Rodent Islets

Mouse and rat islets are isolated in-house through the following procedure. A typical isolation is performed on two animals, either mice or rats, simultaneously. Each pancreas is treated separately from the surgical stage onward. Buffer solutions must be prepared fresh on the day of isolation but can be made from dilution of a Mg^{2+} and Ca^{2+} free 10X stock solution if desired. One liter of Ca^{2+} free solution should be prepared with the following composition (in mM): 137 NaCl, 5.4 KCl, 0.41 NaH_2PO_4, 0.41 Na_2HPO_4, 1 $MgCl_2$, 5 *d*-glucose, 10 HEPES adjusted to pH 7.37 ± 0.02 with NaOH. Following adjustment of pH, remove 100 mL of buffer solution. To the remaining 900 ml of solution, add 1.26 mM $CaCl_2$ from a 1 M stock solution, mix thoroughly and filter both solutions through a sterile, 0.22 μm pore size, bottle top membrane filter (Nalgene). Both solutions should then be stored on ice and bubbled with O_2 for 5 min each with sterile gas dispersion stones.

Immediately prior to animal surgery, gradient and enzyme solutions should be prepared. Enzyme solution is prepared by dissolving Sigma Collagenase Type XI (0.7 mg/ml for mice and 1.5 mg/ml for rats) in Ca^{2+} free buffer solution. Typically, 10 ml of collagenase solution is prepared for each mouse to be sacrificed and 30 ml for each rat. The enzyme solution is then stored on ice until injection. When ordering collagenase, the activity should be between 1200 and 1600 activity units as determined by Sigma. This information can be readily obtained from technical assistance prior to placing the order to ensure that the lot delivered falls within this range. Activity outside of this range leads to poor islet yields and structural integrity. Once a particular lot number of collagenase has been used and determined to provide suitable islet quality and yield, a six-month to one-year supply can be ordered and stored at –4° C without loss of activity.

Gradient solution is prepared by dissolving Ficoll Type 400 DL (Sigma) into Ca^{2+} containing buffer solution. Typically, 50 g of 23% (w/w) Ficoll solution is prepared at maintained at room temperature. Following dissolution of the Ficoll, the pH of the 23% solution should be adjusted with 0.5 M NaOH to closely match that of the buffer solution. Gradient pH can vary from buffer pH by as much as 0.03 pH units without adversely affecting islet isolation. Attempts to adjust pH with HCl (if desired pH is overshot) should be minimized, as Ficoll is a modified sucrose product that undergoes acid-catalyzed decomposition. From the 23% Ficoll solution, 10 g each of two additional solutions, 20% and 21% (w/w), are prepared by dilution with Ca^{2+} containing buffer.

For islet isolations, rats should be between 125-300 g and mice between 10-40 g. Animals are sacrificed by anesthesia in a dessicator using metophane or diethyl ether followed by cervical dislocation. The exterior of the animal is washed thoroughly with 70% ethanol and a midline incision is made. Following dissection of the abdomen, the digestive organs are moved aside with sterile cotton swabs. The liver is then moved to expose the pancreas and the pancreatic duct is ligated between the liver and the duodenum with silk suture cord (Carolina Biological Supply) using curved forceps.

The enzyme solution is injected into the duct through a sterile syringe (5 ml for mice and 20 ml for rat) and 27 gauge needle. The pancreatic duct meets the duodenum just below the stomach and forms a translucent "teardrop" structure. Place one index finger underneath this structure so that the duodenum rests firmly on it. The needle should then be inserted into this teardrop structure. Extreme caution must be exercised at this point in the procedure. Excessive pressure or movement of the needle and/or syringe will tear the duct making it impossible to inject enzyme solution. Once the needle is inserted, gently inject the enzyme solution. Approximately 2-5 ml should be injected for each mouse and 15-20 ml for each rat. As the enzyme is injected, the duct will visibly enlarge prior to distention of the pancreas. If this does not occur, remove the needle and reinsert into the duct. Ductal injection of the enzyme is the most important aspect of the procedure. If less than 1 ml of collagenase per mouse or 5 ml per rat is injected, the pancreas can be cut out, minced and digested as follows; however, it is unlikely that significant quantities of islets will be obtained.

Following injection, the distended pancreas is removed with dissecting scissors and blunt-tip forceps beginning at the spleen. Caution should be exercised to avoid cutting the stomach and intestines, which leads to contamination of the islet preparation. Following removal, the pancreas is placed into a 20 ml scintillation vial that has been siliconized (Sigmacote) and sterilized prior to use. Approximately 5 ml of enzyme solution is added for mice and 10 ml for rats (multiple pancreases should not be placed into the same vial). The vial is then place into a 37° C water bath and incubated. For rats the incubation time is 18 min, while for mice the incubation time varies depending on animal size and volume injected but is typically 14-16 min (Table A-1). Following incubation, the vial is removed, filled with ice-cold Ca^{2+} free buffer solution and shaken vigorously for 30 s. The resulting suspension is transferred to a sterile, 50 ml centrifuge tube using a sterile transfer pipette. Fifteen ml of additional Ca^{2+} free buffer solution is added to the vial then transferred to the same centrifuge tube. The islets are then washed follows.

After 4 min, Ca^{2+} containing buffer is added to the tube to bring the volume to 50 ml and the solution is mixed well by trituration with a sterile transfer pipette and incubated for 4 min. Solution is then removed by aspiration until only 10 ml remains in the tube. To the tube, 30 ml of Ca^{2+} containing buffer is added, the solution is mixed thoroughly and then incubated for 4 min followed by removal of 30 ml of solution. This washing step is repeated 6-8 times while working with both tubes simultaneously. Since the islets are more dense than the acinar tissue, the washing steps serve to both remove residual enzyme and separate and purify the islet tissue.

Following washing, the islets are centrifuged at 1100 rpm for 20 s and all buffer is removed. The density gradient is then prepared as follows. Twelve ml of 23% Ficoll is added to the islet-containing centrifuge tubes and mixed thoroughly with a sterile spatula. Four ml of 21% Ficoll is then slowly (1-2 ml/min) added to prevent mixing of the layers followed by slow addition of 4 ml of 20% Ficoll and 4 ml of Ca^{2+} containing buffer, respectively. The islets are centrifuged at 1100 rpm for 8 min. The top two layers are then removed, placed into a 50 ml centrifuge tube and washed twice with Ca^{2+} containing buffer. Next, 8 ml of the remaining solution is removed, placed into a 50 ml centrifuge tube and washed twice. This produces two tubes from each original pancreas. Following removal of all buffer, 10 ml of tissue culture media is added to each tube. The media consists of RPMI 1640 (Gibco # 11875-093) supplemented with 10% fetal bovine serum (FBS; (Gibco # 26140-079), 1% penicillin/streptomycin (Gibco # 15140-122) and 10 mM HEPES, pH 7.4. (Note: all tissue culture media and supplements are from Life Technologies/Gibco).

The media from each tube is then transferred individually to 60 mm culture dishes, hand picked using a 10-100 μl Eppendorf pipet with sterile tips under a dissecting microscope and transferred to fresh media in 60 mm culture dishes. Figure A-1 shows a typical mouse islet of Langerhans obtained using the above procedure. Note the density and color, as these are more distinguishing characteristics than the shape for picking islets. The majority of the islets obtained will be located in the top two layers of the Ficoll gradient if sufficient care is taken during gradient preparation. Finally, 100-200 islets are stored per 60 mm culture dish in a humidified incubator at 37° C, 5% CO_2 until use or dispersion into single cells.

From a single rat, approximately 300-500 islets can be obtained with a size range of 50-400 μm diameter and a mean islet diameter of approximately 150-200 μm. The number and size of islets is much more variable for mouse islets depending on both age of the animal and the volume of enzyme injected. The average size of islets increases with the weight of the mice from 10-30 g. Table A-2 shows approximations of both islet number and mean diameter obtained as a function of mouse weight.

Dispersion Of Human, Canine, and Porcine Islets into Single β-cells

Canine, porcine and human islets are all dispersed by the same procedure. The overall goal is 40-50% dissociation of the islets. Successful dispersion should result in clumps of 2-50 cells, as well as single cells. The outlined procedure will produce sufficient numbers of single cells for experimentation without risking the damage introduced by attempts at complete enzymatic dissociation.

Media and balanced salt solution can be prepared up to 1 month in advance. Tissue culture media for canine, porcine and human islets is modified CMRL 1066 media (G-100). Fifty ml of 10X CMRL media (Gibco # 11540-028) is diluted to ~ 450 ml in a 500 ml volumetric flask. To this solution, add 1.1 g $NaHCO_3$, 2.98 g HEPES and 0.65 ml of 10 M NaOH in this order. Dilute to line and mix thoroughly. Adjust pH to 7.37 ± 0.02 using 1 M NaOH. Remove 60 ml of the above solution and replace with 50 ml FBS (Gibco # 26140-079), 5 ml of 200 mM *l*-glutamine (Gibco # 25030-081) and 5 ml of penicillin/streptomycin (Gibco # 15140-122). Filter solution with a sterile, 0.22 μm pore size, bottle top filter into autoclaved 500 ml bottle and store in refrigerator. Hank's Balanced salt solution (HBSS) is prepared by diluting 25 ml of 10X HBSS stock (Gibco #14180-061) to ~ 245 ml in a 250 volumetric flask. To this, 2.5 ml penicillin/streptomycin is added and the pH adjusted to 7.37 ± 0.02 using saturated $NaHCO_3$. After pH is adjusted, solution is diluted to the mark and filtered with a sterile, 0.22 μm pore size filter into an autoclaved 500 ml bottle and stored in refrigerator until use.

Upon receipt, islets are checked for purity, integrity and sterility as described above. Islets are then split into multiple lots with 2,000-4,000 islets placed per 15 ml centrifuge tube. Typical islet shipments contain 5,000 or 10,000 islets so 2 or 4 tubes are processed simultaneously. Immediately prior to dispersion, trypsin solution should be prepared at a concentration of 1 mg/ml (Gibco # 27250-042) in HBSS. Prepare 8 ml per islet tube to be dispersed and filter 7 ml of the trypsin solution into 15 ml centrifuge tubes (1 tube per islet tube) using a sterile, low protein binding syringe filter. Store the trypsin-containing centrifuge tubes at 37° C until use. Additionally, versene (Gibco # 15040-066), G-100 and HBSS should be allowed to warm to room temperature before dispersion.

After transfer to a 15 ml centrifuge tube, the islets are centrifuged at 1300 rpm for 30 s at $18\text{-}20^{\circ}$ C. All media is removed by aspiration and 7 ml of HBSS is added to each tube. The tubes are centrifuged at 1300 rpm for 2 min and HBSS removed. Repeat this step once more. After the last wash, remove all HBSS and replace with 7 ml versene for 7 min. Triturate the islets at 0 and 3.5 min with a sterile transfer pipette. At the end of the versene treatment, centrifuge the islets at 1300 rpm for 2 min. Remove all versene by aspiration and replace with 7 ml of trypsin solution. At this time start the empty centrifuge at 1500 rpm for 5 min at 4° C to cool it for later use. Place islet containing tubes with trypsin into 37° C water bath and shake gently for 3 min. Remove from bath and triturate islets 10-20 times with sterile transfer pipette. Return to water bath for an additional 30 s. Remove tubes, add 7 ml of G-100 to each tube (serum stops trypsin activity) and centrifuge at 4° C for 5 min at 1500 rpm. Remove all media and add 1.5 ml G-100 for each 1000 islets in the tube. Plate 0.1 ml onto a tissue culture plate and check density under an inverted microscope. Adjust density to approximately 10^5 cells/0.1 ml with additional G-100 media if necessary. Once density is correct, plate 0.1 ml of cell suspension onto coverslips or tissue culture dishes (Nunclon or Corning) and incubate at 37° C for 1-2 hours to allow cell attachment. After this incubation period, add 3 ml of G-100 to each plate and incubate overnight before use.

Dispersion of Rodent Islets into Single β-cells

Dispersion of mouse and rat islets follows the experimental protocol outlined below. RPMI 1640 tissue culture media is prepared as mentioned in the islet isolation procedure except for the omission of HEPES. Media can be prepared up to 3 weeks in advance and refrigerated until use. Trypsin enzyme solution is prepared by diluting 0.05% trypsin:EDTA (Gibco # 25300-054) to 0.025% with HBSS prepared as described for human islet isolation. For dispersion, 100-200 islets are dispersed per tube and up to 4 tubes can be processed simultaneously. Prior to dispersion, pre-warm trypsin and RPMI 1640 to 37° C.

Transfer islets from 60 mm culture plates to 15 ml centrifuge tubes using sterile transfer pipettes. Centrifuge the islets at 20° C, 1100 rpm for 20 s. Remove media and add 1 ml of warmed 0.025 % trypsin solution per tube. Place in 37° C water bath for 8 min and shake throughout. Following incubation, triturate each tube 10-15 times with sterile plastic transfer pipette and add 7-10 ml of pre-warmed RPMI. Centrifuge for 2 min at 900 RPM. Remove supernatant and repeat the previous wash. Add 0.04-0.05 ml of RPMI per 15 islets. Mix well with 1 ml sterile pipette and plate onto 35 mm tissue culture dishes (Nunclon only) or glass coverslips (approximately 0.03 ml per dish). Incubate for 1-2 hours and add 3 ml of warmed RPMI per plate.

Table A-1. Incubation times for various mouse weights and injection volumes.

Incubation Time (min)				
Injected Volume (ml)	**Mouse Weight (g)**			
	10-15	**15-20**	**20-30**	**30 +**
1	12	14	16	16
2	11	13	16	16
3	10	12	15	16
4	10	12	14	16
5	10	12	14	15

Table A-2. Islet diameter and yield as a function of mouse weight.

	Mouse weight (g)				
Property	**10-15**	**15-20**	**20-25**	**25-30**	**30+**
Islets per Mouse	~ 75	~100	~150	~150	~175
Islet Diameter (μm)	25-150	50-200	50-250	50-300	50-300
Mode islet diameter (μm)	75	100	125	150	150

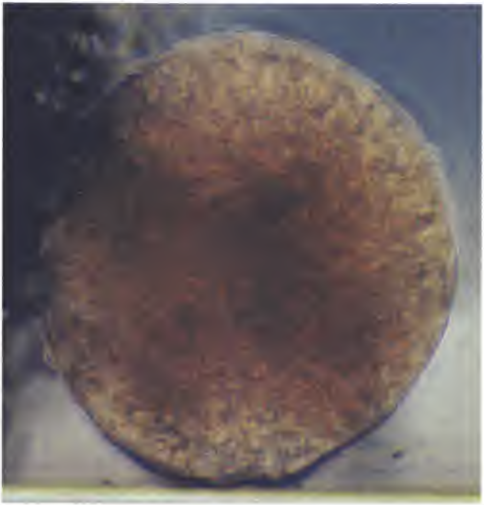

Figure A-1. Typical mouse islet of Langerhans isolated using ductal injection of collagenase. Islet was obtained according to procedure described in text. Glass beads on upper left of islet were used to hold the islet in place and have no significance for the isolation described above. The islet shown is approximately 150 μm in diameter.

APPENDIX B
ANALYSIS OF AMPEROMETRIC CURRENT SPIKES

File Formats

Amperometric current traces are collected with Axoscope data collection software from Axon Instruments. Data is collected in the ".abf" binary file format and then converted to ASCII for data analysis. File structure information for the ".abf" file format is contained within the Axoscope File Support Pack available from Axon Instruments via the internet at *www.axon.com* if future programming applications are warranted. Analysis of individual spike areas, amplitude and width is performed using tim-stat.exe and ts-findn.exe, data analysis programs supplied by Prof. R.M. Wightman. Before data can be analyzed, the ".abf" data files must first be converted to a specific ASCII format and should not exceed 10,000 points per analysis file. Typical amperometric data files contain between 60,000 and 1,500,000 data points and therefore must be fragmented (as described below) into multiple files in order to complete the analysis. The ASCII format used for analysis employs space delimiters and must contain two columns, time (in seconds) and signal (in voltage). A representative section of an analysis file is as follows:

```
0.000 1.001
0.002 1.003
0.004 0.987
0.006 0.993
0.008 1.010
0.010 1.002
```

where the first column is the time (s) followed by a single space then the signal (V). The voltage can be calculated by simply dividing the current at any given point by the amplifier gain used.

Fragmentation of Data Files

Data files are fragmented using in-house software running in the LabWindows environment. The program, axonfrag.c, fragments multiple files based on the filenames assigned by Axoscope and configures the files for automated analysis by ts-findn. The program code is shown below. A brief description of fragmentation and usage are presented here. Ts-findn is a DOS based program that functions based on a series of keystrokes. For automation, the keystroke series for the analysis operations desired must be inserted into the program code in line 146 and 147 as presented below. As the program is written, the data file is opened by ts-findn, filtered with a 60 Hz harmonic notch filter and spikes are determined based on a S/N ratio of 10. Additionally, the keystroke sequence shown contains the output option, which is set to print the spike summary to a dot-matrix printer on LPT1. Any of these properties can be changed by changing the keystroke series that is output by axonfrag.c. Additionally, new functions can be added by adjusting the keystroke series accordingly.

For automated analysis, the files must first be fragmented and formatted by axonfrag.c. Typically all files to be fragmented are copied to a temporary directory before beginning the analysis process. This assists in the later removal of analyzed files. The fragmentation program requires user input as described below. First, the base filename should be input. This is simply the 5 character base filename assigned by Axoscope.

Typically Axoscope filenames are assigned based on the date and the file number. For example, 99401003.abf would be a file collected on April 1, 1999 and would be file number 003. The first and last file to be fragmented should also be entered. Examples of these would be 004 and 027. All files collected in the series between these two file numbers (including the first and last) will be automatically fragmented. Finally, the S/N ratio desired for the analysis and amplifier gain setting for data collection should be entered into the appropriate location. The program determines the number of sub-files to be produced per data file and then begins fragmentation.

In addition to fragmenting the files, the program produces a batch file and series of text files for automated analysis using ts-findn. The file structure for automation of a basefile, 99401 with first and last files 000 and XXX, respectively is as follows:

99401.bat	*Batch File*
99401001.txt	*Keystroke File for Fragmented Files from File 001*
99401001.0	*First Fragmented File from File 001*
99401001.X	*Last Fragmented File from File 001*
99401XXX.txt	*Keystroke File for Fragmented Files from File XXX*
99401XXX.0	*First Fragmented File from File XXX*
99401XXX.X	*Last Fragmented File from File XXX*

Where 99401001.0 is an example of the ASCII fragmented file. The textfile, 99401001.txt contains all of the keystroke commands for each fragmented, ASCII file to be analyzed and the batch file, 99401.bat, automates incorporation of the keystrokes for each file series into ts-findn. Examples of each of these file types can be found below. To run the automated analysis following fragmentation, type the batch file name in DOS and hit enter. For hand calculation of spike files, run tim-stat.exe and open the fragmented ASCII file as desired.

Concerns Using Ts-findn

Automated analysis of current traces obtained generally provides a reliable and reproducible method of analysis for spike characteristics. However, a variety of circumstances can affect the data output and must be addressed. First, the signal-to-noise ratio of the current spikes in the amperometric current traces must be considered. If the S/N ratio is below 5, such as those for mouse and INS-1 cells presented in Chapter 2, it is best to use tim-stat and calculate the spike area by hand. This is more laborious but generates more reproducible spike areas and guarantees all spikes will be found and analyzed.

A second issue that must be considered is the number of spikes per data trace. As the fragmentation program is written, a series of files containing 8192 points is output. This is a limitation of the Lab Windows programming environment, hence there is currently no adjustment in this number. The data files are fragmented at a fixed point, regardless of the position of the current spikes. Ts-findn uses the first 100 points of a data file to calculate the baseline and the root mean square (rms) noise. If a spike is located in this area of the data file, the rms and baseline will be falsely high causing the program to "miss" spikes in the analysis stage. This can be overcome by simple observation. When examining the spike output report, compare the number of spikes counted by eye in the original file to the sum of the spikes found in the fragmented files for each original ".abf" file by ts-findn. If there is a large discrepancy calculate the necessary files by hand.

Finally, when using the Ru-O/CN-Ru modified electrode, the output of the automated file analysis should be monitored closely to ensure that all of the current spikes are found. Due to the drift in the baseline of the electrode, errors are more likely to occur in this analysis than any other. As previously mentioned, ts-findn assigns the first 100 points as the baseline for analysis. This results in reduced numbers of spikes located as well as errors in determination of the spike area for traces with large background drift (> 5 pA/s).

Example File Types

Batch File:

99106.bat

```
type 99106001.txt | ts-findn
type 99106002.txt | ts-findn
```

Keystroke File

99106001.txt

```
 399106001.0
0.1
415r693
10

rlr 399106001.1
0.1
415r693
10

etc.
```

ASCII File.

99106001.0

```
0.0 0.016875
0.002 0.0225
0.004 0.016875
etc.
```

Program Code

```
#include "analysis.h"
#include "formatio.h"
#include "lwsystem.h"
#include "userint.h"
#include "frag.h"
#define TRUE 1

int panel, status;

/* cell fragmentation program for mouse cells.  S/N is variable */

main ()
{
int id;
OpenInterfaceManager();

panel = LoadPanel ("frag.uir", axon);
        if (panel<0)
        {
        FmtOut ("Unable to Load Panel\n");
        exit (0);
        }



        status = DisplayPanel (panel);
         while (TRUE == 1)

        {
        status= GetUserEvent (1, &panel, &id);
        switch (id)
        {
        case 3:  /*Quit Button*/
        exit (0);
        CloseInterfaceManager();
        break;

        case 4:  /*Start Fragmentation*/
        sort();

        break;
        }
        }
}
int sort (void)
{
char filename[20], newfilename[20], outfile[20], num[6], base_file[20];
char text_filename[20], batch_filename[20];
double time_buffer[8191], volt_buffer[8191];
float time_base, ADC_Range, gain, gain2;
double gfactor, x;
int i, l, handle, filetype, first_file, a, last_file, buffer[8191];
int batch_file_handle, text_file_handle, sn;
int format, num_pts_ignored, num_files, file_handle, n, y, z;
int num_remaining;
long j, DataSectPtr, AcqLength, AcqDate, ADC_Res, k;



y=8191;
status = GetCtrlVal (panel, 11, base_file);
status = SetCtrlVal (panel, 5, 1);
status = SetCtrlVal (panel, 8, 1);
status = GetCtrlVal (panel, 12, &first_file);
status = GetCtrlVal (panel, 13, &last_file);
status = GetCtrlVal (panel, 14, &sn);

n = Fmt (batch_filename, "%s.bat", base_file);
batch_file_handle = OpenFile (batch_filename, 0, 1, 1);


        for (a=first_file; a<=last_file; a++)
        {

        n = Fmt (text_filename, "%s%i.txt", base_file, a);
        status = FmtFile (batch_file_handle, "type %s | ts-findn\n",
        text_filename);

        if (a<10)
        {
        n = Fmt (filename, "%s00%i.abf", base_file, a);
        }
```

```
if (a>=10)
{
n = Fmt (filename, "%s0%i.abf", base_file, a);
}


status = SetCtrlVal (panel, 0, filename);
Fmt (newfilename, "%s%i", base_file, a);
status = SetCtrlVal (panel, 1, newfilename);

text_file_handle = OpenFile (text_filename, 0, 1, 1);
handle = OpenFile (filename, 1, 2, 0);
status = SetFilePtr (handle, 10, 0);
status = ScanFile (handle, "%i[b4]>%i[b4]", &AcqLength);
status = SetFilePtr (handle, 20, 0);
status = ScanFile (handle, "%i[b4]>%i[b4]", &AcqDate);
status = SetFilePtr (handle, 36, 0);
status = ScanFile (handle, "%i>%i", &filetype);
status = SetFilePtr (handle, 40, 0);
status = ScanFile (handle, "%i[b4]>%i[b4]", &DataSectPtr);
status = SetFilePtr (handle, 122, 0);
status = ScanFile (handle, "%f[b4]>%f[b4]", &time_base);
status = SetFilePtr (handle, 100, 0);
status = ScanFile (handle, "%i>%i", &format);
status = SetFilePtr (handle, 244, 0);
status = ScanFile (handle, "%f[b4]>%f[b4]", &ADC_Range);
status = SetFilePtr (handle, 252, 0);
status = ScanFile (handle, "%i[b4]>%i[b4]", &ADC_Res);
status = SetFilePtr (handle, 14, 0);
status = ScanFile (handle, "%i>%i", &num_pts_ignored);
status = SetFilePtr (handle, 730, 0);
status = ScanFile (handle, "%f[b4]>%f[b4]", &gain);
status = SetFilePtr (handle, 922, 0);
status = ScanFile (handle, "%f[b4]>%f[b4]", &gain2);



k = DataSectPtr * 512;
num_files = round(AcqLength/8192);
status = SetCtrlVal(panel, 9, num_files);
for (i=0; i<= num_files; i++)
{
        num_remaining = num_files - i;
        status = SetCtrlVal(panel, 10, num_remaining);
        j = k + (long)i*16384;
        Fmt (outfile, "%s.%i", newfilename, i);

        file_handle = OpenFile (outfile, 2, 2, 1);
            gfactor = (ADC_Range/gain) / ADC_Res;
        status = SetFilePtr (handle, j, 0);
        status = ScanFile (handle, "%*i>%*i", y, y, buffer);
        Clear1D (time_buffer, y);
        Clear1D (volt_buffer, y);

        for (z=0; z<y; z++)
        {
        x = time_base/1000000;
        time_buffer[z] = 0 + z*x;
        volt_buffer[z] = buffer[z] * gfactor;
        n = FmtFile (file_handle, "%s<%f %f", time_buffer[z],
        volt_buffer[z]);
        n = WriteFile (file_handle, "\n", 1);
        }
    n = FmtFile (text_file_handle, " 3%s\n0.1\n415r693\n%i\n\nrlr",
    outfile, sn);
    status = CloseFile (file_handle);


    }
    n = WriteFile (text_file_handle, "q", 1);
    status = CloseFile (text_file_handle);
    status = CloseFile (handle);
}
status = SetCtrlVal(panel, 5, 0);
status = SetCtrlVal(panel, 8, 0);
status = CloseFile (batch_file_handle);
}
```

APPENDIX C
MEASUREMENT OF INTRACELLULAR FREE Ca^{2+} IN SINGLE PANCREATIC BETA-CELLS USING FURA-2

Use of Fura-2

Fura-2 is a highly selective, dual excitation, fluorescent Ca^{2+} dye which can easily be loaded into cells in its ester form, fura-2 acetoxymethyl ester (fura-2AM; Grynkiewicz et al., 1985). Once the uncharged ester crosses the plasma membrane, esterases in the cell cleave the five ester groups producing the negatively charged free acid that cannot return across the plasma membrane. The Ca^{2+} binding site on the free acid form of fura-2 is based on the binding structure of EGTA with each fura-2 molecule binding 1 Ca^{2+} ion. Due to the non-destructive nature of the method, measurement of intracellular free Ca^{2+}, $[Ca^{2+}]_i$, by fura-2 microfluorimetry is easily coupled with amperometric detection of exocytosis.

Fura-2 has many properties that make it desirable for measuring Ca^{2+} concentrations within individual cells. It has a quantum yield of 0.23 in the free form and 0.49 when bound (Grynkiewicz et al., 1985). These high values make it possible to monitor fluorescence in the small volume of a single cell and also help to negate the effects of autofluorescence, a lower intensity process (Grynkiewicz et al., 1985). Additionally, when fura-2 is bound to Ca^{2+} the excitation wavelength of the complex is 340 nm while it is 380 nm in the Ca^{2+} free form; however, the emission maximum, 510 nm, remains unchanged (Grynkiewicz et al., 1985). The large Stokes' shift experienced by the dye in the bound form allows accurate quantitation to be performed by ratiometric fluorescence microscopy.

The use of fura-2 for quantitation of $[Ca^{2+}]_i$ within individual cells offers many advantages over other fluorescent dyes and ion selective electrodes. The fluorescence of fura-2 changes very little over the physiological pH range allowing measurements to be made in single cells as well as sub-cellular fractions. Since quantitation is based on a fluorescence ratio, factors such as varying pathlength, absolute dye concentration, heterogeneous dye loading and photobleaching and leakage, typical problems in cellular environments, cancel out because they affect both bound and free fura-2 equally (Grynkiewicz et al., 1985). Finally, fura-2 is highly selective for Ca^{2+} ($K_d = 10^{-7}$ M) over magnesium ($K_d = 10^{-3}$ M), important since resting Ca^{2+} concentration in β-cells is ~100 nM and magnesium is ~1 mM (Tsien and Pozzan, 1989).

Instrumental Diagram

The basic instrument for monitoring $[Ca^{2+}]_i$ in this work consists of a Zeiss Axiovert 100 epifluorescence microscope coupled to a SPEX CMX Cation Monitoring System (Instruments SA). A system diagram is shown in Figure C-1. The CMX system consists of a xenon arc lamp coupled to a splitter. The broad-band illumination of an arc lamp is passed through two individually addressable monochromators with a 5.1 nm bandpass (3 mm slit, 1.7 nm/mm dispersion) before being coupled to the microscope through a fiber optic and focusing optics. Excitation wavelengths (340 and 380 nm for fura-2) are alternately delivered to the specimen through a chopper assembly before the optical fiber. Excitation passes along the optical train of the microscope to a 400 nm long pass dichroic mirror where it is then directed through a high numerical aperture oil immersion objective (Carl Zeiss, Inc., Thornwood, NY; fluar 40 X, N.A. 1.3) onto the specimen, in this case single pancreatic β-cells. The emitted light from the cell is collected back through the dichroic mirror along the optical train of the microscope through a rejection aperture (20 μm for single-cell measurements), and a 510 ± 10 nm bandpass filter onto a photomultiplier tube (PMT) (Hamatsu R928) attached to the microscope.

Instrument Alignment

The most important regular maintenance to be performed on the above mentioned instrument is the alignment of the optical train so that the image in the eyepiece is aligned through the aperture onto the PMT. To align the instrument, a dry coverslip that has been marked in the center with a single dot from a permanent marker pen is placed into a coverslip holder as described for single cell experiments below. A drop of oil is placed on the objective and then the coverslip dish is mounted in the microincubator to hold the dish in place. The objective is then focused onto the dot on the coverslip. Once the dot is in focus, move the coverslip so that the mark is not in the field of view. Next, turn on the 5V light from the shutter housing and observe the two light disks visible in the eyepiece. Adjusting the two optical alignment screws shown in Figure C-2, align the two disks so that they overlap. After this is performed, align the rejection aperture so that the light disk is in the center of the field of view by adjusting the pinhole adjustment screws illustrated in Figure C-2.

Measurements of $[Ca^{2+}]_i$ in Single β-cells by Fura-2 Microfluorimetry

Cells were plated onto 25 mm glass coverslips (Carolina Biological Supply Company, Burlington, NC; AA-63-3017) which had been sterilized in absolute ethanol, air dried and UV irradiated for 30 minutes. Coverslips were then stored in 35 mm tissue culture plates (Corning) until cell suspensions were plated. Cells were plated immediately following isolation and dispersion of islets of Langerhans as discussed in Appendix A. Immediately prior to use, cells were loaded with 2 μM fura-2AM) (Molecular Probes, Eugene, OR; F-1221) at 37° C, 5% CO_2 for 30 minutes. Fura-2 loading solution was prepared by first preparing a 1 mM stock solution of fura-2AM by diluting 50 μg of fura-2AM with 50 μl of dry DMSO. The final loading solution is prepared by 500 fold dilution of fura-2AM stock solution into KRB experimental buffer containing 2.4 mM $CaCl_2$ (3 ml of loading solution should be prepared fresh for each plate to be loaded). Only one plate of cells is loaded at a time.

Following fura-2 loading, coverslips were mounted as the bottom of an open chamber (Medical Systems Corporation, Greenvale, NY; MSC-TD) and placed into a microincubator (Medical Systems Corporation, Greenvale, NY; TC-102) on the stage of an inverted microscope (Carl Zeiss, Inc., Thornwood, NY; Axiovert 100). The microscope was coupled to a Spex CMX cation measurement system equipped for dual excitation monitoring via a fiber optic as described above. The excitation wavelengths were alternated at a rate of 0.16 s and data collected at each wavelength for 0.33 s. This data rate allows one ratio pair to be collected per second. Immediately prior to data collection, the light diversion block shown in Figure C-2 was moved to the closed position. This allows 100% of the emission photons to reach the shutter housing. In the open position, 70% reach the detector housing while the remaining 30% are diverted to the eyepiece.

The emissions generated from excitation at 340 nm (F_{340}) and 380 nM (F_{380}) were used to calculate the fluorescence ratio, R, for the given data traces. Calculation of $[Ca^{2+}]_i$ was performed as previously described (Grynkiewicz et al., 1985) using the following equation:

$[Ca^{2+}]_i = K_d \text{ X } [(R-R_{min})/(R_{max}-R)] \text{ X } (F_{380,\,max}/F_{380,\,min})$.

where R is the experimental ratio, K_d is the binding constant of fura-2 for Ca^{2+} at the experimental temperature, R_{min} is the ratio obtained in the presence of zero free Ca^{2+}, R_{max} is the ratio obtained in saturating Ca^{2+} (~ 40 μM), and $F_{380,max}$ and $F_{380,min}$ are the fluorescence at 380 nm in saturating and zero free Ca^{2+}, respectively. R_{min}, R_{max} $F_{380,max}$ and $F_{380,min}$ are obtained from a two point calibration immediately following single cell experiments. This calibration should be repeated daily using the same aperture to ensure no variations in instrument performance. The calibration is obtained by adding 2 μM fura-2 free acid (Molecular Probes, Eugene, OR; F-1222) to experimental buffer at 37° C containing either 0 mM Ca^{2+} and 1 mM EGTA (R_{min}) or 1 mM Ca^{2+} (R_{max}) and performing an excitation scan from 300-400 nm in triplicate at each concentration. Emission values for 340 nm and 380 nm are obtained from the scans. K_d was taken to be 224 nM at 37° C from the literature (Grynkiewicz et al., 1985) and was independently confirmed on the above system using replicate dilution of Ca^{2+} calibration buffers (Molecular Probes, Eugene,OR; C-3008) as previously reported (Tsien and Pozzan, 1989). Determination of K_d should be performed any time a major instrumental change is observed.

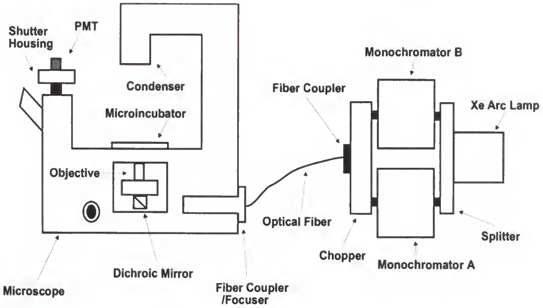

Figure C-1. Instrumental diagram for intracellular free Ca^{2+} measurements.

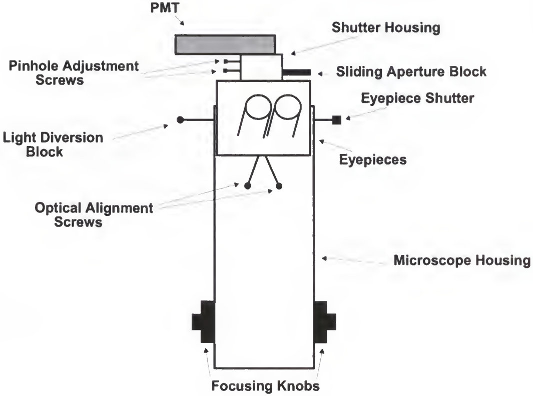

Figure C-2. Front view of Zeiss Axiovert 100 inverted microscope with fluorescence attachment.

REFERENCES

Abdel-Halim, S.M., Guenifi, A., Khan, A., Larsson, O., Berggren, P.-O., Östenson, C.-G., Efendic, S. (1996) *Diabetes* **45**, 934-940.

Alter, C.A., Wolf, B.A. (1995) *Biochem. Biophys. Res. Comm.* **208**, 190-197.

Alvarez de Toledo, G., Fernandez-Chacon, R., Fernandez, J.M. (1993) *Nature* **363**, 554-558.

Ämmalä, C., Ashcroft, F.M., Rorsman, P. (1993) *Nature* **363**, 356-358

Ammon, H.P.T., Verspohl, E. (1976) *Endocrinology* **99**, 1469-1476.

Argoud, G.M., Schade, D.S., Eaton, R.P. (1987) *Diabetes* **36**, 959-962.

Arkhammar, P., Nilsson, T., Rorsman, P., Berggren, P-O. (1987) *J. Biol. Chem.* **262**, 5448-5454.

Asfari, M., Danilo, J., Meda, P., Li, G., Halban, P.A., Wollheim, C.B. (1992) *Endocrinology* **130**, 167-178.

Ashcroft, F.M., Rorsman, P. (1989) *Prog. Biophys. Molec. Biol.* **54**, 87-143.

Aspinwall, C.A., Brooks, S.A., Kennedy, R.T., Lakey, J.R.T. (1997) *J. Biol. Chem.* **272**, 31308-31314.

Aspinwall, C.A., Lakey, J.R.T., Kennedy, R.T. (1999) *J. Biol. Chem.* **274**, 6360-6365.

Atkinson M.A., Maclaren N.K. (1994) *N. Eng. J. Med.* **331**, 1428-1436

Banpied, T.A., Augustine, G.J. (1999) *Proc. Natl. Acad. Sci. USA* **69**, 329-331.

Barnett, D.W., Pressel, D.M., Chern, H.T., Scharp, D.W., Misler, S. (1994) *J. Membrane Biol.* **138**, 113-120.

Beischer, W., Michael, A., Maier, B., Maas, M., Keller, L. (1983) *Diabetologia* **25**, 139.

Berggren, P-O., Larsson, O. (1994) *Biochem. Soc. Trans.* **22**, 12-18.

Berson, S.A., Yalow, R.S. (1966) *Am. J. Med.* **40**, 676-690.

Bertram, R., Smolen, P., Sherman, A., Mears, D., Atwater, I., Martin, F., Soria, B. (1995) *Biophys. J.* **68**, 2323-2332.

Blundell, T., Dodson, G., Hodkin, D., Mercola, D. (1972) *Advances in protein chemistry*, (Anfinsen, C.B., Edsall, J.T., Richards, F.M., eds.) Academic Press: New York, **26**, 279-402.

Bokvist, K., Ämmälä, C., Ashcroft, F.M., Berggren, P-O., Larsson, O., Rorsman, P. (1991) *Proc. R. Soc. Lond. B*, **243**, 139-144.

Bokvist, K., Eliasson, L., Ämmälä, C., Renström, E., Rorsman, P. (1991) *EMBO J.*, **14**, 50-57.

Bonner, F.W., King, L.J., Parke, D.V. (1979) *Chem. Biol. Interact.* **27**, 343-351.

Bonner-Weir, S. (1988) *Diabetes* **37**, 616-621.

Borges, R., Travis, E.R., Hochstetler, S.E., Wightman, R.M. (1997) *J. Biol. Chem.* **272**, 8325-8331.

Bosco, D., Orci, L., Meda, P. (1989) *Exp. Cell Res.* **184**, 72-80.

Bowman, E.J., Siebers, A., Altendorf, K. (1988) *Proc. Nat. Acad. Sci. USA* **85**, 7972-7976.

Bretzel, R.G., Flesch, B.K., Hering, B.J., Brendel, M., Klitscher, D., Brandhorst, H., Schelz, J., Munch, K.P., Federlin, K. (1986) *The immunology of diabetes mellitus,* (Jaworski, M.A., Molnar, G.D., Rajotte, R.V., Singh, B., eds.) Elsevier: Amsterdam, 181-187.

Brown, H., Larsson, O., Bränström, R., Yang, S.-N., Leigbiger, B., Leibiger, I., Fried, G., Moede, T., Deeney, J.T., Brown, G.R., Jacobsson, G., Rhodes, C.J., Braun, J.E.A., Scheller, R.H., Corkey, B.E., Berggren, P.-O., Meister, B. (1998) *EMBO J.* **17**, 5048-5058.

Chen, T.K., Luo, G., Ewing, A.G. (1994) *Anal. Chem.* **66**, 3031-3035.

Chen, M-D., Lin, P-Y., Tsuo, C-T., Wang, J-J., Lin, W-H. (1995) *Biol. Trace Element Res.* **50**, 119-124.

Chow, R.H., von Ruden, L., Neher, E. (1992) *Nature* **356**, 60-62.

Ciolkowski, E.L., Cooper, B.R., Jankowski, J.A., Jorgenson, J.W., Wightman, R.M. (1992) *J. Am. Chem. Soc.* **114**, 2815-2821.

Coore, H.G., Hellman, B., Pihl, E., Täljedal, I-B. (1969) *Biochem. J.* **111**, 107-113.

Cunningham, B.A., Deeney, J.T., Bliss, C.R., Corkey, B.E., Tornheim, K. (1996) *Am. J. Physiol.* **271**, E702-E710.

Dawson, C.M., Lebrun, P., Herchuelz, A., Malaisse, W.J., Goncalves, A.A., Atwater, I. (1986) *Horm. Metab. Res.* **18**, 221-224.

Dean, P.M. (1973) *Diabetologia* **9,** 115-119.

Draznin, B., Goodman, M., Leitner, J.W., Sussman, K.E. (1986) *Endocrinology* **118**, 1054-1058.

Duchen, M.R., Smith, P.A., Ashcroft, F.M. (1993) *Biochem. J.* **294**, 35-42.

Eckholm, R., Ericson, L.E., Lundquist, I. (1971) *Diabetelogia* **7**, 339-348.

Ehrhart, M., Grube, D., Bader, M.F., Aunis, D., Gratzl, M. (1986) *J. Histochem. Cytochem.* **34**, 1673-1682.

Eliasson, L., Renstrom, E., Ammala, C., Berggren, P.-O., Bertorello, A.M., Bokvist, K., Chibalin, A., Deeney, J.T., Flatt, P.R., Gabel, J., Gromada, J., Larsson, O., Lindstrom, P., Rhodes, C.J., Rorsman, P. (1996) *Science* **271**, 813-815.

Emdin, S.O., Dodson, G.G., Cutfield, J.M., Cutfield, S.M. (1980) *Diabetologia* **19**, 174-189.

Epand, R.M., Stafford, A.R., Tyers, M., Nieboer, E. (1985) *Mol. Pharmacol.* **27**, 366-374.

Falck, B., Hellman, B. (1963) *Experientia* **19**, 139-140.

Fernandez-Chacon, R., Alvarez de Toledo, G. (1995) *FEBS Letters* **363**, 221-225.

Finnegan, J.M., Wightman, R.M. (1995) *J. Biol. Chem.* **270**, 5353-5359.

Foster, M.C., Leapman, R.D., Li, M.X., Atwater, I. (1993) *Biophys. J.* **64**, 525-532.

Gao, Z.-Y., Konrad, R.J., Collins, H., Matschinsky, F.M., Rothenberg, P.L., Wolf, B.A. (1996) *Diabetes* **45**, 854-862.

Gazzano, H., Halban, P., Prentki, M., Ballotti, R., Brandenburg, D., Fehlmann, M., Van Obberghen, E. (1985) *Biochem. J.* **226**, 867-872.

Gillis, K.D. (1995) In *Single channel recording* 2nd ed. (Sakmann, B., Neher, E., eds.) Plenum Press: New York, 155-198.

Gillis, K.D., Misler, S. (1992) *Pfulgers Arch.* **420**, 121-123.

Gillis, K.D., Misler, S. (1993) *Pflugers Arch.* **424**, 195-197.

Gold, G., Grodsky, G.M. (1984) *Experentia* **40**, 1105-1114.

Gorski, W., Aspinwall, C.A., Lakey, J.R.T., Kennedy, R.T. (1997) *J. Electroanal. Chem.* **425**, 191-199.

Gray, D.W., Reece-Smith, H., Fairbrother, B., McShane, P., Morris, P.J. (1984) *Transplantation* **37**, 434-437.

Grynkiewicz, G., Poenie, M., Tsien, R.Y. (1985) *J. Biol. Chem.* **260**, 3440-3450.

Guest, P.C., Rhodes, C.J., Hutton, J.C. (1989) *Biochem. J.* **257**, 431-437.

Gylfe, E. (1978) *J. Endocr.* **78**, 239-248.

Harbeck, M.C., Louie, D.C., Howland, J., Wolf, B.A., Rothenberg, P.L. (1996) *Diabetes* **45**, 711-717.

Harris, M.I. (1995) *Diabetes in America 2nd ed.* (Harris, M.I., ed.) NIH Press: Bethesda, MD, 1-14.

Hazama, A., Hayashi, S., Okada, Y. (1998) *Pflugers Arch.* **437**, 31-35.

Hazelwood, R.L. (1989) *The Endocrine Pancreas* Prentice Hall: Englewood Cliffs, N.J.

Hellman, B., Lernmark, A., Sehlin, J., Täljedal, I.-B. (1972) *Biochem. Pharmacol.* **21**, 695-706.

Helmerhorst, E., Stokes, G.B. (1986) *Arch. Biochem. Biophys.* **245**, 238-247.

Hering, B.J., Browatzki, C.C., Schultz, A., Bretzel, R.G., Federlin, K.F. (1993) *Cell Transplantation* **2**, 269-282.

Hiriart, M., Ramirez-Medeles, M.C. (1993) *Mole. Cell. Endocrin.* **93**, 63-69.

Holst, L.S., Mulder, H., Manganiello, V., Sundler, F., Ahren, B., Holm, C., Degerman, E. (1998) *Biochem. Biophys. Res. Comm.* **250**, 181-186.

Holz, G.,G., Leech, C.A., Heller, R.S., Castonguay, M., Habener, J.F. (1999) *J. Biol. Chem.* **274**, 14147-14156.

Hopkins, W.F., Fatherazi, S., Peter-Riesch, B., Corkey, B.E., Cook, D.L. (1992) *J. Membr. Biol.* **129**, 287-295.

Howell, S., (1994) *Diabetologia* **37**, S30-S35.

Huang, L., Shen, H., Atkinson, M.A., Kennedy, R.T. (1995) *Proc. Natl. Acad. Sci. USA* **92**, 9608-9612.

Hurley, L.S. (1969) *Am. J. Clin. Nutr.* **22**, 1332-1341.

Hutton, J.C. (1982) *Biochem. J.* **204**, 171-178.

Hutton, J.C. (1989) *Diabetologia* **32**, 271-281.

Hutton, J.C., Peshavaria, M., Johnston, C.F., Ravazzola, M., Orci, L. (1988) *Endocrinology* **122**, 1014-1020.

Hutton, J.C., Peshavaria, M., Tooke, N.E. (1983) *Biochem. J.* **210**, 803-810.

Ishihara, H., Asano, T., Tsukuda, K., Katagiri, H., Inukai, K., Anai, M., Kikuchi, M., Yazaki, Y., Miyazaki, J.-I., Oka, Y. (1993) *Diabetologia* **36,** 1139-1145.

Islam, M.S., Leibiger, I., Leibiger, B., Rossi, D., Sorrentino, V., Ekstrom, T.J., Westerland, H., Andrade, F.H., Berggren, P.-O. (1998) *Proc. Natl. Acad. Sci. USA* **95**, 6145-6150.

Iversen, J., Miles, D.W. (1971) *Diabetes* **20**,1-5.

Jaim-Etcheverry, G., Zieher, L.M. (1968) *Endocrinology* **96**, 662-677.

Jankowski, J.A., Finnegan, J.M., Wightman, R.M. (1994) *J. Neurochem.* **63**, 1739-1747.

Jankowski, J.A., Schroeder, T.J., Ciolkowski, E.L., Wightman, R.M. (1993) *J. Biol. Chem.* **268**, 14694-14700.

Johnson, J.H., Ogawa, A., Chen, L., Orci, L., Newgard, C.B., Alam, T., Unger, R.H. (1990) *Science* **250**, 546-549.

Kahn, B. (1998) *Cell* **92**, 593-596.

Kahn, S.E., McCulloch, D.K., Porte, D. Jr. (1997) In *International textbook of diabetes mellitus* 2nd ed. (Alberi, K.G.M.M., Zimmet, P., DeFronzo, R.A., Keen, H. eds.) John Wiley and Sons: New York, 337-353.

Kawagoe, K.T., Zimmerman, J.B., Wightman, R.M. (1993) *J. Neurosci. Methods* **48**, 225-240.

Kelly, R.S., Wightman, R.M. (1986) *Anal. Chim. Acta* **187**, 79-87.

Kennedy, R.T., Huang, L., Aspinwall, C.A. (1996) *J. Am. Chem. Soc.* **118**, 1795-1796.

Kennedy, R.T., Huang, L., Atkinson, M.A., Dush, P. (1993) *Anal. Chem.* **65**, 1882-1887.

Kindmark, H., Kohler, M., Efendic, S., Rorsman, P., Larsson, O., Berggren, P.-O. (1992) *FEBS Letters* **303**, 85-90.

Komatsu, M., Schermerhorn, T., Noda, M., Straub, S.G., Aizawa, T., Sharp, G.W.G. (1997) *Diabetes* **46**, 1928-1938.

Kulkarni, R.N., Brüning, J.C., Winnay, J.N., Magnuson, M.A., Kahn, C.R. (1998a) *Diabetes* **47**, A57.

Kulkarni, R.N., Brüning, J.C., Winnay, J.N., Postic, C., Magnuson, M.A., Kahn, C.R. (1999) *Cell* **96**, 329-339.

Kulkarni, R.N., Winnay, J.N., Brüning, J.C., Hanahan, D. (1998b) *Diabetes* **47**, A57.

Kuromi, H., Mizuno, N., Seino, S. (1995) *Diabetes* **44**, 1213-1217.

Lakey, J.R.T., Warnock, G.L., Rajotte, R.V. (1996) *Transplantation* **61**, 506-508.

Lakey, J.R.T., Warnock, G.L., Rajotte, R.V. (1997) *Cell Transplantation* **4**, 163-172.

Larsson, L.-I., Sundler, F., Håkanson, R. (1976) *Diabetologia* **12**, 211-226.

Larsson, O., Ämmälä, C., Bokvist, K., Fredholm, B.,Rorsman, P. (1993) *J. Physiol.* (London) **463**, 349-365.

Leibiger, I.B., Leibiger, B., Moede, T., Berggren, P.-O. (1998) *Molecular Cell* **1**, 933-938.

Leszczyszyn, D.J., Jankowski, J.A., Viveros, O.H., Diliberto, E.J., Near, J.A., Wightman, R.M. (1990) *J. Biol. Chem.* **265**, 14736-14737.

Li, G.D., Miani, D., Dunne, M.J., Pralong, W.F., Theler, J.M., Petersen, O.H., Wollheim, C.B. (1991) *J. Biol. Chem.* **266**, 3449-3457.

Liang, Y., Matschinsky, F. (1994) *Ann. Rev. Nutr.* **14**, 59-81.

Liu, Y.-J., Grapengiesser, E., Gylfe, E., Hellman, B. (1996) *Arch. Biochem. Biophys.* **334**, 295-302.

Liljenquist, J.E., Horwitz, D.L., Jennings, A.S., Chiasson, J.-L., Keller, U., Rubenstein, A.H. (1978) *Diabetes* **27**, 563-570.

Longo, E.A., Tornheim, K., Deeney, J.T., Varnum, B.A., Tillotson, D., Prentki, M., Corkey, B.E. (1991) *J. Biol. Chem.* **266**, 9314-9319.

Loreti, L., Dunbar, J.C., Chen, S., Foá, P.P. (1974) *Diabetologia* **10**, 309-315.

Luzi, L., Batezzati, A., Perseghin, G., Bianchi, E., Vergani, S., Secchi, A., La Rocca, E., Staudacher, C., Spotti, D., Ferrari, G., Di Carlo, V., Pozza, G. (1992) *Diabetes* **41**, 1632-1639.

Maes, E., Pipeleers, D. (1984) *Endocrinology* **114**, 2205-2209.

Mahadevan, I.B., Kimber, M.C., Lincoln, S.E., Tiekink, E.R.T., Ward, A.D., Betts, W.H., Forbes, I.J., Zalewski, P.D. (1996) *Aust. J. Chem.* **49**, 561-568.

Maki, L.W., Keizer, J. (1995) *Am. J. Phys.* **268**, C780-C791.

Malaisse, W.J. (1994) *Diabetologia* **37**, S36-S42.

Malaisse, W.J., Malaisse-Lagae, F., Lacy, P.E., Wright, P.H. (1967) *Proc. Soc. Exp. Biol. Med.* **124**, 497-500.

Marincola, F., Frank, W., Clark, W., Douglas, M., Merrell, R. (1983) *Diabetes* **32**, 1162-1167.

Martin, B.C., Warram, J., Krowlewski, A., Bergman, R., Soeldner, J., Kahn, C.R. (1992) *Lancet* **340**, 925-929.

Matthews, E.K., McKay, D.B., O'Connor, M.D.L., Borowitz, J.L. (1982) *Biochim. Biophys. Acta* **715**, 80-89.

Michel, E., Parsons, J.A. (1990) *J. Histochem. Cytochem.* **38**, 965-973.

Moens, K., Himberg, H., Flamez, D., Huypens, P., Quartier, E., Ling, Z., Pipeleers, D., Gremlich, S., Thorens, B., Schuit, F. (1996) *Diabetes* **45**, 257-261.

Moore, A.W., Jorgenson, J.W. (1993) *Anal. Chem.* **65**, 188-191.

Mortimer, C. H., Carr, D., Lind, T., Bloom, S.R., Mallinson, C.N., Schally, A.V., Tunbridge, W.M.G., Yeomans, L., Coy, D.H., Kastin, A., Besser, G.M., Hall, R. (1974) *Lancet* **1**, 697-701.

Moser, M., Warnock, G.L. (1991) *Clin. Invest. Med.* **14**, A144.

Nanavati, C., Fernandez, J.M. (1993) *Science* **259**, 963-965.

Norman, A.W., Litwack, G. (1997) *Hormones* 2nd ed., Academic Press: San Diego, 193-227.

Oberhauser, A.F., Robinson, I.M., Fernandez, J.M. (1996) *Biophys J.* **71**, 1131-1139.

Okamoto, H. (1999) *Mole. Cell. Biochem.* **193**, 115-118.

O'Rahilly, S., Turner, R., Matthews, D. (1988) *N. Eng. J. Med.* **318**, 1225-1230.

Orci, L. (1982) *Diabetes* **31**, 538-565.

Orci, L. (1985) *Diabetologia* **28**, 528-546.

Orci, L., Ravazzola, M., Amherdt, M., Madsen, O., Perrelet, A., Vassalli, J-D., Anderson, R.G.W. (1986) *J. Cell Biol.* **103**, 2273-2281.

Orci, L., Vassalli, J.-D., Perrelet, A. (1988) *Sci. Am.* 85-94.

Owman, C., Håkanson, R., Sundler, F. (1973) *Fed. Proc.* **32**, 1785-1791.

Pace, C.S., Matchinsky, F.M., Lacy, P.E., Conant, S. (1977) *Biochim. Biophys. Acta* **497**, 408-414.

Paras, C.D., Kennedy, R.T. (1995) *Anal. Chem.* **67**, 3633-3637.

Paras, C.D., Kennedy, R.T. (1997) *Electroanalysis* **9**, 203-208.

Paras, C.D., Qian, W.J., Lakey, J.R.T., Tan, W.H., Kennedy, R.T. (1999) manuscript submitted for publication.

Patel, Y.C., Amherdt, M., Orci, L. (1982) *Science* **217**, 1155-1156.

Penner, R. (1995) In *Single channel recording* 2^{nd} ed. (Sakmann, B., Neher, E., eds.) Plenum Press: New York, 3-30.

Pfeifer, M.A., Halter, J.B., Porte, D. Jr. (1981) *Am. J. Med.* **70**, 579-588.

Pihel, K., Travis, E.R., Borges, R., Wightman, R.M. (1996) *Biophys. J.* **71**, 1633-1640.

Pipeleers, D.G. (1994) *Diabetologia* **37**, S57-S64.

Pipeleers, D.G., in't Veld, P., Maes, E., Van De Winkel, M. (1982) *Proc. Natl. Acad. Sci. USA* **79**, 7322-7325.

Pipeleers, D.G., Pipeleers-Marichal, M.A. (1981) *Diabetologia* **20**, 654-663.

Polonsky, K.S. (1995) *Diabetes* **44**, 705-717.

Pralong, W. F., Bartley, C., Wollheim, C.B. (1990) *EMBO J.* **9**, 53-59.

Prentki, M., Tornheim, K., Corkey, B.E. (1997) *Diabetologia* **40**, S32-S41.

Rahamimoff, R., Fernandez, J.M. (1997) *Neuron* **18**, 17-27.

Rajan, A.S., Aguilar-Bryan, L., Nelson, D.A., Yaney, G.C., Hsu, W.H., Kunze, D.L., Boyd, A.E. (1990) *Diabetes Care* **13**, 340-363.

Rajotte, R.V., Lakey, J.R.T., Warnock, G.L. (1995) In *Methods in cell transplantation* (Ricordi, C., ed.) RG Landes: Austin, TX, 517-524.

Rajotte, R.V., Mazur, P. (1981) *Cryobiology* **18**, 17-31.

Ricordi, C., Lacy, P.E., Finke, E.H., Olack, B.J., Scharp, D.W. (1988) *Diabetes* **37**, 413-420.

Robinson, I.M., Finnegan, J.M., Monck, J.R., Wightman, R.M., Fernandez, J.M. (1995) *Proc. Nat. Acad. Sci. USA* **92**, 2474-2478.

Rothenberg, P.L., Willison, L.D., Simon, J., Wolf, B.A. (1995) *Diabetes* **44**, 802-809.

Sandler, S., Andersson, A. (1987) *Cryobiology* **24**, 285-291.

Scharp, D.W., Lacy, P.E., Santiago, J.V. (1991) *Transplantation* **51**, 76-85.

Scharp, D.W., Lacy, P.E., Santiago, J.V., McCullough, C.S., Weide, L.G., Falqui, L., Marchetti, P., Gingerich, R.L., Jaffe, A.S., Cryer, P.E., Anderson, C.B., Flye, M.W. (1990) *Diabetes* **39**, 515-518.

Schatz, H., Pfeiffer, E.F. (1977) *J. Endocrin.* **74**, 243-249.

Schroeder, T.J., Borges, R., Finnegan, J.M., Pihel, K., Amatore, C., Wightman, R.M. (1996) *Biophys. J.* **70**, 1061-1068.

Schroeder, T.J., Jankowski, J.A., Kawagoe, K.T., Wightman, R.M., Lefrou, C., Amatore, C. (1992) *Anal. Chem.* **64**, 3077-3083.

Schuit, F.C., Derde, M.P., Pipleers, D.G. (1989) *Diabetologia* **32**, 207-212.

Scott, A.M., Atwater, I., Rojas, E. (1981) *Diabetologia* **21**, 470-475.

Smith, P.A., Duchen, M.R., Ashcroft, F.M. (1995) *Pflugers Arch.* **430**, 808-818.

Sodoyez, J.C., Sodoyez-Goffaux, F., Foá, P.P. (1969) *Proc. Soc. Exp. Biol. Med.* **130**, 568-571.

Stagner, J., Samols, E., Polonsky, K., Pugh, W. (1986) *J. Clin. Invest.* **78**, 1193-1198.

Sun, X.J., Pons, S., Wang, L.M., Zhang, Y.T., Yenush, L., Burks, D., Myers, M.G., Glasheen, E., Copeland, N.G., Jenkins, N.A., Pierce, J.H., White, M.F. (1997) *Mol. Endocrinol.* **11**, 251-262.

Taborsky, G.J. Jr. (1983) *Am. J. Phys.* **245**, E598-E603.

Takahashi, N., Kadowaki, T., Yazaki, Y., Ellis-Davies, G.C.R., Miyashita, Y., Kasai, H. (1999) *Proc. Natl. Acad. Sci. USA* **96**, 760-765.

Takahashi, N., Kadowaki, T., Yazaki, Y., Miyashita, Y., Kasai, H. (1997) *J. Cell Biol.* **138**, 55-64.

Tamemoto, H., Kadowaki, T., Tobe, K., Yagi, T., Sakura, H., Hayakawa, T., Terauchi, Y., Ueki, K., Kaburagi, Y., Satoh, S., Sekihara, H., Furuta, Y., Ikawa, Y., Kasuga, M., Yazaki, Y., Aizawa, S. (1994) *Nature* **372**, 182-186.

Tanaka, R., Shima, K., Sawazaki, N., Matsuyama, T., Kumahara, Y., Yanaihara, N. (1980) *Endocrinol. Jap.* **27**, 343-348.

Tanford, C., Epstein, J. (1954) *J. Am. Chem. Soc.* **76**, 2170-2176.

Tang, J., Pugh, W., Polonsky, K.S., Zhang, H. (1996) *Am. J. Physiol.* **270**, E504-E512.

Tao, L., Aspinwall, C.A., Kennedy, R.T. (1998) *Electrophoresis* **19**, 403-408.

Tatham, P.E.R., Duchen, M.R., Millar, J. (1991) P*flugers Arch.* **419**, 409-414.

Taylor, S. (1999) *Cell* **97**, 9-12.

Taylor, S., Accili, D., Imai, Y. (1994) *Diabetes* **43**, 735-740.

Tess, M.E., Cox, J.A. (1998) *Electroanalysis* **10**, 1237-1240.

Theler, J.-M., Mollard, P., Guerineau, N., Vacher, P., Pralong, W.F., Schlegel, W., Wollheim, W.B. (1992) *J. Biol. Chem.* **267,** 18110-18117.

Toroptsev, I.V., Eshchenko, V.A., Troshkin, V.G. (1974) *Bull. Exp. Biol. Med.* **77**, 119-121.

Tsien, R.Y., Bacskai, B.J. (1995) In *Handbook of biological confocal microscopy*, 2nd ed. (Pawley, J.B. ed.) Plenum Press: New York, 459-478.

Tsien, R.Y., Pozzan, T. (1989) *Meth. Enzymol.* **172,** 230-262.

Unger, R.H. (1991) *Science* **251**, 1200-1205.

Van Schravendijk, C.F.H., Heylen, L., Van den Brande, J.L., Pipeleers, D.G. (1990) *Diabetologia* **33**, 649-653.

Velloso, L.A., Carneiro, E.M., Crepaldi, S.C., Boschero, A.C., Saad, M.J.A. (1995) *FEBS Letters* **377**, 353-357.

Verspohl, E.J., Ammon, H.P.T. (1980) *J. Clin. Invest.* **65**, 1230-1237.

Vionnet, N., Stoffel, M., Takeda, J., Yasuda, K., Bell, G.I., Zouali, H., Lesage, S., Velho, G., Iris, F., Passa, P., Froguel, P., Cohen, D. (1992) *Nature* **356**, 721-722.

Walker, A., Glavinovic, M.I., Trifaro, J.-M. (1996) *Pflug. Arch.* **431**, 729-735.

Warnock, G.L., Ao, Z., Lakey, J.R.T., Rajotte, R.V. (1994a) In *Pancreatic islet transplantation: Procurement of pancreatic islets* (Lanza, R.P., Chick, W.L. eds.) RG Landes: Austin, TX, **1**, 81-95.

Warnock, G.L., Kneteman, N.M., Rajotte, R.V. (1991) *The endocrine pancreas* (Samols, E., ed.) Raven Press: New York, 487-517.

Warnock, G.L., Kneteman, N.M., Ryan, E.A., Rabinovitch, A., Rajotte, R.V. (1992) *Diabetologia* **35**, 89-95.

Warnock, G.L., Lakey, J.R.T., Ao, Z., Rajotte, R.V. (1994b) *Transplant. Proc.* **26**, 3438.

Webb, D.-L., Islam, M.S., Efanov, A.M., Brown, G., Kohler, M., Larsson, O., Berggren, P.-O. (1996) *J. Biol. Chem.* **271**, 19074-19079.

White, M.F. (1997) *Diabetologia* **40**, S2-S17.

White, N.S. (1995) In *Handbook of biological confocal microscopy.* 2nd ed. (Pawley, J.B. ed.) Plenum Press: New York, 459-478..

Wightman, R.M., Jankowski, J.A., Kennedy, R.T., Kawagoe, K.T., Schroeder, T.J., Leszczyszyn, D.J., Near, J.A., Diliberto, E.J., Viveros, O.H. (1991) *Proc. Natl. Acad. Sci. USA* **88**, 10754-10758.

Wightman, R.M., Schroeder, T.J., Finnegan, J.M., Ciolkowski, E.L., Pihel, K. (1995) *Biophysical J.* **68**, 383-390.

Willmott, N.J., Galione, A., Smith, P.A. (1995) *FEBS Letters* **371**, 99-104.

Withers, D.J., Gutierrez, J.S., Towery, H., Burks, D.J., Ren, J.-M., Previs, S., Zhang, Y., Bernal, D., Pons, S., Shulman, G.I., Bonner-Weir, S., White, M.F. (1998) *Nature* **391**, 900-904.

Xu, G., Gao, Z.-Y., Wolf, B.A. (1998a) *Diabetes* **47**, A57.

Xu, G., Howland, J., Rothenberg, P.L. (1996) *Biochem. J.* **318**, 623-629.

Xu, G., Marshall, C.A., Lin, T.-A., Kwon, G., Munivenkatappa, R.B., Hill, J.R., Lawrence, J.C. Jr., McDaniel, M.L. (1998b) *J. Biol. Chem.* **273**, 4485-4491.

Xu, G., Rothenberg, P.L. (1998) *Diabetes* **47**, 1243-1252.

Yamagata, K., Furuta, H., Oda, N., Kaisaki, P.J., Menzel, S., Cox, N.J., Fajans, S.S., Signorini, S., Stoffel, M., Bell, G.I. (1996) *Nature* **384**, 458-460.

Yoshimori, T., Yamamoto, A., Moriyama, Y., Futai, M., Tashiro, Y. (1991) *J. Biol. Chem.* **266**, 17707-17712.

Zalewski, P.D., Forbes, I.J., Betts, W.H. (1993) *Biochem. J.* **296**, 403-408.

Zhou, Z., Misler, S. (1995) *Proc. Natl. Acad. Sci. USA* **92**, 6938-6942.

Zhou, Z., Misler, S. (1996) *J. Biol. Chem.* **270**, 270-277.

Zimmerberg, J. (1987) *Biosci. Rep.* **7**, 251-268.

BIOGRAPHICAL SKETCH

Craig Alan Aspinwall was born January 26, 1972, in Marietta, GA. He graduated *magna cum laude* from Berry College, in Rome, GA, with a Bachelor of Science degree in chemistry in April, 1994. In August, 1994 he began graduate studies under the direction of Dr. Robert T. Kennedy in the Chemistry Department at the University of Florida. He completed his research in June 1999, obtaining a Doctor of Philosophy degree.

I certify that I have read this study and that in my opinion it conforms to acceptable standards of scholarly presentation and is fully adequate, in scope and quality, as a dissertation for the degree of Doctor of Philosophy.

Robert

Robert T. Kennedy, Chairman
Professor of Chemistry

I certify that I have read this study and that in my opinion it conforms to acceptable standards of scholarly presentation and is fully adequate, in scope and quality, as a dissertation for the degree of Doctor of Philosophy.

Richard A. Yost
Professor of Chemistry

I certify that I have read this study and that in my opinion it conforms to acceptable standards of scholarly presentation and is fully adequate, in scope and quality, as a dissertation for the degree of Doctor of Philosophy.

Kathryn R. Williams

Kathryn R. Williams
Associate in Chemistry

I certify that I have read this study and that in my opinion it conforms to acceptable standards of scholarly presentation and is fully adequate, in scope and quality, as a dissertation for the degree of Doctor of Philosophy.

Jon D. Stewart
Assistant Professor of Chemistry

I certify that I have read this study and that in my opinion it conforms to acceptable standards of scholarly presentation and is fully adequate, in scope and quality, as a dissertation for the degree of Doctor of Philosophy.

Mark A. Atkinson
Professor of Pathology, Immunology, and
Laboratory Medicine

This dissertation was submitted to the Graduate Faculty of the Department of Chemistry in the College of Liberal Arts and Sciences and to the Graduate School and was accepted as partial fulfillment of the requirements for the degree of Doctor of Philosophy.

August 1999

Dean, Graduate School